INVESTIGATE THE FEASIBILITY OF IMPLEMENTING EARTH-TO-AIR HEAT EXCHANGER (EAHE) AS A SUSTAINABLE COOLING SYSTEM IN MALAYSIA

THIEM WOH MUN

UNIVERSITY TUNKU ABDUL RAHMAN

INVESTIGATE THE FEASIBILITY OF IMPLEMENTING EARTH-TO-AIR HEAT EXCHANGER (EAHE) AS A SUSTAINABLE COOLING SYSTEM IN MALAYSIA

THIEM WOH MUN

A project report submitted in partial fulfilment of the requirements for the award of Bachelor of Engineering (Hons.) Mechanical Engineering

Faculty of Engineering and Science
Universiti Tunku Abdul Rahman

May 2015

DECLARATION

I hereby declare that this progress report is based on my original work except for citations and quotations which have been duly acknowledged. I also declare that it has not been previously and concurrently submitted for any other degree or award at UTAR or other institutions.

Signature   :

Name   :   Thiem Woh Mun

ID No.   :   10UEB05467

Date   :   8 May 2015

APPROVAL FOR SUBMISSION

I certify that this progress report entitled **"INVESTIGATE THE FEASIBILITY OF IMPLEMENTING EARTH-TO-AIR HEAT EXCHANGER (EAHE) AS A SUSTAINABLE COOLING SYSTEM IN MALAYSIA"** was prepared by **THIEM WOH MUN** has met the required standard for submission in partial fulfilment of the requirements for the award of Bachelor of Engineering (Hons.) Mechanical Engineering at Universiti Tunku Abdul Rahman.

Approved by,

Signature   :

Supervisor   :

Date   :

The copyright of this report belongs to the author under the terms of the copyright Act 1987 as qualified by Intellectual Property Policy of Universiti Tunku Abdul Rahman. Due acknowledgement shall always be made of the use of any material contained in, or derived from, this report.

Specially dedicated to

my beloved mother, father, brother and sister.

ACKNOWLEDGEMENTS

I would like to thank everyone who had contributed to the successful completion of this project report. I would like to express my gratitude to my research supervisor, Dr. Tan Yong Chai for his invaluable advice, guidance and his enormous patience throughout the development of the research.

In addition, I would also like to express my gratitude to my loving parent and family members and friends who had helped and given me encouragement throughout this progress report. I am thankful to all my final year project group members for sharing valuable knowledge with me.

INVESTIGATE THE FEASIBILITY OF IMPLEMENTING EARTH-TO-AIR HEAT EXCHANGER (EAHE) AS A SUSTAINABLE COOLING SYSTEM IN MALAYSIA

ABSTRACT

This project aims to evaluate the potential of implementing Earth-to-Air Heat Exchanger (EAHE) to provide space cooling and air conditioning in Malaysia. The benefit of this passive cooling technology in tropical climate such as Malaysia is unrecognized at current time due to lack of development in this field. Based on experimental measurement, the suitable depth for the installation of the pipe of EAHE prototype system in this project was determined to be 1.5 m. The difference of ground temperature at the depth of 1.5 m and 2.0 m was also determined to be very small with a difference of only $0.1\,^{\circ}$C.

To design the EAHE prototype system for this studies, a cooling load analysis based on Residential Load Factor (RLF) method has been conducted on the experimental residential room. The cooling load determined from RLF method was 952 W. The EAHE prototype system designed in this project intended to reject heat of the amount imposed by the determined cooling load under the worst condition. The EAHE prototype system finalized and tested in this project has selected PVC pipe of 3 in (80 mm) nominal diameter. The pipe length of the EAHE prototype has been designed to be 11.6 m long.

Besides, a centrifugal exhaust has been designed and fabricated in this project that was used in the EAHE prototype system. The centrifugal fan was designed by a trial-and-error approach using Flow Simulation of SolidWorks. The simulated and experimental suction velocity was determined to be 17.1 m/s and 16.5 m/s with a percentage difference of 3.64 %.

Experimental studies performed on the EAHE prototype system has shown that the average ideal and actual percentage reduction of cooling load achieved were 37.57 % and 16.21 % respectively. The average heat rejected by the EAHE and from the room were 357.70 W and 154.28 W respectively. The results obtained also shown that the EAHE efficiency stays in the range of 30 – 50 % for most of the time and the prototype had achieved an average EAHE efficiency of 48.87 %. The average ideal and actual Coefficients of Performance (COPs) achieved by the EAHE prototype were 7.15 and 3.09 respectively. It was also shown that the actual COP of the EAHE prototype stays in the range of 3.0 – 4.4 for most of the time.

In conclusion, the EAHE prototype did reasonably well performance in terms of COPs. However, it did not achieved very well performance in percentage reduction of cooling load and EAHE efficiency due to the effect of heat gained by the insulation. Therefore, it can be concluded that it is feasible to implement EAHE cooling system in Malaysia if thermal insulation of the system could be carefully designed.

TABLE OF CONTENTS

LIST OF TABLES

LIST OF FIGURES

LIST OF SYMBOLS / ABBREVIATIONS

A	net surface area, ft^2
A_{cf}	conditioned floor area of building, ft^2
A_{es}	building exposed surface area, ft^2
A_L	building effective leakage area, ft^2
A_{ul}	unit leakage area factor, in^2/ft^2
q_{opq}	opaque surface cooling load, Btu/h
CF_{opq}	surface cooling factor, $Btu/h.ft^2$
COP_{actual}	actual coefficient of performance of the EAHE
COP_{ideal}	ideal coefficient of performance of the EAHE
C_s	air sensible heat factor, Btu/h·cfm
D_i	inner diameter of the pipe, m
D_o	outer diameter of the pipe, m
DR	daily cooling range, °F
f	friction factor
h_a	convective heat transfer coefficient of air, $W/m^2·K$
k	thermal conductivity of the component, W/m·K
k_a	thermal conductivity of the air, W/m·K
k_p	thermal conductivity of the PVC pipe, W/m·K
L	length of the pipe, m
$\dot{m}_a$	mass flow rate of air, kg/s
N_{oc}	number of occupants
Nu	Nusselt number
OF_b	opaque surface cooling factors
OF_r	opaque surface cooling factors
OF_t,	opaque surface cooling factors

P_{fan}	rated power of the fan, W
Pr	Prandlt number
$Q_{bal,hr}$	balanced ventilation flow rate via HRV/ERV equipment, cfm
$Q_{bal,oth}$	other balanced ventilation supply airflow rate, cfm
Q_i	infiltration leakage rate assuming no mechanical pressurization, cfm
Q_{unbal}	unbalanced airflow rate, cfm
Q_v	required ventilation flow rate, cfm
Q_{vi}	combine infiltration/ventilation flow rate, cfm
$q_{gained/rejected}$	heat gained or rejected, W
q_{ig}	cooling load (sensible) due to internal heat gains, Btu/h
q_{load}	total heat gain of the room from cooling load analysis, W
$q_{rejected,EAHE}$	heat rejected by the EAHE prototype, W
$q_{rejected,rooom}$	heat rejected from the room, W
q_{vi}	ventilation/infiltration cooling load, Btu/h
$R_{conductive}$	conductive thermal resistance of the pipe, K/W
$R_{convective}$	convective thermal resistance from air to inner pipe surface, K/W
Re	Reynolds number
R_{total}	total thermal resistance, K/W
t	thickness of the component, m
U	construction U-factor, Btu/h ft^2 ^{o}F
V_{avg}	average velocity in the EAHE pipe system, m/s
V_o	outlet velocity of the EAHE system or suction inlet velocity of the fan, m/s
V_i	inlet velocity of the EAHE system
ΔT	difference of temperature, K
$\Delta T_{room\text{-}ground}$	temperature difference of room and ground temperature, K
Δt	cooling design temperature difference, ^{o}F
ε_s	HRV/ERV sensible effectiveness
μ	dynamic viscosity of the air, kg/m s
η_{EAHE}	EAHE efficiency
ρ	density of air, kg/m^3

EAHE	Earth-to-Air Heat Exchanger
°C	degree Celsius
s	second
m	meter
J	Joule
W	Watt
Pa	Pascal
kg	kilogram

LIST OF APPENDICES

CHAPTER 1

INTRODUCTION

1.1 Background

The world energy consumption is increasing over the time horizon while the fossil fuels are still expected to be the largest supply of the worldwide energy consumption. Nevertheless, nuclear and renewable energy are growing fast due to the relatively high price of fossil fuels especially petroleum and other liquid fuels as shown in Figure 1.1 (EIA U.S. Energy information Administration, 2013). In Malaysia, the energy demand of residential and commercial sectors has increased by over 118 and 124 percent from year 2000 to 2012. Most of the energy consumed in these two sectors are used in cooling and conditioning the indoor air of a building as shown in Figure 1.2 (Energy Commission, 2013). Renewable energy combine with energy efficient design suggested a sustainable and reliable solution for the worldwide energy crisis.

There is a growing interest in heating, ventilation and air conditioning (HVAC) based on renewable energy particularly in the development of green building. Geothermal energy which exploits the use of renewable energy stored in the ground is one of the energy sources currently in demand (Geothermal Panel of the European Technology Platform on Renewable Heating and Cooling, 2012). There are generally three types of geothermal energy that could be extracted or harvested corresponding to three level of depth of the ground which are deep, swallow and very swallow (or near-surface). Deep geothermal energy can be extracted using deep drilling holes for electricity generation. Geothermal power plant

utilizes steam (over 150ºC) produced from reservoir of hot water found three to six km below the surface of ground for this purpose (Germany Energy Agency, 2002).
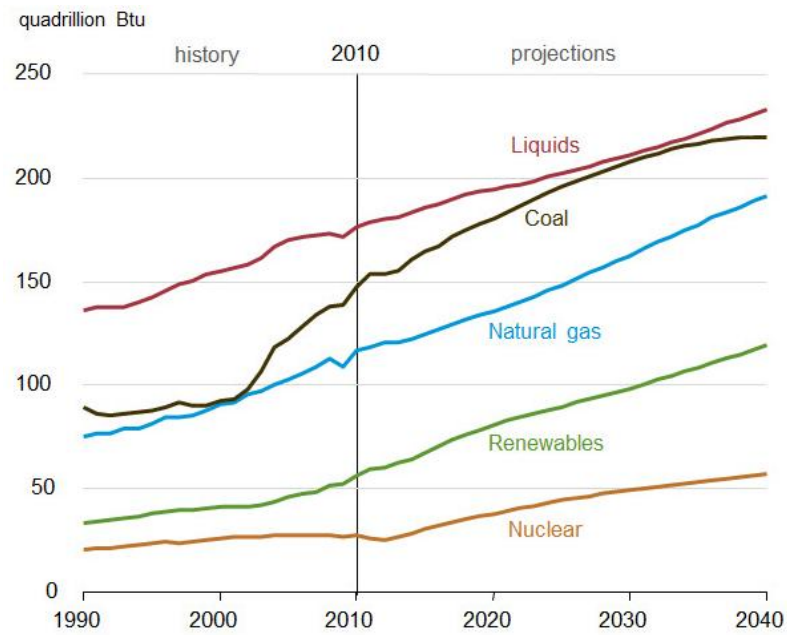
Figure 1.1: International Energy Outlook 2013 on World Energy Consumption by Fuel Type (EIA U.S. Energy information Administration, 2013)
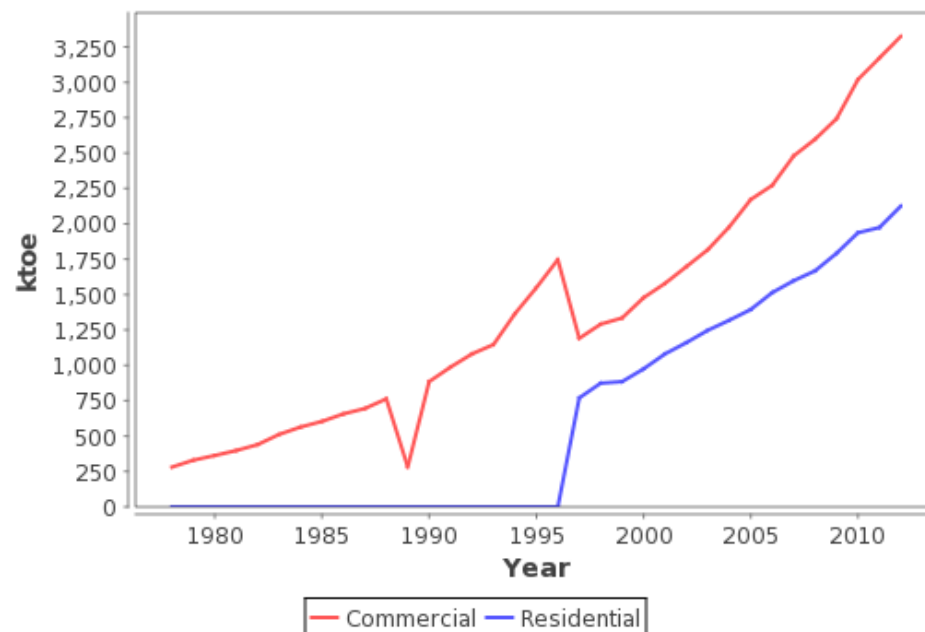
Figure 1.2: Electricity Consumption of Residential and Commercial Sectors of Malaysia (Energy Commission, 2013)

Swallow geothermal energy can be extracted using deep bore heat exchangers, a closed system for geothermal energy production consists of a single borehole at a depth of over 400 m. Double pipe heat exchangers are inserted into it and heat is then extracted and delivered to a heat pump circuit at the surface through a circulating hot water. This kind of geothermal heat wells finds it application in the industrial and agriculture heating process (Germany Energy Agency, 2002). The third type of geothermal energy is near-surface geothermal energy which exploits the heat from the upper layers of ground and ground water. At sufficient depth of about 2 m from the ground surface, the ground temperature remains relatively constant, the temperature fluctuations at the surface is attenuated by the high thermal inertia of the soil. The ground temperature at this depth is warmer than air in winter and cooler than the air in summer for a seasonal country.

Passive cooling and heating of a building to a comfortable level can be achieved through buried pipes in the ground, a mechanism called earth-to-air heat exchanger (EAHE). When ambient air is drawn through these buried pipes, the air will be cooled in the summer because the ground temperature is lower. Conversely, the ambient air is heated during winter because the ground temperature is relatively higher. For many years since its discovery, EAHE was well-known as a potent and viable solution to achieve comfort and space cooling whilst reducing energy consumption in a building (Al-Ajmi, Loveday and Hanby, 2006). Besides being emission-free and environment friendly, the main advantages of the EAHE is low operational and maintenance costs and high pre-cooling and pre-heating potential.

The main focus of this study is to investigate the effectiveness of the EAHE in terms of cooling potential in Malaysia which has a tropical climate. Generally, an EAHE consists of a network of buried pipes where hot air is sucked in at the inlet end by the blower or fan to the outlet end of the pipes. The ground function as a heat sink absorbing the thermal energy given out by the transfer medium of air through heat transfer. Subsequently, the hot ambient air in tropical climate will be cooled down at EAHE outlet ends. In some instances, if the air temperature at the EAHE outlet is sufficiently low, the outlet air from the EAHE can be straightaway used for space cooling. Otherwise, it could be further cooled down by means of an external refrigeration unit. Therefore, EAHE reduced the cooling load and energy consumed

of the building in either case of direct cooling or pre-cooling (Wu, Wang and Zhu, 2007).

Generally, there are two type of EAHE system which are open or closed loop EAHE (Ozgener and Ozgener, 2011). Both open and closed loop EAHE have network of buried pipes connected to the inlet and outlet ends they differentiated from each other by the location of the inlet end. Open loop EAHE typically has an inlet shaft with filter located outside of the building and an outlet located inside the building. It is so called open loop EAHE because the system is open at the inlet end and takes in air from the outdoor as shown in Figure 1.3. Alternatively, a closed loop EAHE typically has both inlet and outlet ends located inside the building. It is so called closed loop EAHE because the buried pipes, inlet and outlet ends and the building space formed a closed system as referred to Figure 1.4. In this study, a closed loop EAHE with the network of buried pipes installed in open spaces (rather than beneath buildings) has been constructed for investigation.
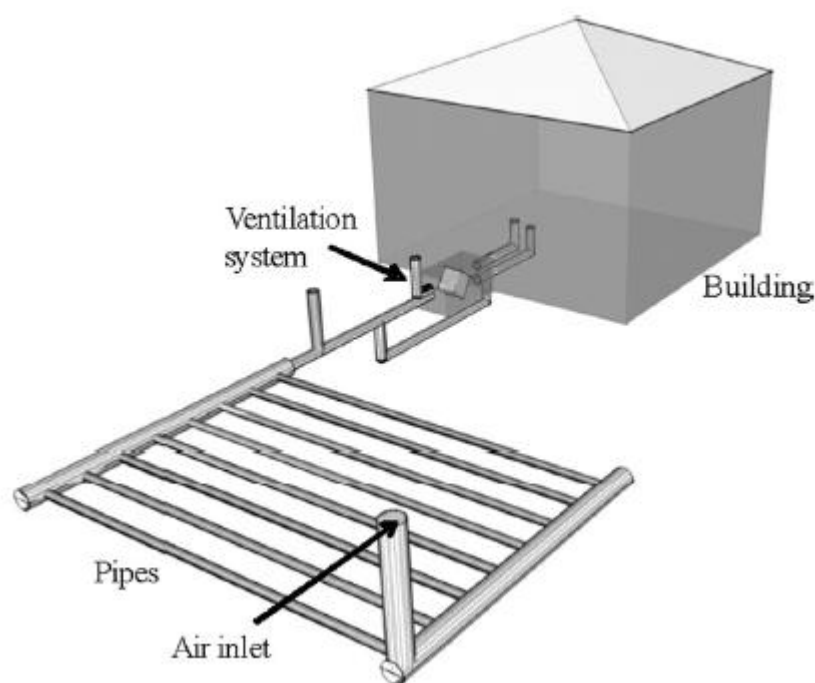
Figure 1.3: Open loop EAHE System (Peretti, et al., 2013)
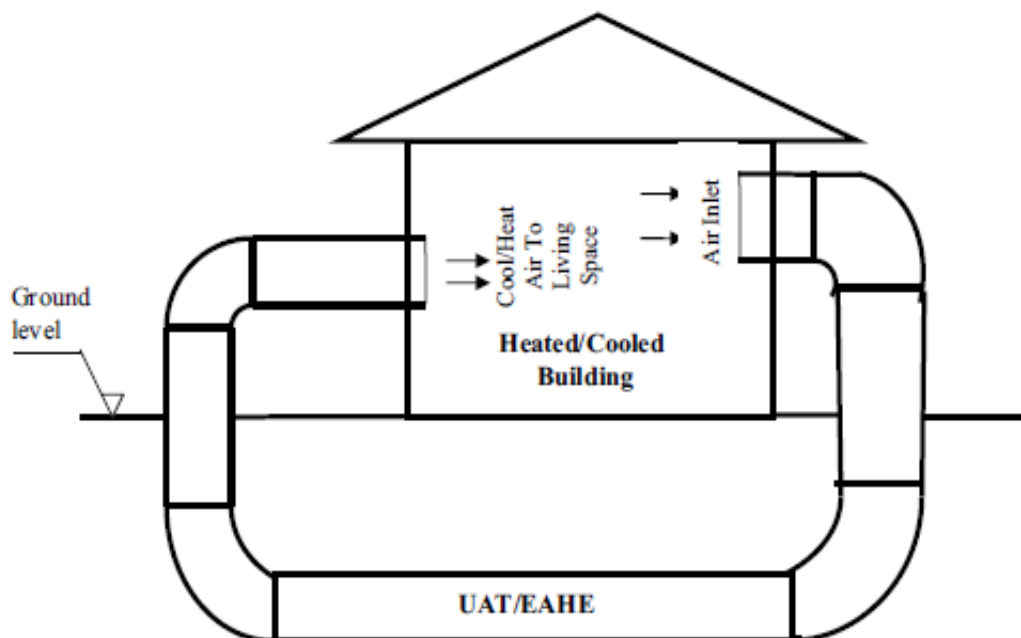
Figure 1.4: Closed loop EAHE System (Ozgener and Ozgener, 2011)

1.2   Problem Statements

This study intended to determine the potential of implementing Earth-to-Air Heat Exchangers (EAHE) in Malaysia as a sustainable option for the purpose of space cooling and air conditioning. It was shown that the cooling performance of several EAHE in other climates are greatly influenced by the ambient air temperature and undisturbed ground temperature where the pipe being buried. (Pretti, et al., 2013). The fact that this passive cooling technology (EAHE) lack of implementation data and records in Malaysia makes the evaluation process rather challenging.

The ground temperature at the depth where EAHE is buried does not always remain constant due to the heat transfer convection and radiation with the surrounding at the surface. By designing the depth of buried pipe as deep as possible will not solve this problem because of the increase in installation cost due to soil digging will not necessary be justified by the increase in cooling performance. Therefore, the main problem in this study was to determine the undisturbed ground temperature profile and suitable depth of ground for EAHE in Malaysia. One of the

feasible solutions to resolve this issue could be by conducting an on-site experimental measurement of ground temperature at various depth.

In general, the EAHE prototype shall be designed and built based on the cooling load imposed by the experimental room or space to be conditioned. It was crucial that cooling load to be known so that the EAHE designed would not be undersized or oversized in terms of cooling capacity. There are many methods available to determine the cooling load some of which as complicated as using computerized numerical solutions while other could be as simple as using empirical factor. Therefore, the next problem was to determine cooling load imposed by the experimental residential room with the chosen method before the EAHE prototype could be designed and built.

The optimization of the cooling performance of the EAHE depends greatly on its operating parameters such as pipe length, diameter, air flow rate and depth of ground (Wu, Wang and Zhu, 2007). Therefore, the next problem in this project was to design and built an EAHE prototype and to determine the optimum size of the prototype in terms of its pipe diameter and length. In addition, an exhaust fan has to be designed and built to provide the static pressure, air flow rate and velocity required by the prototype EAHE system. The process of fan design was also very important because the EAHE prototype should be well balanced in cooling and acoustics performances at the same time. Thus, another problem in this project was to design and fabricate the suitable exhaust fan using the available design methods.

Although there are plenty EAHEs in operation in Europe and other regions of the world, this technology was not yet being commercialized in Malaysia. The determination of the cooling performance and economic considerations of implementation were the foremost issues restraining the development of this technology in Malaysia. Therefore, the last problem in this project was to determine the experimental cooling performance of a designed and built EAHE prototype so as to access its feasibility of implementation in Malaysia.

1.3   Aim and Objectives

Based on the problems identified in the previous section, this project was carried out to resolve all these problems with the aim to access the feasibility of implementing EAHE in Malaysia. In short, the five (5) objectives that were to be achieved through this final year project include:

1. To determine the suitable depth for the installation of earth-to-air heat exchanger (EAHE) pipe by experimental measurement.
2. To determine the cooling load of the experimental residential room using Residential Load Factor (RLF) method proposed by ASHRAE.
3. To design and fabricate a centrifugal exhaust fan that can provide the static pressure, air flow rate and velocity required by the prototype EAHE system.
4. To design an EAHE prototype system in terms of pipe diameter and length to output the cooling capacity imposed by the experimental residential room's cooling load.
5. To analyse and evaluate the experimental cooling performance of the EAHE prototype system.

CHAPTER 2

LITERATURE REVIEW

2.1   Undisturbed Ground Temperature by Experiment Investigation

The undisturbed ground temperature is the main operating parameter during the EAHE design process. It was proposed that the undisturbed ground temperature will be affected by the depth of ground. Although the deeper into the ground the more constant the ground temperature, installing EAHE too deep will not be justified by the increase of installation cost. Therefore, finding the suitable depth of ground for the EAHE installation is very important during the design process.

In practice, most of the EAHE in operation was installed at a depth of 3 m to 4 m. Ghosal and Tiwari (2006) performed a parametric studies by conducting experiments in Delhi, India to illustrate the effects of operating parameters including the depth of ground on the thermal performance. This study has demonstrated that the cooling performance of the integrated EAHE increased with increasing depth of ground up to 4 m in a hot and dry climate as shown in Figure 2.1. However, this result might not be applicable in other region of the world with different climate. Pfafferott (2003) evaluated the energy efficiency with a standardized method of three EAHEs in Germany with the depth of pipe of 2-3 m, 2 m and 2.3 m below the ground.

Sanusi, Li and Zamri (2014) analysed the potential of EAHE in Malaysia in terms of ground temperature and ambient temperature. The ambient temperature, ground surface temperature, and ground temperature at the depth of 1 m, 2m, 3 m, 4

m and 5 m were measured during the first stage of the investigation. Then, soil temperature at the depth of 0.5 m, 1.0 m and 1.5 m were investigated for one year. The results of this study shown that at a depth of below 1 m, the soil temperature increases with depth up to 5 m. The annual amplitude or the fluctuation of the soil temperature decreases from 0.5 m to 1.0 m and then 1.5 m. The optimum depth of ground for EAHE installation obtained in this study was 1 m below the ground. At the depth of 1 m, the maximum differences between the outdoor ambient temperature and the soil temperature was determine to be about 7 ℃.
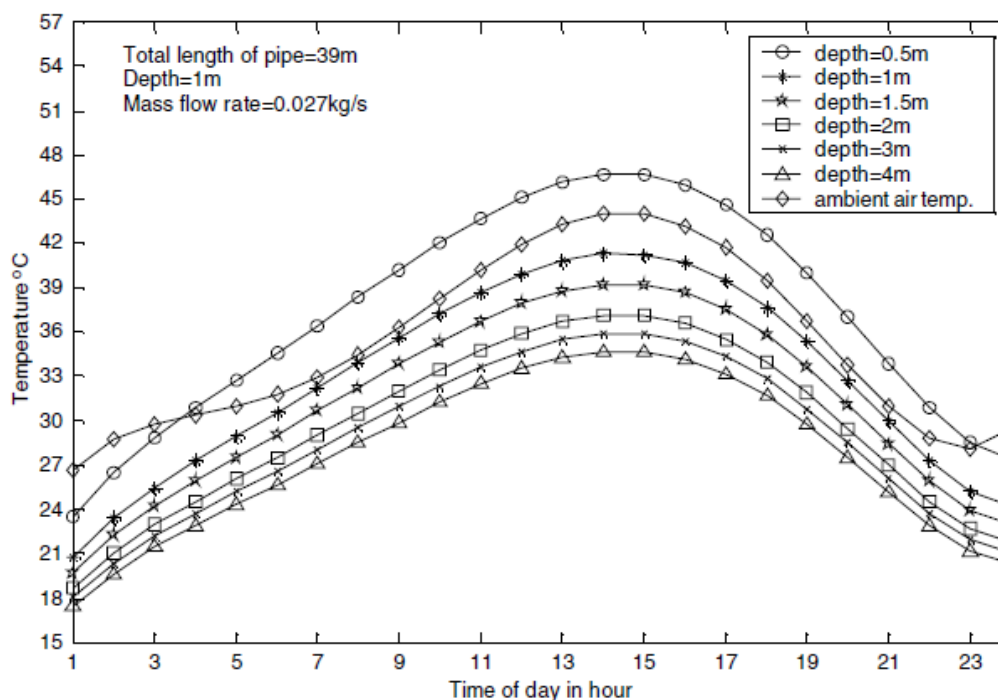
Figure 2.1: Effect of Depth of Ground on Indoor Air Temperature (Ghosal and Tiwari, 2006)

Another factor that is also affecting the undisturbed ground temperature is whether there is shading effect on the ground surface. In Malaysia, Nik, Kasran and Hassan (1986) shown that the soil temperature under shading such as forest were regularly lower than that of the open area by about 4 to 6 ℃. For open area, significant differences in soil temperature were observed at various depth (up to 30cm from the ground surface). It was also shown in this study that the soil temperature for open area shown high fluctuation at the depth of 5 cm. In other

words, the "shading effect" of the forest cover caused a lower soil temperature amplitude. Besides, the soil temperature decreased with depth in the open area whilst not obvious under forest. The presence of a "shading effect" was the most important modifying factor in soil temperature besides other factors such as slope and elevation as demonstrated in this research.

2.2   EAHE Pipe Diameter Selection

The pipe diameter is the most critical and important aspect in the design of EAHE system. This is because an oversizing EAHE system would not be economical as the system was not fully utilized the cooling capacity offered but cause the system to be over-cost. On the other hand, an undersized system would not be able to attain the required cooling capacity (heat rejection) imposed by the cooling load of the conditioned spaced.

Typical pipe diameters for the EAHE system are 10 cm to 30 cm but could be as large as 1 m in some cases for larger commercial building (Peretti, et al., 2013). By using software simulation it was shown that an increase in the pipe diameter results in a decrease in the difference between outlet air temperature and environment temperature for constant average air velocity. However, it was shown that with the increased of pipe diameter the cooling capacity of the EAHE system would also be increased which has an important role in EAHE design (Wu, Wang and Zhu, 2007).

However, one parametric study conducted in tropical climate (Thailand) had demonstrated that increasing pipe diameter, lengths and air velocity could improve the performance of EAHE system particularly on pipe diameter and air velocity. It was found out in this study that the Coefficient of Performance (COP) of the EAHE system could be improved or enlarged significantly with the increased of pipe diameter and air velocity. Increasing pipe diameter was found to have effect in reducing the air velocity through EAHE system and hence would also reduce the heat transfer rate but the cooling capacity was increased. Therefore, the average COP

would be higher, however, the outlet temperature would be higher as well. (Mongkon, et al., 2014).

2.3   EAHE Pipe Length Selection

It is important that the length of the EAHE to be sufficiently long so that outlet temperature could be as close to the ground temperature as possible which means a more complete heat transfer process could took place. It would be desirable if the pipe length could be made as long as possible so that the outlet temperature could be as low as possible, however, the additional cost might not be able to justifiable by the improvement in cooling performance.

A transient and implicit model developed by Wu, Wang and Zhu (2007) predicted that increasing the pipe length could increases the cooling capacity of the EAHE system. This numerical and computational mathematical model predictd that the longer the pipe length the lower the outlet temperature could be. The average outlet temperature obtained for three different pipe length obtained were 29.85℃ for 20 m pipe, 27.95 ℃ for 40 m and 26.65 ℃ for 60 m (Wu, Wang and Zhu, 2007). However, there would be no significant advantage in using EAHE with pipe length more than 70 m long and the exact optimum pipe length would mostly depends on local climate condition as reported in one literature review of EAHE cooling system (Peretti, et al., 2013).

2.4   Evaluation of Cooling Performance of EAHE in Different Climate

The cooling performance of the EAHE can be evaluated using a range of approaches depending requirements of the researchers. Generally, cooling performance could be evaluated with the specific cooling energy supply per annum, heat transfer NTU and h_{mean}, temperature ratio Θ, cooling capacity Q and coefficient of performance (or energy efficiency) COP of the EAHE system.

Mongkon, et al. (2014) evaluated the cooling performance of an EAHE system in the agriculture greenhouse under the tropical climate of Thailand. It was found in this study that the operating nature of the EAHE system could be divided into two periods: heating and cooling periods. The cooling period was from approximately 10 am to 5 pm with high inlet temperature. The maximum COP of this cooling period from the prediction of mathematical model was 2.41 whilst the actual COP attained was observed to be 1.9. The experimental setup of this study was as shown in Figure 2.5.
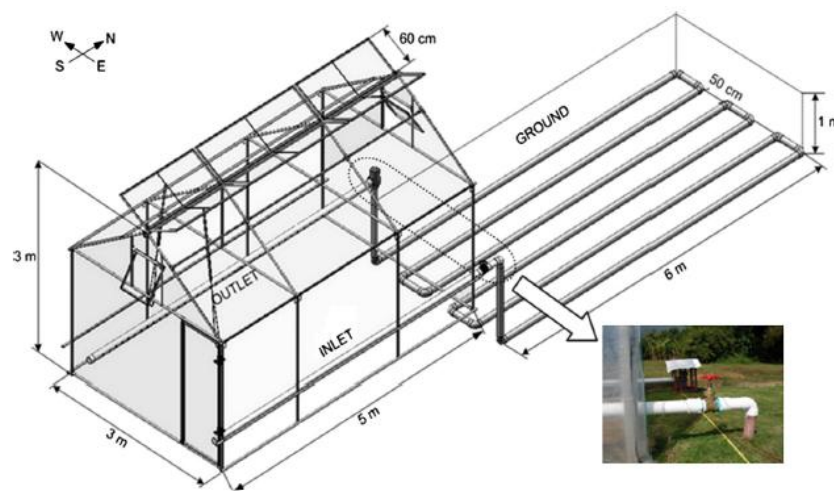
Figure 2.2: Experimental Setup of EAHE (Mongkon, et al., 2013)

Ghosal and Tiwari (2004) conducted an experimental validation to investigate the cooling and heating performance of an EAHE buried under the bare and covered (under greenhouse) surface at Delhi, India. This study reported 3-4℃ decrease of greenhouse air temperature in summer with integrated EAHE buried under bare surface. This study shows that EAHE pipes buried under covered surface reduces the cooling performance as compared to those under bare surface. The air temperature inside the greenhouse increased by 1-2℃ due to the increase of outlet temperature by 3-4℃ with EAHE buried under covered surface. This study demonstrated the evaluation of the cooling performance of EAHE based on thermal load leveling (TLL). It gives an indication about the temperature fluctuation inside the greenhouse. The highest TLL value obtained by the system was 0.67 at January.

Wu, Wang and Zhu (2007) evaluated the mathematical model of soil and EAHE against the experimental system installed in Guangzhou, Southern China. It was reported that a maximum daily cooling capacity of 74.6 kWh could be obtained from the EAHE system installed in the mentioned region of China. The maximum cooling capacity was achieved by pipe of 60 m in length and 0.3m in diameter. This study also shown that the cooling capacity or performance of the EAHE could be increased by increasing the length and the diameter of the buried pipe. The maximum cooling capacity achieved by the EAHE in this study was 74.6 kWh daily.
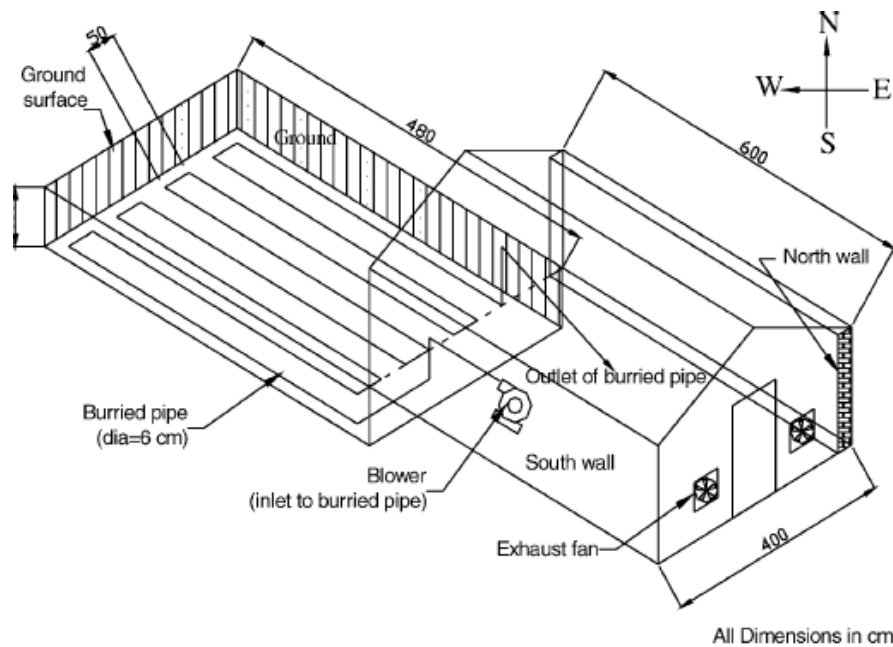
Figure 2.3: Experimental Setup of EAHE (Ghosal and Tiwari, 2003)

Al-Ajmi, Loveday and Hanby (2006) conducted a theoretical study on the cooling potential of EAHE for desert climate in Kuwait. Based on the theoretical model developed, it was concluded that the optimal EAHE configuration required a pipe length of 60 m, pipe diameter of 0.25 m, buried depth of 4 m, and air mass flow rate of 100 kg/h. This configuration when integrated to a 300 m^2 building was able to give a reduction of 2.8 ℃ when the ambient temperature was at the peak value of 45 ℃ in the summer. However, it was also concluded that the EAHE system alone was not sufficient to maintain the indoor temperature within comfort range. In other words, EAHE could reduce the cooling load but it must be combined with traditional air conditioning unit in order to be implemented in extreme desert climate.

Reimann (2007) has presented a paper of experimental investigation of CoolTek house in Melaka, Malaysia integrated with EAHE. There were no windows in the air-conditioned region of the CoolTek house as shown in the Figure 2.4. There was a solar chimney that expelled out the warm light air from the house and drained in ground cooled EAHE air from the two inlets at the floor. These two upper portion of EAHE pipes will be connected to a sub-soil chamber which then will be connected to the lower portion of the EAHE pipe at sub-soil depth. Then, a small fan was mounted in the solar chimney opening to mechanically drawn in cooled EAHE air and force expel air from the solar chimney. The EAHE outlet temperature was able to achieve a stable temperature of approximately 27.7 ℃ both at day and night time. This system was able to provide sufficient cooling capacity by reducing the sensible cooling load by 9.8%.
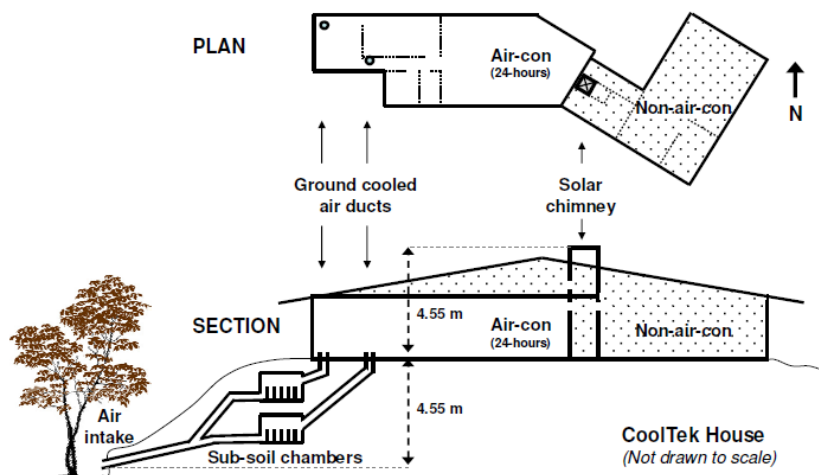
Figure 2.4: CoolTek house with integrated EAHE layout (Reimann, 2007)

CHAPTER 3

METHODOLOGY

3.1   Experimental Location and Setup

3.1.1   Experimental Location

The EAHE study has been conducted in University Tunku Abdul Rahman (UTAR) Lee Kong Chian Faculty of Engineering and Science (LKC FES) as shown in Figure 3.1. The coordinate location of the experiment site is 3°13'00.60'' N 101°43'57.01'' E. The exact location of the experiment site location is shows as the area within the blue circle in Figure 3.1.

Figure 3.1: Bird-eye view of experiment location through Google Maps (2015)

3.1.2 Experimental Residential Room

The experimental residential room is a small room that has a dimension of 2970mm (length), 4470mm (width) and 3230mm (height). The wall of this room was built with lightweight concrete and covered with clay roof tiles. This experimental residential room consists of a plastic door and an opened window area in default. The window area was later being covered with plywood to eliminate the heat gain through fenestration. Figure 3.2 and 3.3 show the room in different view point.

Figure 3.2: Experimental Residential Room View 1

Figure 3.3: Experimental Residential Room View 2

3.2 Measurement of Ground, Room and Environment Temperature

3.2.1 Preparation of the K-type Thermocouples

The undisturbed ground temperature, T_g at the depth of 0.5m, 1.0m, 1.5m and 2.0m was measured for 3 days. After cutting the thermocouples into desired length for each depth of ground, one of the end which left on the ground was marked with duct tape marking. This allows us to differentiate one thermocouple from another after all of them were buried into the same holes. Then, the hot junction of the thermocouples (the end buried into the ground) were also twisted together and shaped as shown in Figure 3.6.

Figure 3.4: Marking by Duct Tape for Thermocouples

Figure 3.5: Shaping of Hot Junction of the Thermocouple

3.2.2   Drilling of Hole by JKR Probe and Insertion of Thermocouples

Thermocouples were inserted into the ground to measure the ground temperature at different depth aforementioned. To drill a hole into the ground for the insertion of the thermocouples, an apparatus called JKR probe was borrowed from Civil Lab of UTAR. JKR probe is a tool that can be used to create a small hole on the ground deep into the desired depth up to 30 feet (9m).

The process of drilling a hole for the insertion of thermocouples began with the assembling of the JKR probe. The drilling head was connected to the metal rod along the screw thread. Next, the weight hammer was attached to the other end of the metal. After placing the assembly on the spot where hole was to be drilled, the weight hammer was lifted up and allowed to free fall to punch the metal rod by its inertia into the ground. This process of punching was continued until most of the length of metal rod has gone into the ground. Then, the weight hammer was removed temporary and connector was attached to allow another metal rod to join on the previous metal rod. The weight hammer was then re-attached and the process of punching the ground continued until the desired maximum depth of 2.0 m was reached.

Finally, K-type thermocouples that has been prepared for each depth was inserted into the ground one by one started from the deepest one to the shallowest one. Last but not least, the hole with thermocouple inserted were filled up with soil to ensure there was a direct contact of thermocouples with the soil at each depth.

Figure 3.6: JKR Probe

Figure 3.7: Hole Drilled by using JKR Probe

3.2.3 On-site Measurement of Ground, Room (before EAHE) and Environment Temperature

Before the cooling analysis and EAHE prototype design can be done, three temperature profiles were needed to be taken which are the ground, room and environment temperatures. These temperatures has been measured for three sunny days and the average temperature reading were obtained and used in the subsequent cooling load analysis and EAHE prototype design. For each day, temperatures were measured for every hour from 8am to 6pm, for a total of 11 hours.

The ground temperature at each depth of 0.5m, 1.0m, 1.5m and 2.0m were measured after the thermocouple has been inserted into the ground as described in Section 3.2.2 for three days. The room temperature profile before the installation of the EAHE was also taken for three days to determine the temperature profile of the room without the EAHE system. Then, this room temperature profile were compared to the room temperature profile with EAHE installed to evaluate the cooling performance of the system. Besides, the highest room temperature was also recorded which is needed in the cooling load analysis. Finally, the environment temperature was also measured for three days.

The instrument that was used to measure the temperatures was the infra-red thermometer (Model: TM-909AL) as shown in Figure 3.8. This infra-red

thermometer had been borrowed from the Mechatronics Laboratory of UTAR. By inserting the cold junction into the sockets of the infra-red thermometer and placing the hot junction to where temperature to be measured, the infra-red thermometer can capture the small potential difference between the hot and cold junctions. This potential difference is then shown as a digital output of temperature reading on the infra-red thermometer. Table 3.1 shows the technical specification of the K-type thermocouple when it is connected to the thermometer.

Figure 3.8: K-type/Infra-red Thermometer

Table 3.1: Technical Specification of K-type Thermocouple

Measurement Range	$-100℃$ to $1300℃$
Measurement Resolution	$0.1℃$
Measurement Accuracy	$\pm(1\% + 1℃)$

3.3   Cooling Load Analysis

Cooling load of the experimental residential room was calculated using Residential Load Factor (RLF) method as suggested by ASHRAE. This method is a simplified version of the more detailed Residential Heat Balance (RHB) method. However, this method could provide sufficient accuracy and especially useful in situation where detailed analysis is impractical.

3.3.1   Cooling Load due to Heat Gain through Opaque Surfaces

Heat gains through opaque surfaces such as walls, floor slabs ceiling and door can be caused by the difference of air temperature across these surfaces. Besides, heat gains through these surfaces could also because of solar gains which incident on the surfaces. The equation used to estimate the cooling load due to heat gains through opaque surfaces using RLF method are given as shown in below.

$$q_{opq} = A \times CF_{opq} \tag{3.1}$$

$$CF_{opq} = U(OF_t \Delta t + OF_b + OF_r DR) \tag{3.2}$$

where

q_{opq}	= opaque surface cooling load, Btu/h
A	= net surface area, ft^2
CF_{opq}	= surface cooling factor, Btu/h.ft^2
U	= construction U-factor, Btu/h ft^2 ^{o}F
Δt	= cooling design temperature difference, ^{o}F
OF_t, OF_b, OF_r	= opaque surface cooling factors
DR	= daily cooling range, ^{o}F

Figure 3.9 shows the opaque surface factors for different situation. These factors represent the construction specific physical characteristics associated with each surfaces. Figure 3.10 shows that roof solar absorptance, α_{roof}.

Surface Type	OF_t	OF_b, °F	OF_r
Ceiling or wall adjacent to vented attic	0.62	$25.7\,\alpha_{roof} - 8.1$	−0.19
Ceiling/roof assembly	1	$68.9\,\alpha_{roof} - 12.6$	−0.36
Wall (wood frame) or door with solar exposure	1	14.8	−0.36
Wall (wood frame) or door (shaded)	1	0	−0.36
Floor over ambient	1	0	−0.06
Floor over crawlspace	0.33	0	−0.28
Slab floor (see Slab Floor section)			

Figure 3.9: Opaque Surface Cooling Factor Coefficients (ASHRAE, 2009)

Material	Color			
	White	Light	Medium	Dark
Asphalt shingles	0.75	0.75	0.85	0.92
Tile	0.30	0.40	0.80	0.80
Metal	0.35	0.50	0.70	0.90
Elastomeric coating	0.30			

Figure 3.10: Roof Solar Absorptance (ASHRAE, 2009)

3.3.2 Cooling Load due to Infiltration/Ventilation

The cooling load as a result of ventilation and infiltration can be calculated based on equations shown below.

$$q_{vi} = C_s \left[Q_{vi} + (1 - \varepsilon_s) Q_{bal,hr} + Q_{bal,oth} \right] \Delta t \qquad (3.3)$$

where

q_{vi} = ventilation/infiltration cooling load, Btu/h

C_s = air sensible heat factor, 1.1 Btu/h cfm at sea level

Q_{vi} = combine infiltration/ventilation flow rate, cfm

ε_s = HRV/ERV sensible effectiveness

$Q_{bal,hr}$ = balanced ventilation flow rate via HRV/ERV equipment, cfm

[assumed $Q_{bal,hr} = 0$]

$Q_{bal,oth}$ = other balanced ventilation supply airflow rate, cfm

[assumed $Q_{bal,oth} = 0$]

Δt = cooling design temperature difference, °F

$$Q_{vi} = Q_v + \max\left(Q_{unbal}, Q_i + 0.5Q_{unbal}\right) \tag{3.4}$$

where

Q_{vi} = combine infiltration/ventilation flow rate, cfm

Q_v = required ventilation flow rate, cfm [assumed Q_v= 0 for single zone]

Q_{unbal} = unbalanced airflow rate, cfm [assumed Q_{unbal} = 0]

Q_i = infiltration leakage rate assuming no mechanical pressurization, cfm

Therefore

$$Q_{vi} = Q_i \tag{3.5}$$

while

$$Q_i = A_L \times IDF \tag{3.6}$$

where

A_L = building effective leakage area

IDF = infiltration driving force, cfm/in^2 (refer Figure 3.11)

$$A_L = A_{es} \times A_{ul} \tag{3.7}$$

where

A_{es} = building exposed surface area, ft^2

A_{ul} = unit leakage area factor, in^2/ft^2 (refer Figure 3.12)

$H,$	Heating Design Temperature, °F					Cooling Design Temperature, °F		
ft	−40	−20	0	20	40	85	95	105
8	1.40	1.27	1.14	1.01	0.88	0.41	0.48	0.55
10	1.57	1.41	1.25	1.09	0.92	0.43	0.52	0.61
12	1.75	1.55	1.36	1.16	0.97	0.45	0.55	0.66
14	1.92	1.70	1.47	1.24	1.02	0.47	0.59	0.71
16	2.10	1.84	1.58	1.32	1.06	0.48	0.62	0.76
18	2.27	1.98	1.69	1.40	1.11	0.50	0.66	0.82
20	2.45	2.12	1.80	1.48	1.15	0.52	0.69	0.87
22	2.62	2.27	1.91	1.55	1.20	0.54	0.73	0.92
24	2.80	2.41	2.02	1.63	1.24	0.55	0.76	0.98

Figure 3.11: Typical Values of IDF (ASHRAE, 2009)

Construction	Description	A_{ul} (in^2/ft^2)
Tight	Construction supervised by air-sealing specialist	0.01
Good	Carefully sealed construction by knowledgeable builder	0.02
Average	Typical current production housing	0.04
Leaky	Typical pre-1970 houses	0.08
Very leaky	Old houses in original condition	0.15

Figure 3.12: Unit Leakage Area Factor (ASHREA, 2009)

3.3.3   Cooling Load due to Internal Heat Gains

According to the ASHRAE Handbook-Fundamentals, the cooling load contributed by internal heat gains sources such as occupants, lighting and equipment (or appliances) can be estimated by the following equation. For the purpose of cooling load estimation for the EAHE design, it will be assumed that the room is occupied by two people throughout the whole day.

$$q_{ig} = 464 + 0.7A_{cf} + 75N_{oc} \tag{3.8}$$

where

q_{ig} = cooling load (sensible) due to internal heat gains, Btu/h

A_{cf} = conditioned floor area of building, ft^2

N_{oc} = number of occupants [assumed $N_{oc} = 2$]

3.4 EAHE Prototype Design

3.4.1 EAHE Prototype Design Strategy

The procedures involved in the designing of the EAHE prototype system was based on a trial-and-error approach. This is necessary because the requirement of static pressure of the fan depends on the pressure drop of the EAHE pipe. This pressure drop was only known after the pipe diameter and length of the EAHE prototype has been designed. However, the design of the pipe diameter and length required the mass flow rate and velocity of the fan that was going to supply to the system. Therefore, it forms a cycle and required a trial-and-error approach to design the EAHE prototype system.

3.4.2 Fan Design and Fabrication

The previous version of EAHE prototype system being designed have chosen axial exhaust fan to drive the air through the pipe of the system. However, axial fan used in the system lacks the static pressure to overcome the pressure loss of the pipe system required. For this reason, a centrifugal fan was designed and fabricated in this project.

A stand fan motor of rated power 50W has been used as the prime mover to drive the designed centrifugal fan impeller. The centrifugal fan casing and impeller was fabricated from hard-cardboard and plywood. These material were chosen to minimize the additional loading on the motor especially for the fan impeller that could be caused by its weight.

Since the suction inlet of the centrifugal exhaust fan was connected directly to the outlet end of the EAHE pipe system, it is reasonable to assume that the outlet air velocity of the EAHE pipe system to be equal to the suction inlet air velocity of the centrifugal exhaust fan. Therefore, we can set a design value for the outlet air velocity for the EAHE pipe system and let it equal to the suction inlet air velocity of the centrifugal fan to start the trial-and-error procedures.

As the air flow from the one end to the other, its velocity will dropped as a result of friction and losses. The common practise was to set the average velocity between the inlet and outlet value based on the ASHREA recommendation. This recommendation suggested certain maximum air velocity in the main and branch duct to avoid unnecessary acoustic problem, which is to control the sound and vibration of the system. Figure 3.13 shows the recommended air velocity in our project's case which is 2600 fpm or 13.6 m/s. Then, a higher value is set as the design value at the suction inlet of the centrifugal fan for example, 16 m/s so that an average velocity of about 13.6 m/s can be achieved in the EAHE pipe system. The following equation was used to calculate the average velocity of the EAHE pipe system.

$$V_{avg} = \frac{V_o + V_i}{2} = 13.6 \, \text{m/s (recommended)} \qquad (3.9)$$

where

V_{avg} = average velocity in the EAHE pipe system, m/s

V_o = outlet velocity of the EAHE system or suction inlet velocity of the fan, m/s

V_i = inlet velocity of the EAHE system

ASHRAE
Sound and Vibration Control

Table 3 - Maximum Recommended Duct Airflow Velocities Needed to Achieve Specified Acoustic Design Criteria				
		Maximum Airflow Velocity, fpm		
Main Duct Location	Design RC (N)	Rectangular Duct	Circular Duct	Increased Flow Circular vs Rectangular
In Shaft or above drywall ceiling	45	3,500	5,000	1.43
	35	2,500	3,500	1.40
	25	1,700	2,500	1.47
Above suspended acoustic ceiling	45	2,500	4,500	1.80
	35	1,750	3,000	1.71
	25	1,200	2,000	1.67
Duct located within occupied space	45	2,000	3,900	1.95
	35	1,450	2,600	1.79
	25	950	1,700	1.79

Notes:
1. Branch ducts should have airflow velocities of about 80% of the values listed.
2. Velocities in final runouts to outlets should be 50% of the values or less.
3. Elbows and other fittings can increase airflow noise substantially, depending on the type. Therefore, duct airflow velocities should be reduced accordingly.

Figure 3.13: Maximum Recommended Air Flow Velocity (ASHREA, 2009)

The centrifugal exhaust fan used in the EAHE prototype was designed based on a trial-and-error approach using Flow Simulation of SolidWorks. Those steps involved in the designing of the centrifugal exhaust fan were as listed below.

1. The impeller and casing of the centrifugal was first designed to give a trial value of air velocity, mass flow rate and static pressure.

2. The air velocity and mass flow rate parameters were used to design the optimum pipe diameter and length of the EAHE pipe system as shown in Section 3.4.3.

3. The EAHE pipe design determined from Step 2 was modelled in SolidWorks and simulated with the exhaust centrifugal fan.

4. The average velocity in the EAHE pipe as provided by the result of the simulation was compared with the recommended average velocity of 13.6 m/s.

5. If the average velocity acquired was less than the recommended value, then the process was repeated by altering the fan design to give a higher air velocity, mass flow rate and static pressure else the design will be finalized if the average velocity was almost equal and slightly higher than the recommended value.

3.4.3   Pipe Diameter and Length Selection of EAHE Prototype

The required pipe length of EAHE prototype was calculated for five different nominal diameters which were 1 in (25mm), 2 in (50mm), 3 in (80mm), 4 in (100mm) and 5 in (125 mm). By fixing the material of pipe as PVC and with the determined heat rejection rate from the cooling load analysis, the selection of which diameter of PVC pipe to be used was based on the shortest required pipe length because this will minimize the area of ground used. Figure 3.14 shows the Microsoft Excel Spreadsheet used for the calculation of required pipe length. Figure 3.15 is the catalogue of PVC pipe from ATKC e-Commerce Warehouse which shows the standard PVC pipe with grade and dimension available in the market.

The lowest grade with the thinnest pipe wall was selected for each of the different nominal diameters which were input into the Microsoft Excel Spreadsheet for the calculation of pipe length required. This is because the thinnest pipe wall will give the lowest possible conductive resistance associated with the pipe for each of the different nominal diameters. The heat transfer equations that were used to calculate the required pipe length for each of the different nominal diameters were listed in the following pages.

Inner diameter of pipe, Di	0.0577	m		Constant	Values	
Outer diameter of pipe, Do	0.0602	m		Specific heat of air, Cpa	1.005	kj/kg.K
Air velocity	13.2	m/s		Density of air, pa	1.205	kg/m3
Mass flow rate	0.04160	kg/s		Thermal conductivity of PVC, kp	0.19	W/m.K
				Themal conductivity of air, ka	0.0257	W/m.K
Reynold number, Re	58934			Dynamic viscosity of air, µa	0.000015573	m2/s
Friction factor, f	0.02019			Volume flow rate, Q	0.034520076	m3/s
Prantl number, Pr	0.61			In Re	10.9841702	
Nusselt number, Nu	110.24			Temperature difference, dTmax	8.3	C
Convective coefficient, ha	49.1014			Heat extraction, qdot	952	W
Rcond/L	0.03552	K/W				
Rconv/L	0.11234	K/W				
Rtotal/L	0.14786	K/W				
Length, L	16.9596	m				

Figure 3.14: Microsoft Excel Spreadsheet for Pipe Diameter and Length Selection

STANDARD				MS 762				MS 628								MS 762	
				Wall Thickness (MM)													
Normal Size		Outside Diameter (mm)		Class O		Class B (PN 6)		Class C (PN 9)		Class D (PN 12)		Class E (PN 15)				Class 7	
in	mm	Min	Max	Min	Max	Min	Max	Min	Max	Min	Max	Min	Max			Min	Max
1/2	15	21.2	21.5									1.7	2.1			3.7	4.3
3/4	20	26.6	26.9									1.9	2.5			3.9	4.5
1	25	33.4	33.7									2.2	2.7			4.5	5.2
1 1/4	32	42.1	42.4							2.2	2.7	2.7	3.2			4.8	5.5
1 1/2	40	48.1	48.4							2.5	3.0	3.1	3.7			5.1	5.9
2	50	60.2	60.5					2.5	3.0	3.1	3.7	3.9	4.5			5.5	6.3
2 1/2	65	75.0	75.3	1.8	2.2			3.0	3.5	3.9	4.5	4.8	5.5				
3	80	88.7	89.1	1.8	2.2	2.9	3.4	3.5	4.1	4.6	5.3	5.7	6.6				
4	100	114.1	114.5	2.3	2.8	3.4	4.0	4.5	5.2	6.0	6.9	7.3	8.4				
5	125	140.0	140.4	2.6	3.1	3.8	4.4	5.5	6.4	7.3	8.4	9.0	10.4				
6	155	168.0	168.5	3.1	3.7	4.5	5.2	6.6	7.6	8.8	10.2	10.8	12.5				
8	200	218.8	219.4	3.1	3.7	5.3	6.1	7.8	9.0	10.3	11.9	12.6	14.5				
10	250	272.6	273.4	3.1	3.7	6.6	7.6	9.7	11.2	12.8	14.8	15.7	18.1				
12	300	323.4	324.3	3.1	3.7	7.8	9.0	11.5	13.3	15.2	17.7	18.7	21.6				

STANDARD			Wall Thickness (MM)			
			JIS K 6741			
Normal Size	Outside Diameter (mm)		Type VU (AE) 6.0 BAR		Type VP (AW) 10.0 BAR	
mm	Min	Max	Min	Max	Min	Max
200	215.3	216.7	6.5	7.5	10.3	11.7
250	266.1	267.9	7.8	9.0	12.7	14.5
300	317.0	319.0	9.2	10.6	15.1	17.3

Figure 3.15: PVC Pipe Catalogue (ATKC e-Commerce Warehouse, 2015)

$$R_{conductive} = \frac{\ln(D_o / D_i)}{2 \times \pi \times L \times k_p} \qquad (3.10)$$

where

$R_{conductive}$ = conductive thermal resistance of the pipe, K/W

D_o = outer diameter of the pipe, m

D_i = inner diameter of the pipe, m

L = length of the pipe, m

k_p = thermal conductivity of the PVC pipe, W/m·K

It was assumed that fully developed turbulent flow of air was provided inside the ground pipe. The convective thermal resistance associated with the convection heat transfer between the air flowing in the ground pipe and the pipe inner surface can be expressed as Equation 3.11.

$$R_{convective} = \frac{1}{\pi \times D_i \times h_a \times L} \qquad (3.11)$$

where

$R_{convective}$ = convective thermal resistance from air to inner pipe surface, K/W

h_a = convective heat transfer coefficient of air, W/m^2 $\cdot$K

D_i = inner radius of the soil annulus/nominal radius of the ground pipe, m

L = length of the pipe, m

The convective heat transfer coefficient, h_a of the above formula can be calculated by the formula below provided that Nusselt number, Nu was known

$$h_a = Nu \times \frac{k_a}{D_i} \qquad (3.12)$$

where

h_a = convective heat transfer coefficient of air, W/m^2 $\cdot$K

Nu = Nusselt number

D_i = inner diameter of the ground pipe, m

k_a = thermal conductivity of the air, W/m $\cdot$K

The Nusselt number for a fully developed laminar and turbulent flow in a circular pipe can be obtained by a correlation valid over large Reynold number and Prantl number ranges as proposed by Gnielinski (Incopera, 2002). This correlation is valid for $0.5 \leq Pr \leq 2000$ and $300 \leq Re \leq 5\times 10^6$.

$$Nu = \frac{\left(\frac{f}{8}\right)(Re-1000)Pr}{1+12.7\left(\frac{f}{8}\right)^{0.5}(Pr^{2/3}-1)} \qquad (3.13)$$

where

Nu = Nusselt number

f = friction factor

Pr = Prandlt number

Re = Reynolds number

Friction factor appears in the above equation can be determined using Petukhov's relationship which is particularly valid for smooth pipe as shown in Equation 3.14.

$$f = (0.79 \ln \text{Re} - 1.64)^{-2} \tag{3.14}$$

where

f = friction factor
Re = Reynolds number

$$\text{Pr} = \frac{c_{pa} \times \mu}{k_a} \tag{3.15}$$

where

Pr = Prantl number
C_{pa} = specific heat capacity of air, J/kg·K
k_a = thermal conductivity of air, W/m·K

Reynolds number appear in the above equation can be determined by the following Equation 3.16.

$$\text{Re} = \frac{4 \dot{m}_a}{\pi \times D_i \times \mu} \tag{3.16}$$

where

Re = Reynolds number
D_i = inner diameter of the ground pipe, m
μ = dynamic viscosity of the air, kg/m s
$\dot{m}_a$ = mass flow rate of air, kg/s

$$\dot{m}_a = \frac{\rho \times \pi \times D_i^2 \times V_{avg}}{4} \tag{3.17}$$

where

$\overset{\bullet}{m}_a$ = mass flow rate of air, kg/s

ρ = density of air, kg/m^3

D_i = inner diameter of the ground pipe, m

V_{avg} = average velocity in the EAHE pipe system, m/s

The total thermal resistance, R_{total} associated with this heat transfer can be calculated by Equation 3.18.

$$R_{total} = R_{conductive} + R_{convective} \qquad (3.18)$$

where

R_{total} = total thermal resistance, K/W

$R_{convective}$ = convective thermal resistance between air flowing and pipe inner surface, K/W

$R_{conductive}$ = conductive thermal resistance of the pipe, K/W

Finally, the required length of the EAHE can be calculated as shown in Equation 3.19.

$$L = \frac{q_{load} \times R_{total}}{\Delta T_{room-ground}} \qquad (3.19)$$

where

L = length of the pipe, m

q_{load} = total heat gain of the room from cooling load analysis, W

$\Delta T_{room\text{-}ground}$ = temperature difference of room and ground temperature, K

R_{total} = total thermal resistance, K/W

3.5 **Data Collection and Analysis of the EAHE Prototype System**

3.5.1 **Data Collection of the EAHE Prototype System**

Data collection was conducted on the EAHE prototype system that was designed and built. The collection of temperature readings were accomplished by using K-type thermocouple and K-type/infra-red thermometer similar to Section 3.2. The following temperature readings were collected to conduct the data analysis

1. Room temperature, T_r
2. EAHE inlet temperature, T_i
3. EAHE outlet temperature, T_o
4. Room inlet temperature before insulation, T_i'
5. Room outlet temperature after insulation, T_o'
6. Environment temperature, $T_{environ}$

The exact location on the EAHE prototype system where each of the above mentioned temperature will be taken can be found in Figure 4.30 of Section 4.4 in which the full view of the finalized EAHE prototype system design was given.

3.5.2 **Temperature Data Analysis of the EAHE Prototype System**

After the collection of various temperature data of the EAHE prototype system has been conducted for three days, the collected data were then analysed. Each and every of the temperature profile mentioned in the previous section was analysed in terms of trends, peak values and temperature difference with another temperature profile to get a more in-depth understanding of the EAHE prototype system.

3.5.3   Heat Analysis of the EAHE Prototype System

There was heat rejected by the EAHE prototype along the pipe length buried underground. However, it was also important to analyse the portion heat rejected by the room over the total heat rejected by the EAHE prototype system. Besides, there was heat gained between the room inlet before insulation and EAHE inlet after insulation and between the EAHE outlet before insulation and room outlet after insulation due to imperfect insulation. Furthermore, there was also heat gained that was analysed.

Therefore, heat analysis was carried out on two different heat gained and rejected on four different segments of the EAHE prototype system which were listed here.

1. Heat gained by the insulation at the inlet segment. This heat gained based on the temperature difference between the room inlet temperature before insulation, T_i' and EAHE inlet temperature after insulation, T_i.

2. Heat gained by the insulation at the outlet segment. This heat gained was based on the temperature difference EAHE outlet temperature before insulation, T_o and room outlet temperature after insulation, T_o'

3. Heat rejected by the EAHE system. This heat rejected was based on the temperature difference between EAHE inlet after insulation, T_i and EAHE outlet temperature before insulation, T_o.

4. Heat rejected from the room. This heat rejected was based on the temperature difference between room inlet temperature before insulation, T_i' and room outlet temperature after insulation, T_o'.

The heat gained or rejected on different segment of the EAHE prototype can be defined as the heat transfer rate as a result of the temperature differences of that particular segment. The equation that expressed heat gained or rejected in terms of these variables can be expressed as shown in Equation 3.20.

$$q_{gained/rejected} = \dot{m}_a\, c_{pa} \Delta T \tag{3.20}$$

where

$q_{gained/rejected}$ = heat gained or rejected, W

c_{pa} = specific heat capacity of the air, J/kg K

$\dot{m}_a$ = mass flow rate of air, kg/s

ΔT = difference of temperature, K

3.5.4 Cooling Performance of EAHE Prototype

The first parameters that can be used to evaluate the cooling performance of a cooling system such as the EAHE prototype system under study is percentage of cooling effect. The percentage of cooling effect can be expressed as shown in Equation 3.21 and 3.22.

$$\% \text{ Reduction of Cooling Load (ideal)} = \frac{q_{rejected,EAHE}}{q_{load}} \times 100\% \qquad (3.21)$$

$$\% \text{ Reduction of Cooling Load (actual)} = \frac{q_{rejected,rooom}}{q_{load}} \times 100\% \qquad (3.22)$$

where

q_{load} = total cooling load, W

$q_{rejected,EAHE}$ = heat rejected by the EAHE prototype, W

$q_{rejected,rooom}$ = heat rejected from the room, W

The ideal percentage reduction of cooling load is the fraction of heat rejected by the EAHE over the total cooling load without the consideration of imperfect insulation. On the other hand, actual percentage reduction of cooling is the fraction of heat rejected from the room over the total cooling load with the consideration of imperfect insulation.

The second parameter that can be used to evaluate the cooling performance of an EAHE cooling system is called the EAHE efficiency. EAHE efficiency was defined as the fraction of heat rejected from the room to the total heat rejected by the EAHE into the ground. Therefore, EAHE efficiency can be calculated by the following Equation 3.23.

$$\eta_{EAHE} = \frac{q_{rejected,rooom}}{q_{rejected,EAHE}} \times 100\% \tag{3.23}$$

where

η_{EAHE} = EAHE efficiency

$q_{rejected,rooom}$ = heat rejected from the room, W

$q_{rejected,EAHE}$ = heat rejected by the EAHE prototype, W

Besides, the cooling performance of the EAHE prototype could also be evaluated by its energy efficiency which can be described by the dimensionless parameter called coefficient of performance (COP). Two different COPs of the EAHE prototype were analysed which are the COP_{ideal} and COP_{actual}. COP_{ideal} is the ideal coefficient of performance of the EAHE prototype without the consideration of imperfect insulation. It is defined as the ratio of heat rejected by the EAHE system over the power dissipated which is fan power. On the other hand, COP_{actual} actual coefficient of performance of the EAHE prototype with the consideration of imperfect insulation. It is defined as the ratio of heat rejected from the room over the power dissipated which is also the fan power. The equation for the calculation of COP_{ideal} and COP_{actual} are shown in Equation 3.24 and 3.25.

$$COP_{ideal} = \frac{q_{rejected,EAHE}}{P_{fan}} = \frac{\dot{m}_a c_{pa}(T_i - T_o)}{P_{fan}} \tag{3.24}$$

where

COP_{ideal} = ideal coefficient of performance of the EAHE

$q_{rejected,EAHE}$ = cooling capacity/heat transfer rate from the air to the ground, W

P_{fan} = rated power of the fan, W

$$COP_{actual} = \frac{q_{rejected,room}}{P_{fan}} = \frac{\dot{m}_a \, c_{pa} \left(T_i^{'} - T_o^{'} \right)}{P_{fan}}$$
(3.25)

where

COP_{actual} = actual coefficient of performance of the EAHE

$q_{rejected,room}$ = cooling capacity/heat transfer rate from the air to the ground, W

P_{fan} = rated power of the fan, W

CHAPTER 4

RESULTS AND DISCUSSION

4.1   Ground, Room and Environment Temperature Profile

Using the procedures mentioned in Section 3.2, the ground temperatures at different depth, room temperatures without EAHE system, and environment temperatures had been measured and recorded for 3 days continuously. The measurement had been conducted from 8am in the morning until 6pm in the evening each day. The full detail of these measurement for these three days had been tabulated in tables and presented in graphs in Appendix A.

In order to analyse the variation and trends of the ground, room and environment temperature profile captured, these temperature has been sum up and averaged to get the mean temperatures at the specific period of time. The mean daily ground, room and environment temperature obtained for these three days was tabulated and presented in Table 4.1. Besides, the mean daily ground, room and temperature for these three days was also plotted into a graph as shown in Figure 4.1.

From the temperature data obtained and shown in Figure 4.1 and 4.2, it could be observed that the room temperature mostly influenced by the environment temperature. As can be observed from the aforementioned figures, the room temperature increased as the environment temperature increased from morning 8am to afternoon 1pm. At 1pm in the afternoon, the environment temperatures reached its peak or maximum temperature.

Table 4.1: Mean Ground, Room and Environment Temperatures

| Description / Time	0.5 m (ºC)	1.0 m (ºC)	1.5 m (ºC)	2.0 m (ºC)	Room temperature, $T_r{'}$ (ºC)	Environment temperature, T_{env} (ºC)
08:00 AM	27.9	27.7	27.4	27.4	28.5	27.0
09:00 AM	27.8	27.6	27.3	27.3	29.8	27.8
10:00 AM	28.4	27.9	27.2	27.2	31.1	32.0
11:00 AM	29.2	28.1	27.1	27	32.3	34.0
12:00 PM	29.8	28.5	27.6	27.3	33.8	35.6
01:00 PM	30.6	28.8	28.3	27.9	35.2	37.0
02:00 PM	31.1	29.4	28.6	28.4	36.5	36.7
03:00 PM	31.5	30.5	29	28.7	37.3	36.2
04:00 PM	30.6	30.8	29.3	29.2	36.8	35.5
05:00 PM	29.5	29.9	29.5	29.4	35.9	33.5
06:00 PM	28.8	29.0	29.0	28.9	35.0	30.7
Max temperature	31.5	30.8	29.5	29.4	37.3	37.0
Min temperature	27.8	27.6	27.1	27.0	28.5	27.0
Temperature range	3.7	3.2	2.4	2.4	8.8	10.0
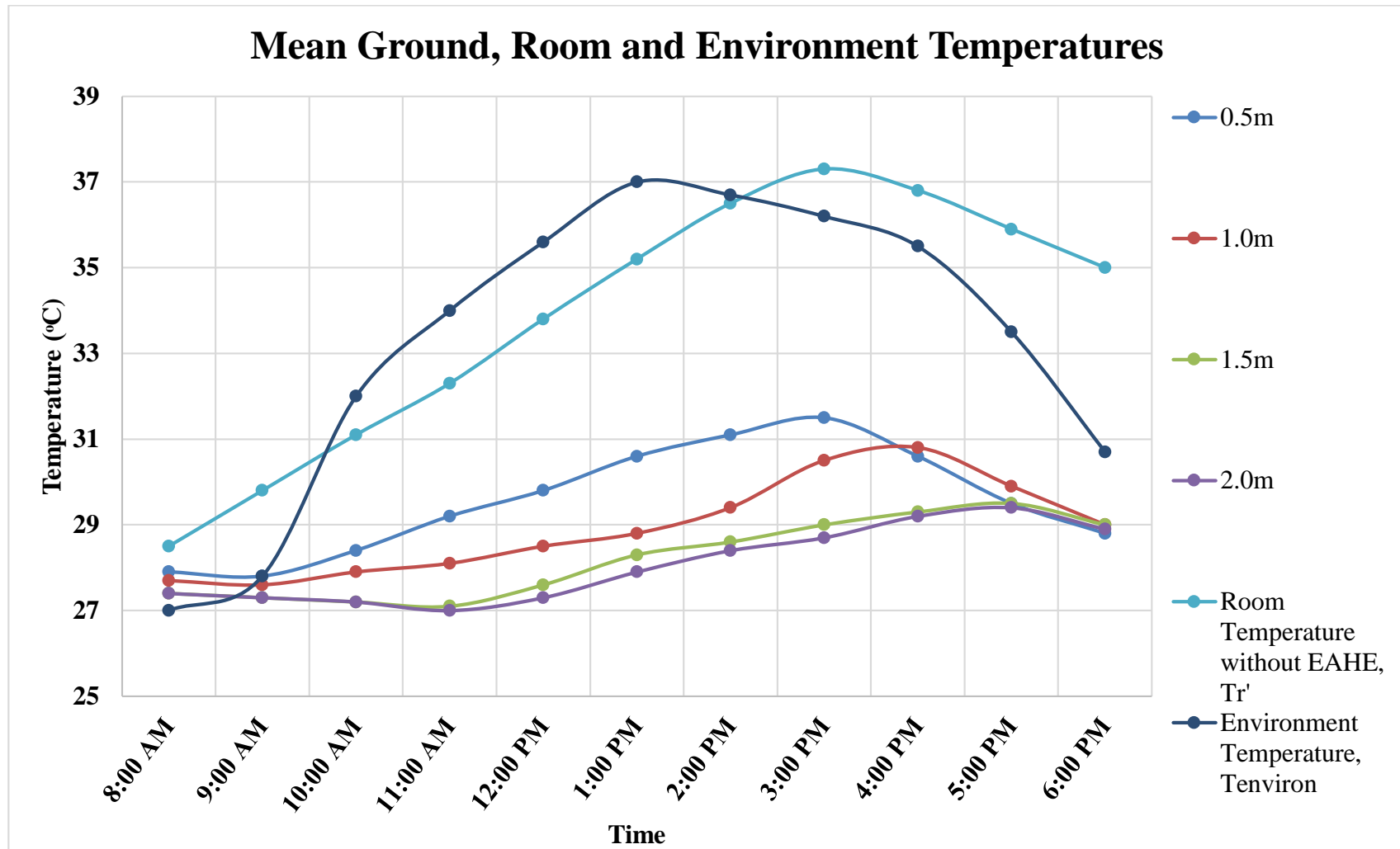
Figure 4.1: Mean Ground, Room and Environment Temperatures
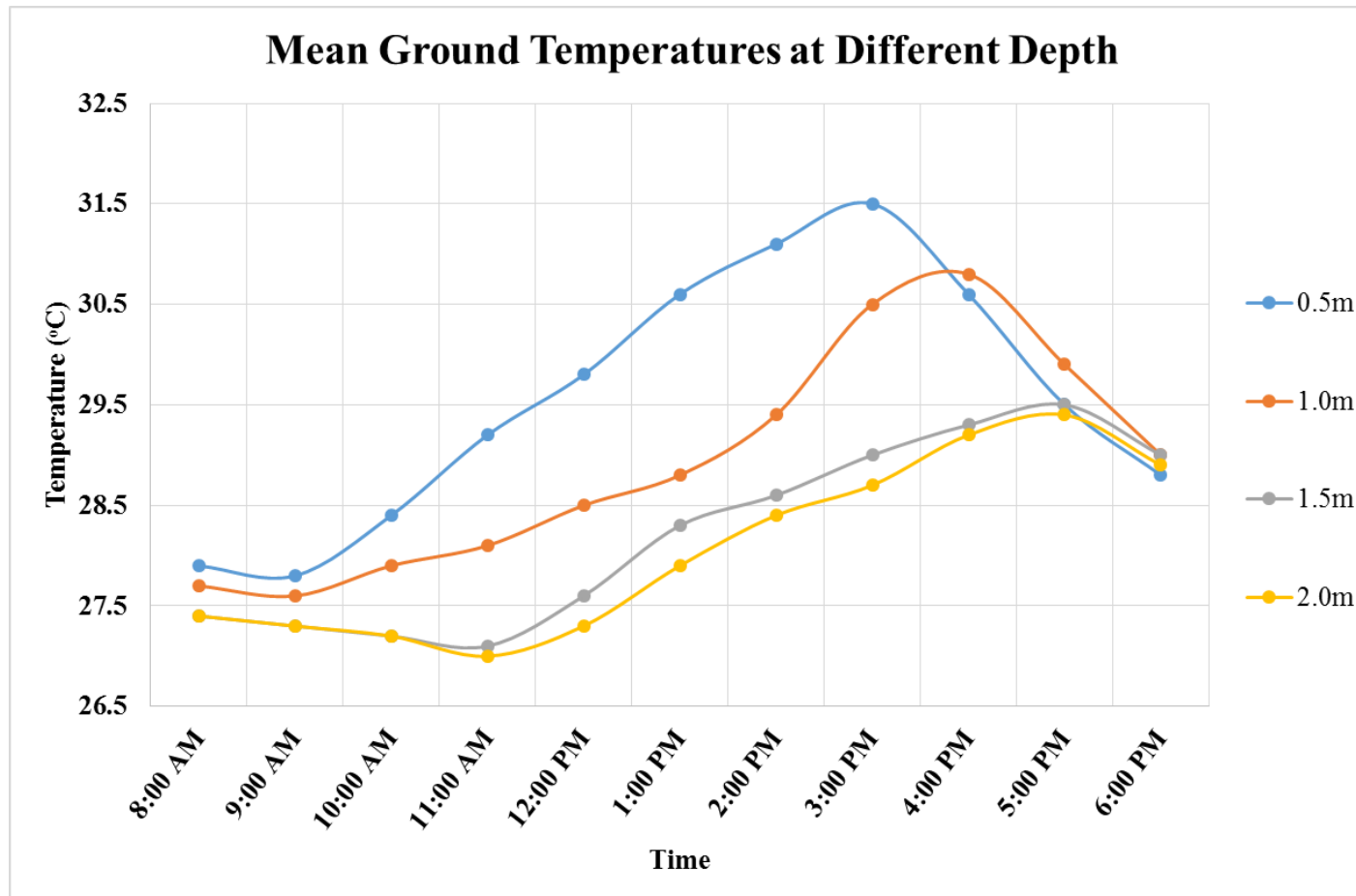
Figure 4.2: Mean Ground Temperatures at Different Depth

However, the room temperature did not reaches its maximum temperatures at this time of the day. The room temperature continued to increase until it reaches its peak temperature at about 3pm in the afternoon. Therefore, a delayed or shifted response can be observed from the variation of room temperature as compared to the environment temperature. Although there was a shift of response between room and environment temperature, both of these temperature decreased almost linearly together after the shift which is 4pm onwards.

This shift in the temperature response of the room temperature could be due to the heat accumulation in the room after its peak temperature. This is because the room lacks ventilation as compared to the environment in which heat could be carried away by the convective heat transfer of the ambient air. By relying solely on the conductive heat transfer through the room's wall, the room temperature only started to decrease after a period of time when the environment temperatures had already decreased. Therefore, it could be concluded that the room temperature without the EAHE was directly influenced by the environment temperature whereby both of them have the same temperature trends while the room temperature had a damped response from the environment temperature at late afternoon due to heat accumulation.

On the other hand, it could be observed that the ground temperature at all the depth decreases slightly in the morning from 8am to 9am in the morning until the minimum temperature attained. The minimum ground temperature at the depth of 0.5m, 1.0 m, 1.5 m and 2.0m were 27.8°C, 27.6°C, 27.1°C and 27.0°C respectively. After the minimum ground temperature had been attained, the ground temperature at each depth will start to increase with different rate of increment. As could be observed from the Figure 4.3 above, the rate of increment in ground temperature decreases as the depth of ground increased.

Beside this, the maximum temperature attained by the ground at different depth also decreased as the depth of ground increased as shown in Figure 4.2. The maximum ground temperature at the depth of 0.5m, 1.0 m, 1.5 m and 2.0m were 31.5°C, 30.8°C, 29.5°C and 29.4°C respectively. Besides, the mean daily range of the ground temperature was also decreased as the depth of ground increased as shown in

Table 4.1. After the maximum temperature had been attained, the ground temperature started to decrease at a different rate. The rate of decrement in temperature decreased as the depth of ground increases as shown in Figure 4.2 above. Therefore, it could be concluded that the fluctuation of ground temperature in terms of mean daily temperature range decreased as the depth of the ground increases. This could be due to the effect of fluctuating solar radiation on the ground (which contribute to the radiation heat gain) would decrease as we go deeper into the ground.

As can be observed in Figure 4.2, the difference of ground temperature at the depth of 1.5 m and 2.0 was very small during all the period of time. The difference in mean maximum and minimum temperature at the depth of 1.5 m and 2.0 m was just 0.1 ℃. Thus, it has been decided that the pipe of the EAHE prototype should be buried at the depth of 1.5m. The additional costing and time that might be incurred to go 0.5 m deeper cannot be justified by the very slight decrease of mean maximum and minimum temperature. In a nutshell, the ideal or suitable depth for the installation of the pipe of EAHE prototype by experimental measurement was 1.5 m.

4.2   Cooling Load Analysis with Residential Load Factor (RLF) Method

To determine the cooling load of the experimental residential room using the Residential Load Factor (RLF) method as described in Section 3.3, a site investigation has been conducted in order to find out the characteristics of the room. Figure 4.3 shows the detail dimensions of the room that had been measured and was drawn in technical drawing. All the dimensions shown in the drawing are in millimeters, mm.

The type of material and construction specification of the roof, walls, doors and wood covered window were investigated to determine the parameters needed for the cooling load analysis. Figures 4.4, 4.5, 4.6 and 4.7 show the pictures taken for the roof, wall, doors and wood covered window. The construction U-factor for the roof and wall has been determined from Figure 4.8 and 4.9 as suggested by previous student involved in the same project Tan Kien Seng. The construction U-factor of the

plastic door and wood covered windows was calculated based on the following formula.

$$U = \frac{k}{t} \qquad (4.1)$$

Where

U = construction U-factor, W/m^2 K

k = thermal conductivity of the component, W/m K

t = thickness of the component, m
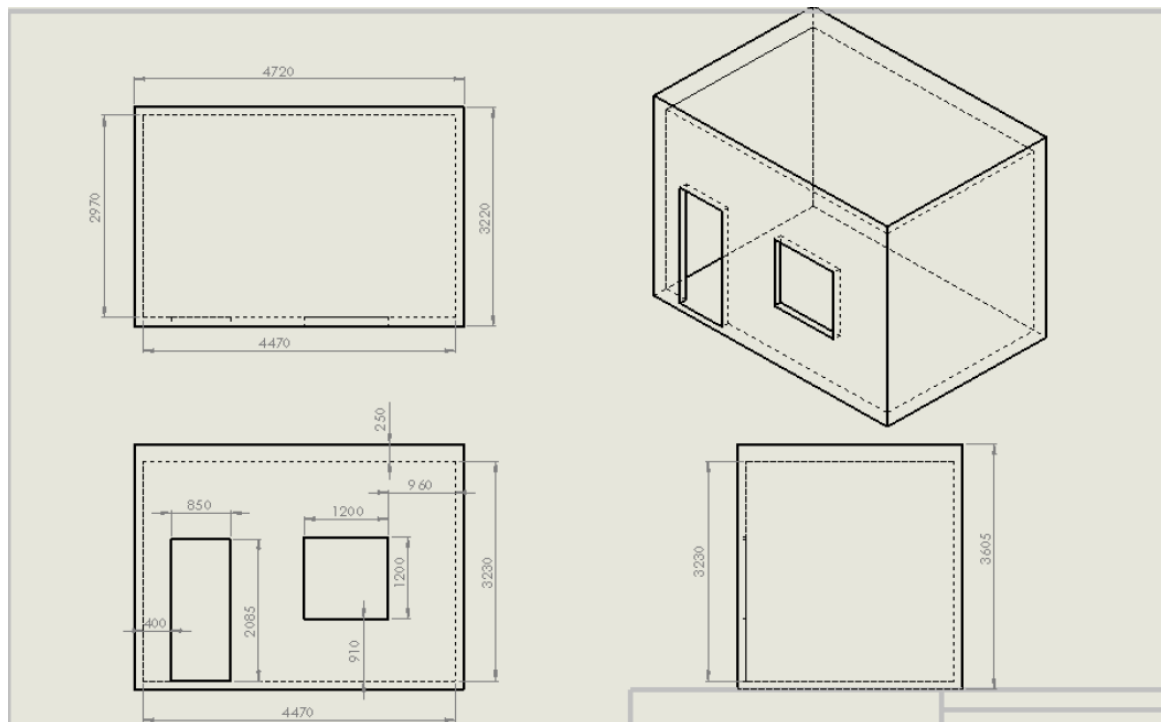
Figure 4.3: Detail Dimensions of the Experimental Residential Room

Figure 4.4: Roof tiles of the Experimental Residential Room

Figure 4.5: Concrete ceiling of the Experimental Residential Room

Figure 4.6: Walls of the Experimental Residential Room

Figure 4.7: Door and Wood Covered Window of the Experimental Residential Room

	TABLE 3 Roof Types			
	Layers (Inside to Outside)	**Description**	**U (Btu/h·ft² °F)**	**U (W/m² K)**
1	E0 A3 B25 E3 E2 A0	Steel deck with 3.33 in. (85 mm) insulation	0.080	0.454
2	E0 A3 BI4 E3 E2 A0	Steel deck with 5 in. (125 mm) insulation	0.055	0.312
3	E0 E5 E4 C12 E3 E2 A0	2 in. (50 mm) h.w. concrete deck with suspended ceiling	0.232	1.317
4	E0 E1 BI5 E4 B7 A0	Attic roof with 6 in. (150 mm) insulation	0.043	0.244
5	E0 BI4 C12 E3 E2 A0	5 in. (125 mm) insulation with 2 in. (50 mm) h.w. concrete deck	0.055	0.312
6	E0 C5 BI7 E3 E2 A0	4 in. (100 mm) h.w. concrete deck with 0.3 in. (8 mm) insulation	0.371	2.107
7	E0 B22 C12 E3 E2 C12 A0	1.67 in. (40 mm) insulation with 2 in. (50 mm) h.w. concrete RTS	0.138	0.784
8	E0 B16 C13 E3 E2 A0	0.15 in. (4 mm) insul. with 6 in. (150 mm) h.w. concrete deck	0.424	2.407
9	E0 E5 E4 B12 C14 E3 E2 A0	3 in. (75 mm) insul. with 4 in. (100 mm) l.w. conc. deck and susp. clg.	0.057	0.324
10	E0 E5 E4 C15 B16 E3 E2 A0	6 in. (150 mm) l.w. conc. dk with 0.15 in. (4 mm) ins. and susp. clg.	0.104	0.591
11	E0 C5 BI5 E3 E2 A0	4 in. (100 mm) h.w. concrete deck with 6 in. (150 mm) insulation	0.046	0.261

Figure 4.8: Roof Type of the Experimental Residential Room with Suggested U-factor (Tan, 2013)

TABLE 2
Wall Types

	Layers (Inside to Outside)	Description	U (Btu/h·ft²·°F)	U (W/m² K)
1	E0 A3 B1 B13 A3 A0	Steel siding with 4 in. (100 mm) insulation	0.066	0.375
2	E0 E1 B14 A1 A0	Frame wall with 5 in. (125 mm) insulation	0.055	0.312
3	E0 C3 B5 A6 A0	4 in. (100 mm) h.w. concrete block with 1 in. (25 mm) insulation	0.191	1.084
4	E0 E1 B6 C12 A0	2 in. (50 mm) insulation with 2 in. (50 mm) h.w. concrete	0.047	0.267
5	E0 A6 B21 C7 A0	1.36 in. (35 mm) insulation with 8 in. (200 mm) l.w. concrete block	0.129	0.732
6	E0 E1 B2 C5 A1 A0	1 in. (25 mm) insulation with 4 in. (100 mm) h.w. concrete	0.199	1.130
7	E0 A6 C5 B3 A3 A0	4 in. (100 mm) h.w. concrete with 2 in. (50 mm) insulation	0.122	0.693
8	E0 A2 C12 B5 A6 A0	Face brick and 2 in. (50 mm) h.w. concrete with 1 in. (25 mm) insul.	0.195	1.107
9	E0 A6 B15 B10 A0	6 in. (150 mm) insulation with 2 in. (50 mm) wood	0.042	0.238
10	E0 E1 C2 B5 A2 A0	4 in. (100 mm) l.w. conc. block with 1 in. (25 mm) insul. and face brick	0.155	0.880
11	E0 E1 C8 B6 A1 A0	8 in. (200 mm) h.w. concrete block with 2 in. (50 mm) insulation	0.109	0.619
12	E0 E1 B1 C10 A1 A0	8 in. (200 mm) h.w. concrete	0.339	1.925

Figure 4.9: Wall Type of the Experimental Residential Room with Suggested U-factor (Tan, 2013)

Table 4.2 summarizes the characteristics of the experimental residential room of this project along with the associated construction U-factors.

Table 4.2: Mean Daily Ground, Room and Environment Temperatures

Component	Description	Factors
Roof	Concrete flat roof with wood frame ceiling and light clay tiles	$U = 0.232 \text{ Btu/h} \cdot \text{ft}^2 \cdot °\text{C}$
Exterior walls	Light weight concrete block walls with three (3) walls exposed to solar radiation while one (1) was shaded.	$U = 0.155 \text{ Btu/h} \cdot \text{ft}^2 \cdot °\text{C}$
Door	Plastic door made of PVC of $k = 0.19 \text{ W/m} \cdot \text{K}$ with a thickness of $t = 27 \ mm$	$U = 1.24 \text{ Btu/h} \cdot \text{ft}^2 \cdot °\text{C}$
Window	Plywood wood, $k = 0.13 \text{ W/m} \cdot \text{K}$ covered window with a thickness of $t = 10 \text{ mm}$ that is being shaded from solar.	$U = 2.29 \text{ Btu/h} \cdot \text{ft}^2 \cdot °\text{C}$
Construction	Leaky	$A_{ul} = 0.08 \text{ in}^2/\text{ft}^2$

To define the indoor and outdoor design condition for the cooling system, the common practice suggested by the ASHRAE Handbook – Fundamental of 2009 has been taken into consideration. The typical practice for cooling purpose is to design the indoor conditions at 75 °F (23. 8 °C) to 85 °F (29.4 °C) dry bulb temperature as suggested by ASHRAE. As decided by our project team the design indoor temperature was set to 85 °F. On the other hand, the outdoor design conditions for cooling load calculation should be selected from the climate data of the specific location. The outdoor design temperature should be the mean maximum air temperature taken from the warmest month of Kuala Lumpur, Malaysia which is March. To find the daily range for the designed EAHE cooling system, the difference between the mean maximum and minimum temperatures of the warmest month should be used. Based on the climate data obtained from website of Malaysia Metrological Department, the mean maximum and minimum temperature of March are 35 °C (95 °F) 25 °C (77 °F) and as shown in Figure 4.10 and 4.11.

RAJAH 2B : PURATA SUHU MAXIMUM BULANAN (°C)
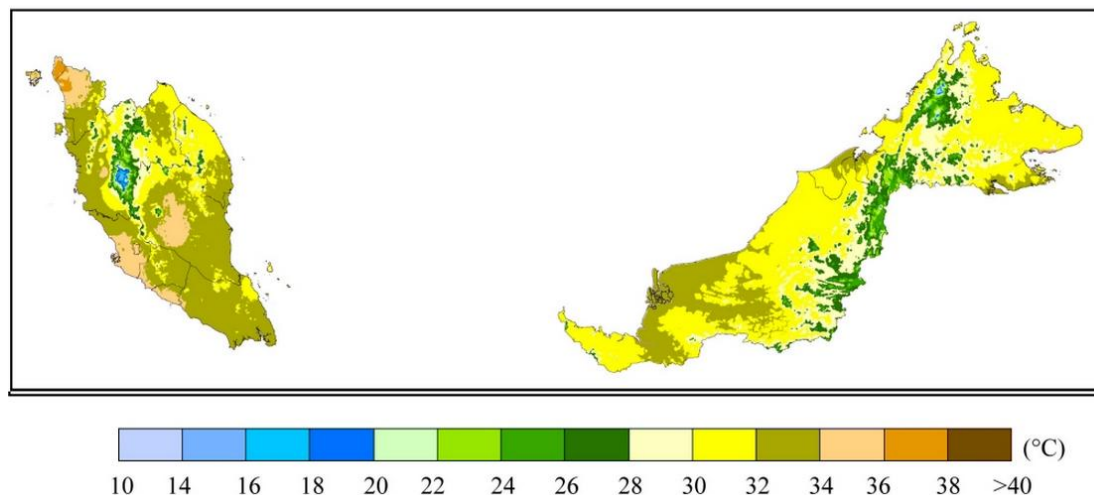
Figure 4.10: Mean Maximum Temperature Distribution of Malaysia at March (Malaysia Metrological Department, 2015)

RAJAH 2C : PURATA SUHU MINIMUM BULANAN (°C)
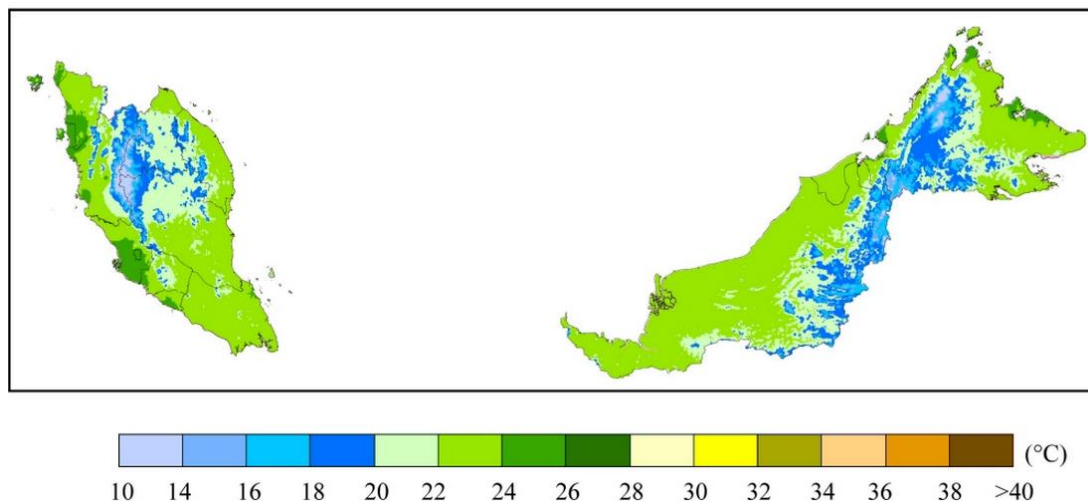
Figure 4.11: Mean Minimum Temperature Distribution of Malaysia at March (Malaysia Metrological Department, 2015)

Table 4.3 summarized the design condition of the EAHE cooling system for the experimental residential room. Table 4.4 summarized the experimental residential room component parameters for the calculation of cooling load using RLF method. Table 4.5 summarized the experimental residential room opaque surface factors.

Table 4.3: Experimental Residential Room Design Conditions

Item	Values
Latitude	3°13'00.60'' N
Indoor temperature	85 ℉
Outdoor temperature	95 ℉
Daily range	18 ℉
Wind speed	7.5 mph (suggested by ASHRAE)
Design Δt	10 ℉

Table 4.4: Experimental Residential Room Component Parameter

Component	Quantity
Ceiling	15.1984 m^2 = 163.94 ft^2
Door	1.7723 m^2 = 19.07 ft^2
Window	1.44 m^2 = 15.5 ft^2
Walls	30.412 m^2 = 327.35 ft^2 (unshaded)
	14.4381 m^2 = 155.41 ft^2 (shaded)
Floor area	15.1984 m^2 = 163.94 ft^2
Total exposed surface	63.2608 m^2 = 680.93 ft^2
Volume	42.8816 m^2 = 461.57 ft^2
Wall height	3.23 m = 10 ft

Table 4.5: Experimental Residential Room Opaque Surface Factors

Component	U-factor, Btu/h·ft·^{o}F	OF$_t$	OF$_b$	OF$_r$	CF$_{opq}$
Ceiling	0.232	1.0	14.96	-0.36	4.2874
Door	1.24	1.0	14.8	-0.36	22.7168
Window	2.29	1.0	14.8	-0.36	8.0608
Wall (unshaded)	0.155	1.0	14.8	-0.36	2.8396
Wall (shaded)	0.155	1.0	0	-0.36	8.0608

A sample calculation for the opaque surface cooling load due to heat gains at these opaque surfaces was given below.

For ceiling,

$$CF_{opq} = U(OF_t \Delta t + OF_b + OF_r DR)$$
$$= 0.232[1.0(10) + 14.96 + (-0.36 \times 18)]]$$
$$= 4.2874$$
$$q_{opq} = A \times CF_{opq}$$
$$= 163.6 \times 4.2874$$

$$= 701.41 \, \text{Btu/h}$$

For door,

$$CF_{opq} = U(OF_t \Delta t + OF_b + OF_r DR)$$
$$= 1.24[1.0(10) + 14.8 + (-0.36 \times 18)]]$$
$$= 22.7168$$

$$q_{opq} = A \times CF_{opq}$$
$$= 19.08 \times 22.7168$$
$$= 433.44 \, \text{Btu/h}$$

For window,

$$CF_{opq} = U(OF_t \Delta t + OF_b + OF_r DR)$$
$$= 2.29[1.0(10) + 0 + (-0.36 \times 18)]]$$
$$= 8.0608$$

$$q_{opq} = A \times CF_{opq}$$
$$= 15.5 \times 8.0608$$
$$= 124.94 \, \text{Btu/h}$$

For wall (unshaded)

$$CF_{opq} = U(OF_t \Delta t + OF_b + OF_r DR)$$
$$= 0.155[1.0(10) + 14.8 + (-0.36 \times 18)]]$$
$$= 2.8396$$

$$q_{opq} = A \times CF_{opq}$$
$$= 327.35 \times 2.8396$$
$$= 929.54 \, \text{Btu/h}$$

For wall (shaded),

$$CF_{opq} = U(OF_t \Delta t + OF_b + OF_r DR)$$
$$= 0.155[1.0(10) + 0 + (-0.36 \times 18)]]$$
$$= 0.5456$$

$$q_{opq} = A \times CF_{opq}$$
$$= 155.41 \times 0.5456$$
$$= 84.79 \, \text{Btu/h}$$

Total opaque surfaces cooling load, $q_{opq,total}$

$$q_{opq,total} = 701.41 + 433.44 + 124.94 + 84.79 = 2,274.12 \, \text{Btu/h}$$

A sample calculation for the infiltration/ventilation cooling load that was contributing to the total cooling load was given below. Since there was no ventilator in the experimental residential room, therefore we have assumed that

$$Q_{vi} = Q_i$$

Building total exposed area, $A_{es} = 680.93 \, \text{ft}^2$

Unit leakage area factor, $A_{ul} = 0.04 \, \text{cfm/in}^2$ (according to Figure 3.12)

Thus,

$$A_L = A_{es} \times A_{ul}$$
$$= 680.93 \times 0.08$$
$$= 54.47 \, \text{cfm}$$

Infiltration driving force, IDF = 0.41 (according to Figure 3.11)

Thus,

$$Q_i = A_L \times IDF$$
$$= 54.47 \times 0.41$$
$$= 22.33 \, \text{cfm}$$

$$Q_{vi} = Q_i = 22.33 \, \text{cfm}$$

Ventilation/infiltration cooling load, q_{vi}

$$q_{vi} = C_s [Q_{vi} + (1 - \varepsilon_s)Q_{bal,hr} + Q_{bal,oth}]\Delta t$$
$$= 1.1[22.33 + (1 - \varepsilon_s)0 + 0]10$$
$$= 245.63 \text{ Btu/h}$$

A sample calculation for the cooling load due to internal heat gains that was contributing to the total cooling load was given below. For the purpose of cooling load estimation for the EAHE design, it will be assumed that the room is occupied by two people throughout the whole day.

Cooling load due to internal heat gains, q_{ig}

$$q_{ig} = 464 + 0.7A_{cf} + 75N_{oc}$$
$$= 464 + 0.7(163.94) + 75(2)$$
$$728.76 \text{ Btu/h}$$

Table 4.6 shows the cooling load contributed by opaque surfaces, infiltration/ventilation and internal heat gains along with the total cooling load. The total cooling load as calculated and tabulated in Table 4.5 was 952 W. To sum up, the cooling load of the experimental residential room as determined by using Residential Load Factor (RLF) method was 952 W.

Table 4.6: Experimental Residential Room Cooling Loads

Component	Cooling Load, Btu/h
Opaque surfaces	2,274.12 Btu/h
Infiltration/ventilation	245.63 Btu/h
Internal gain	728.76 Btu/h
Total Cooling Load	$\mathbf{3,248.51 \text{ Btu/h} = 952 \text{ W}}$

4.3   EAHE Prototype Design

4.3.1   Fan Design and Fabrication

Three most important parameters to be determined in the design of centrifugal exhaust fan for the EAHE prototype was the mass flow rate, suction velocity and static pressure. The mass flow rate and velocity at the suction inlet of the centrifugal exhaust fan was required as an input parameter during the designing of pipe diameter and length for the EAHE prototype system. Based on the designed pipe diameter and length, the pressure drop of the EAHE pipe layout must not exceed the static pressure provided by the designed centrifugal exhaust fan as well.

Figure 4.12 shows the solid modelling of the finalized centrifugal exhaust fan in SolidWorks. Figure 4.13 and 4.14 shows the impeller and casing of the finalized centrifugal exhaust fan in solid modelling. Figure 4.15 shows the actual appearance of the fabricated centrifugal exhaust fan. Figure 4.16 shows the fan impeller of the fabricated centrifugal exhaust fan. Figure 4.17 shows the casing of the fabricated centrifugal exhaust fan. Figure 4.18 shows the supporting structure of the fabricated centrifugal exhaust fan.

Figure 4.12: Finalized Centrifugal Exhaust Fan in Solid Modelling
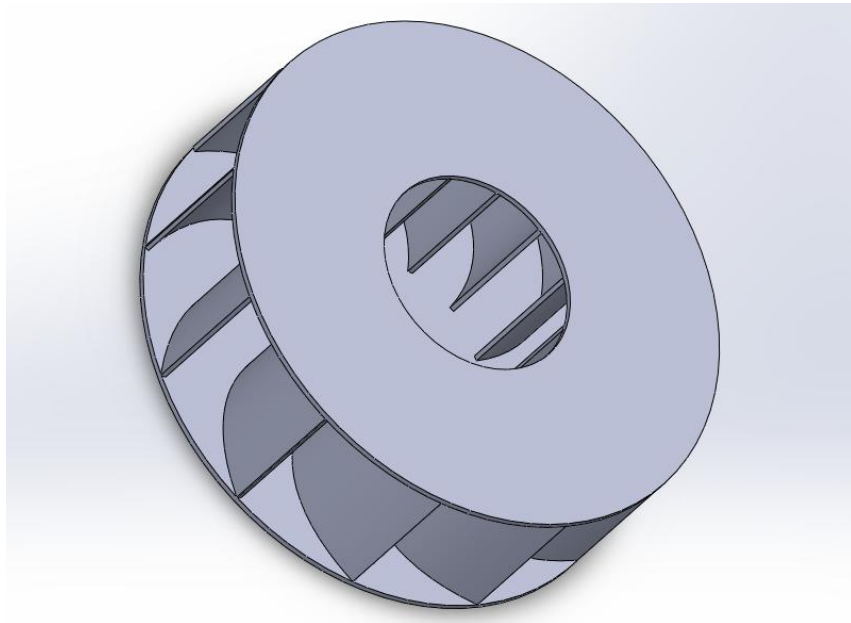
Figure 4.13: Impeller of Finalized Centrifugal Exhaust Fan in Solid Modelling
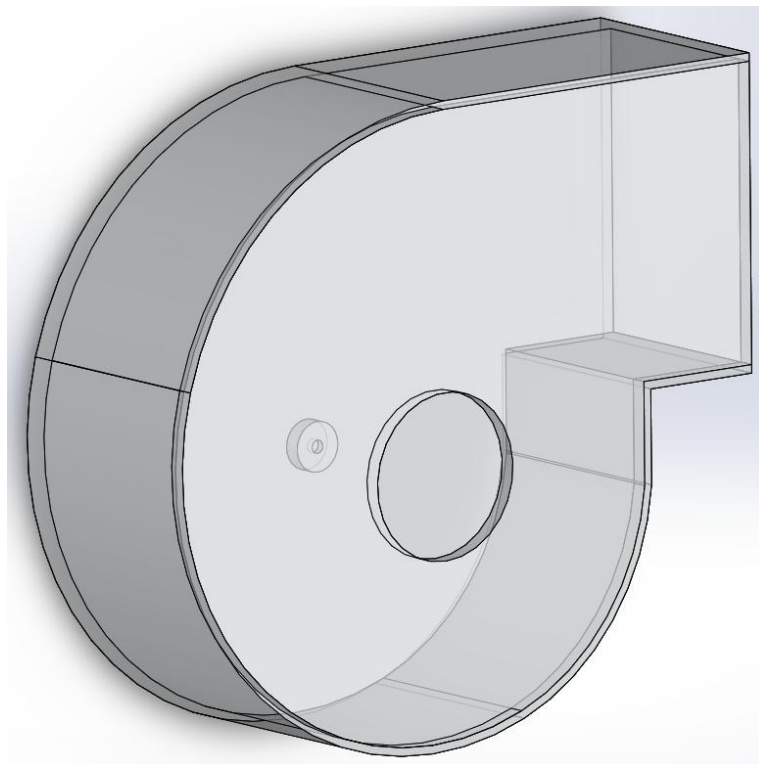
Figure 4.14: Casing of Finalized Centrifugal Exhaust Fan in Solid Modelling
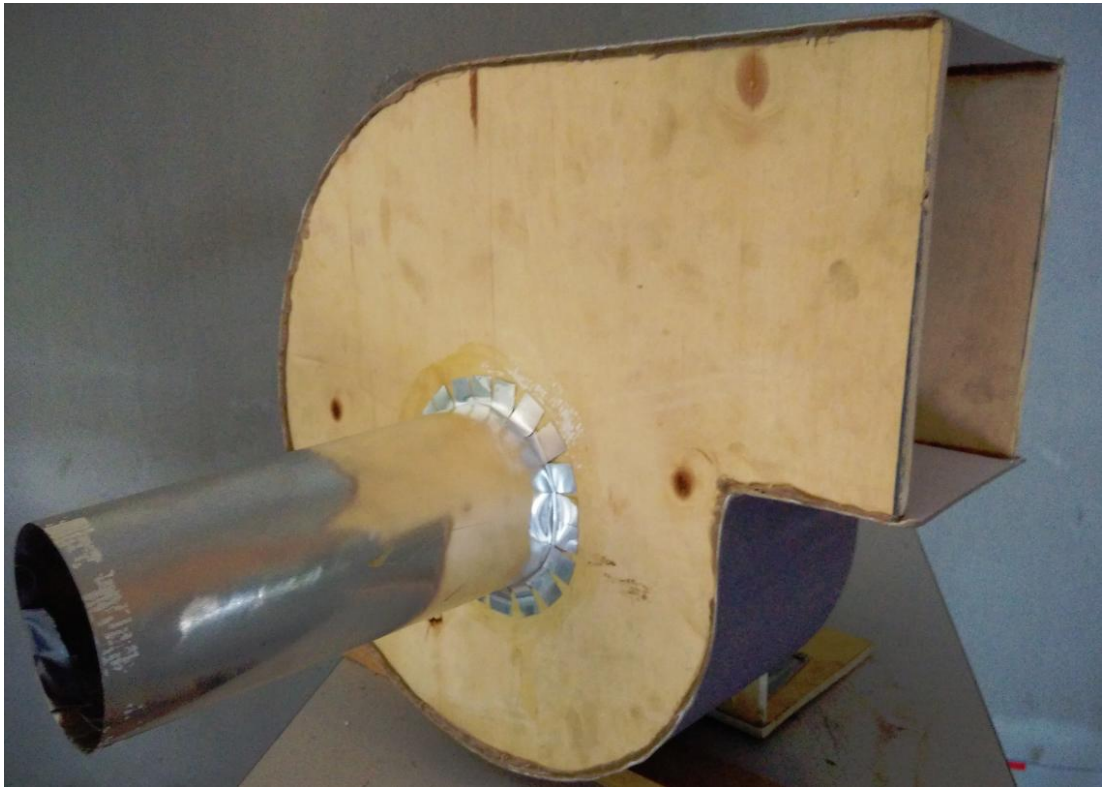
Figure 4.15: Actual Appearance of the Fabricated Centrifugal Exhaust Fan
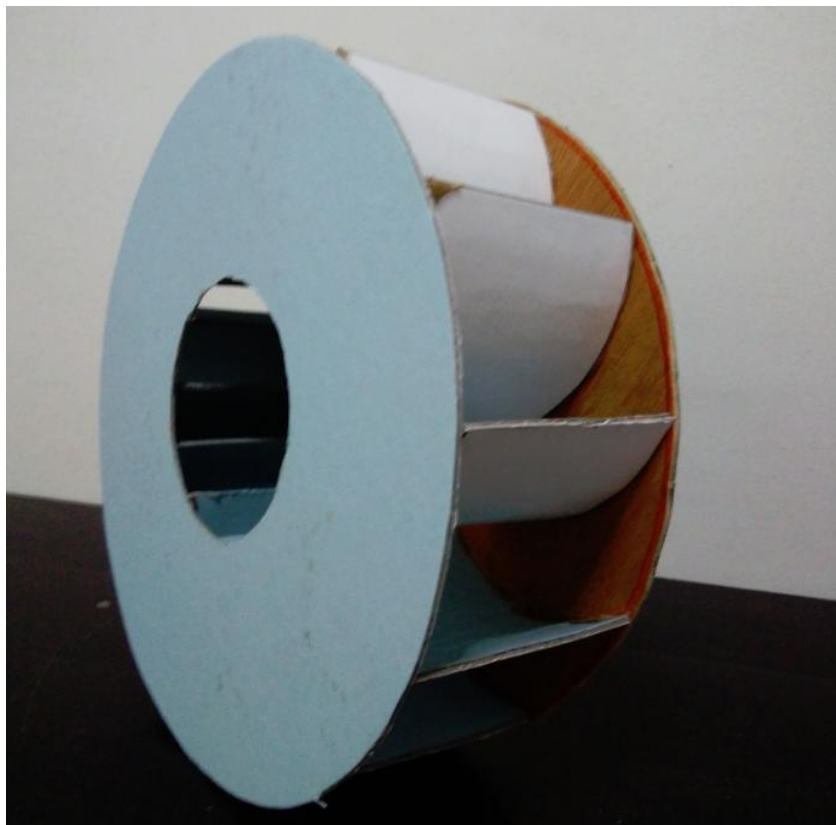
Figure 4.16: Impeller of the Fabricated Centrifugal Exhaust Fan
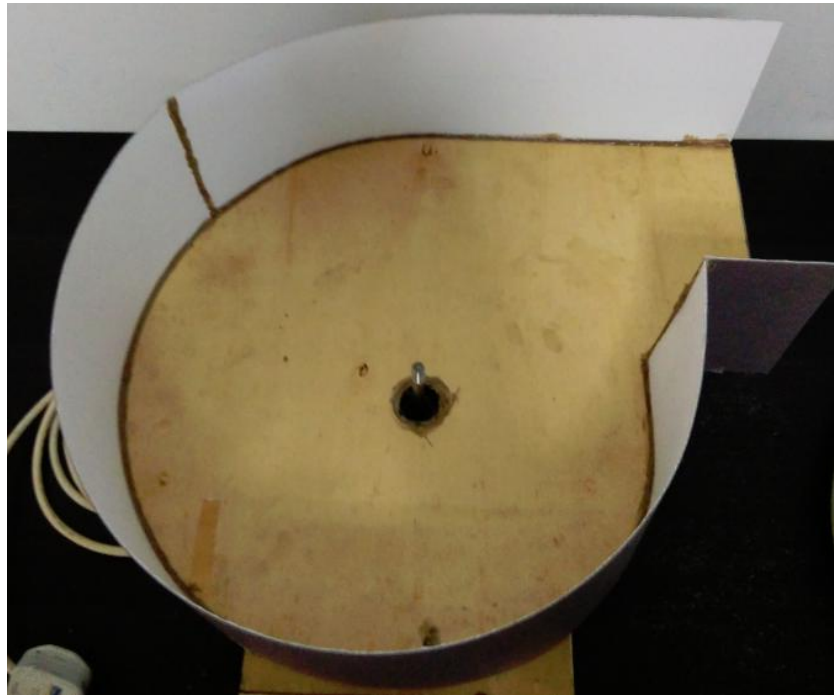
Figure 4.17: Casing/Housing of the Fabricated Centrifugal Exhaust Fan

Figure 4.18: Supporting Structure of the Fabricated Centrifugal Exhaust Fan

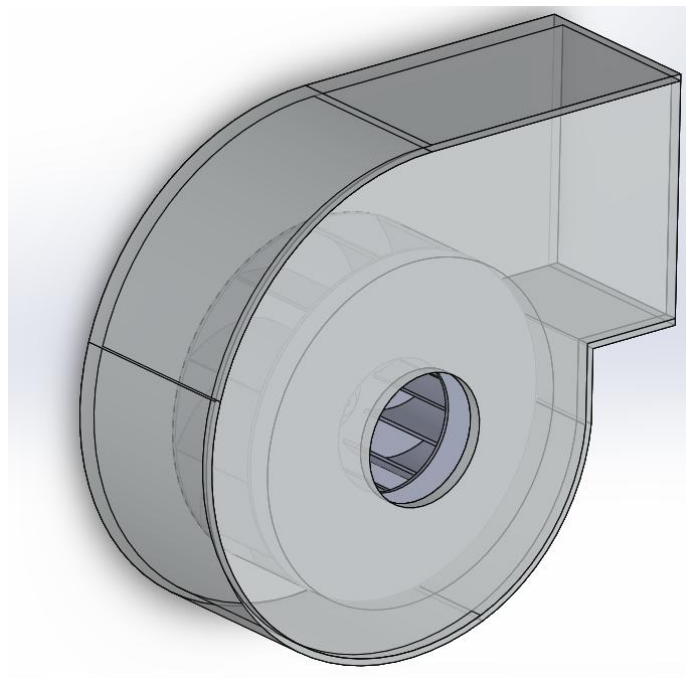The finalized design of the centrifugal exhaust fan was simulated in Flow Simulation of SolidWorks and tested experimentally after it was fabricated to determine and verify some of its important specifications. The finalized design of the centrifugal exhaust fan has the following specification as shown in Table 4.7. Note that the static pressure of the centrifugal exhaust fan could not be determined experimentally because the testing equipment was not available in UTAR. Figure 4.19 shows that the suction velocity of the centrifugal exhaust fan was being tested using an anemometer. Since the diameter of suction opening of the centrifugal fan was known, the mass flow rate can be calculated based on the determined suction velocity.

$$\overset{\bullet}{m}_a = \frac{\rho \times \pi \times D^2_{opening} \times V_{suction}}{4} \tag{4.2}$$

where

$\overset{\bullet}{m}_a$ = mass flow rate of the centrifugal fan, kg/s

$D^2_{opening}$ = diameter of suction opening, m

$V_{suction}$ = suction velocity of centrifugal fan, m/s

For simulated result,

$V_{suction}$ = 17.1 m/s

$D_{opening}$ = 100 mm = 0.1 m

Thus,

$$\overset{\bullet}{m}_a = \frac{\rho \times \pi \times D^2_{opening} \times V_{suction}}{4}$$

$$= \frac{1.205 \times \pi \times 0.10^2 \times 17.1}{4}$$

$$= 0.16186 \text{ kg/s}$$

For experimental result,

$$V_{suction} = 16.5 \text{ m/s}$$

$$D_{opening} = 100 \text{ mm} = 0.1 \text{ m}$$

Thus,

$$\dot{m}_a = \frac{\rho \times \pi \times D^2_{opening} \times V_{suction}}{4}$$

$$= \frac{1.205 \times \pi \times 0.1^2 \times 16.5}{4}$$

$$= 0.15618 \text{ kg/s}$$

The percentage difference of the simulation and experimental value for suction velocity and mass flow rate could be calculated.

$$\% \text{ Difference of Velocity} = \frac{|17.1 - 16.5|}{16.5} \times 100 \% = 3.64 \%$$

$$\% \text{ Difference of Mass Flow Rate} = \frac{|0.16186 - 0.15618|}{0.15618} \times 100 \% = 3.64 \%$$

Table 4.7: Specification of Designed Centrifugal Exhaust Fan

Component	Simulation value	Experimental value
Suction velocity	17.1 m/s	16.5 m/s
Mass flow rate	0.16186 kg/s	0.15618 kg/s
Static Pressure	263 Pa	NA

Figure 4.19: Determination of Experimental Suction Velocity by Anemometer

Figure 4.20 shows the simulation results of the velocity flow trajectory inside the centrifugal exhaust fan. Figure 4.21 shows the simulation results of the pressure flow trajectory inside the centrifugal exhaust fan. Figure 4.22 shows the simulation result of velocity cut plot of the centrifugal exhaust fan at the suction inlet which is showing the suction inlet velocity. Figure 4.23 shows the simulation result of relative pressure of the centrifugal exhaust fan at the suction inlet which is showing the static pressure provided by the fan.
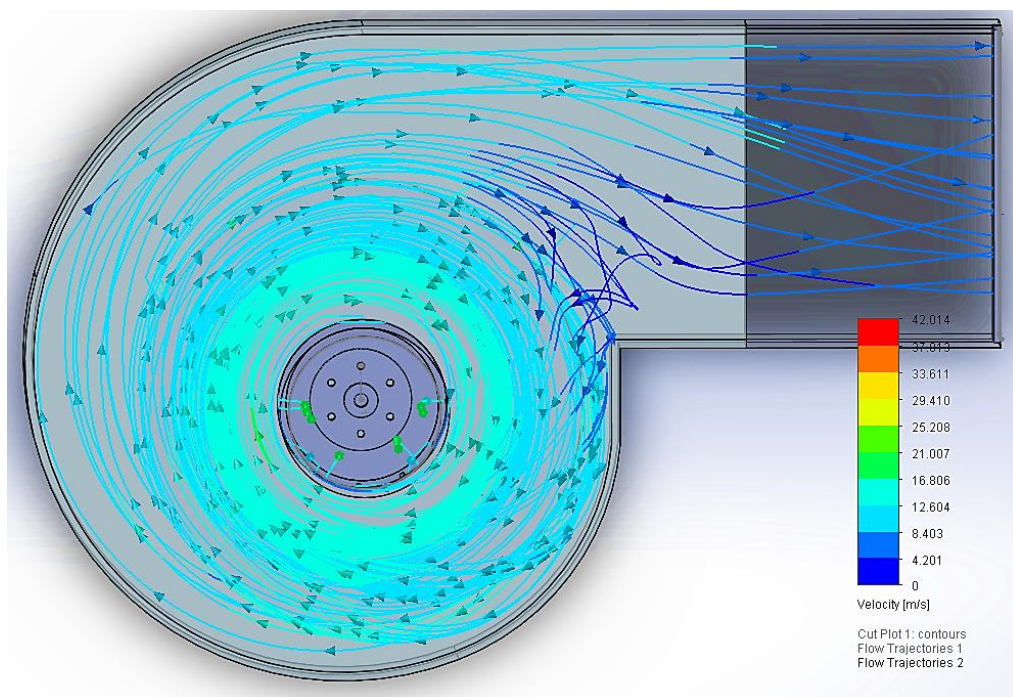
Figure 4.20: Velocity Flow Trajectory in Flow Simulation
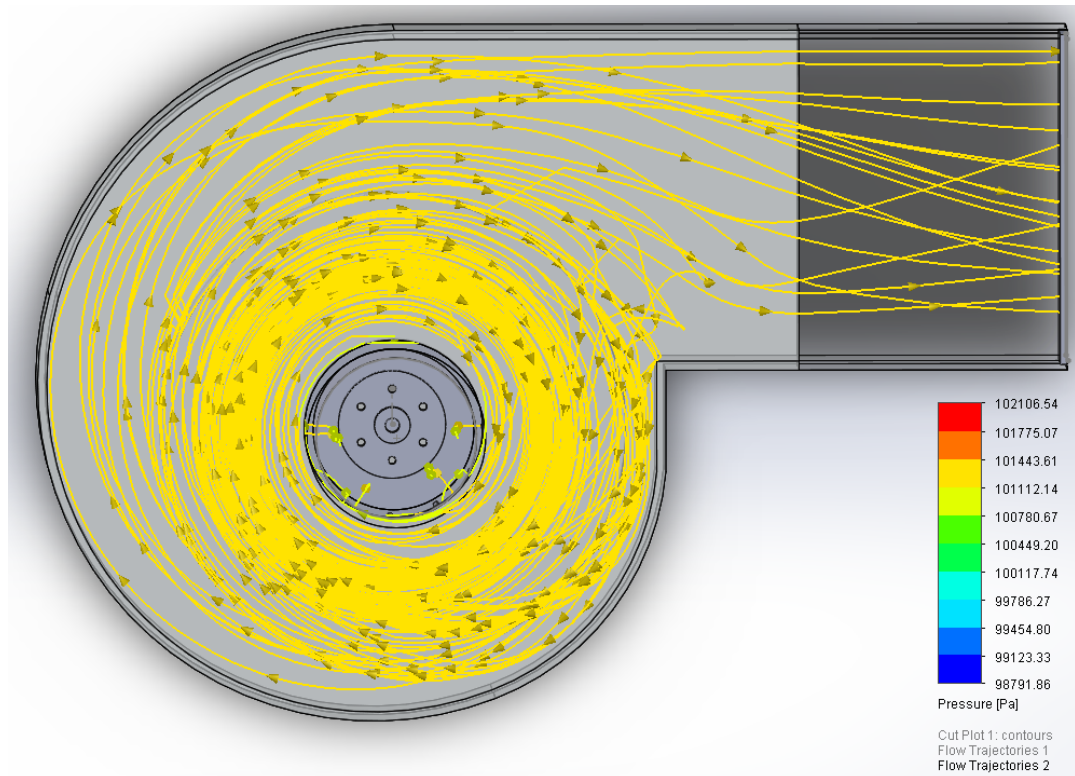
Figure 4.21: Pressure Flow Trajectory in Flow Simulation
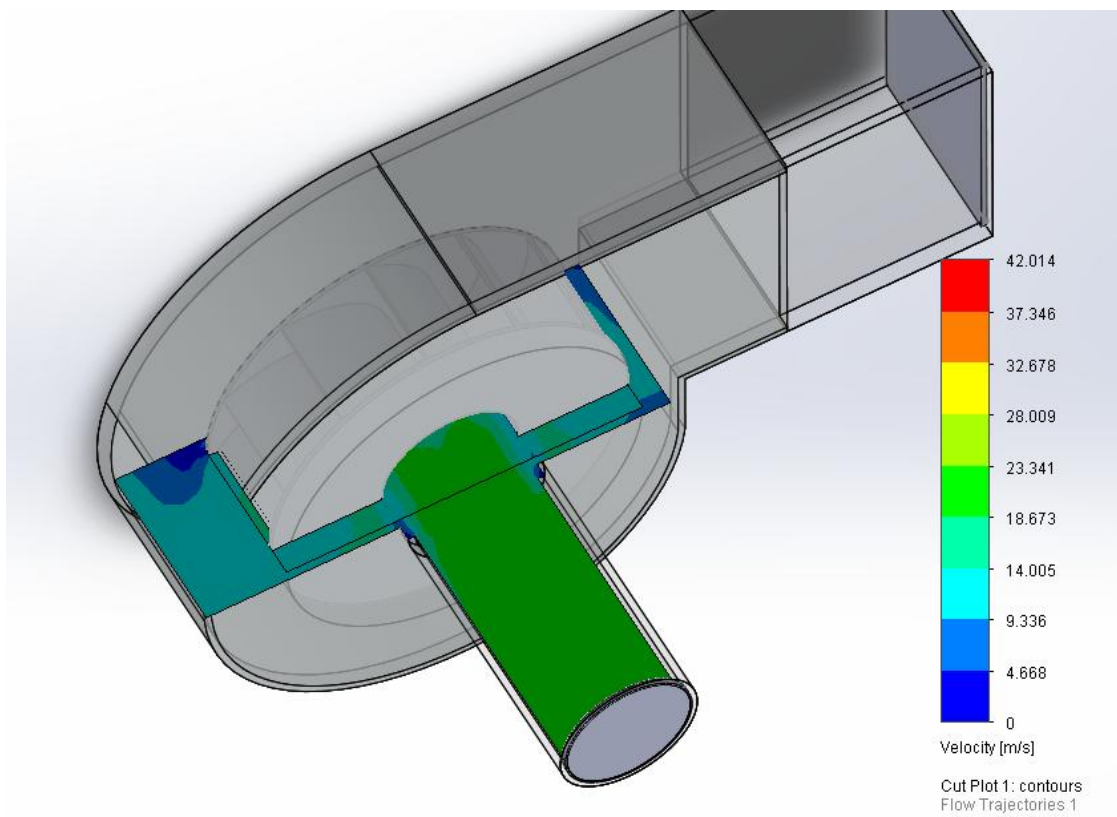
Figure 4.22: Velocity Cut Plot in Flow Simulation
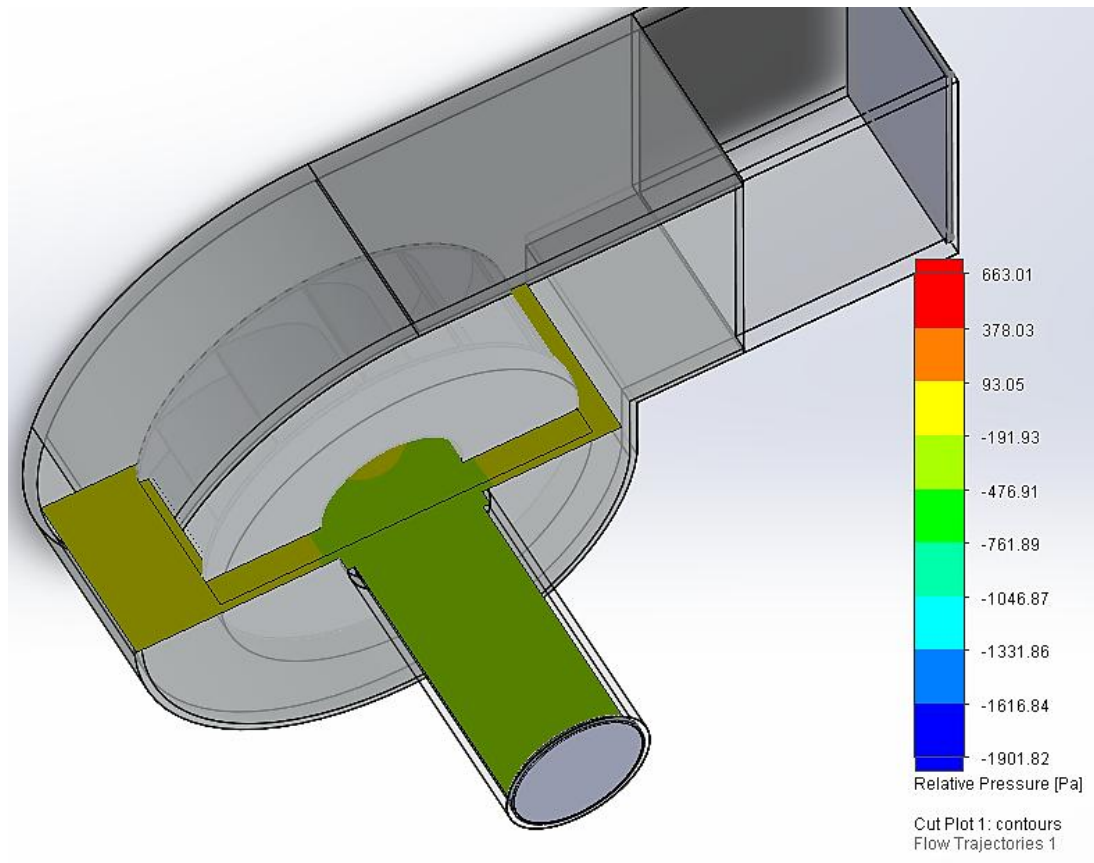
Figure 4.23: Pressure Cut Plot in Flow Simulation

4.3.2   Pipe Diameter and Length Selection of EAHE Prototype

To design the pipe diameter and length of the EAHE prototype system, the air velocity and mass flow rate of the centrifugal exhaust fan designed in the previous Section 4.3.1 was used as the input data in the developed Microsoft Excel Spreadsheet. This developed Microsoft Excel Spread will calculate the required length of the EAHE prototype with the provided data of air velocity, mass flow rate, pipe material characteristics, cooling load and the trial diameter.

The required pipe length of EAHE prototype was calculated for five different nominal diameters which were 1 in (25mm), 2 in (50mm), 3 in (80mm) and 4 in (100 mm) and 5 in (125 mm). By fixing the material of the pipe as PVC and with the pre-determined cooling load, the selection of which nominal diameter of PVC pipe to be used was based on the shortest required pipe length because this will minimize the

area of ground used. The difference of room (without EAHE) and ground temperature, $\Delta T_{room\text{-}ground}$ used in Equation 3.16 given in Section 3.4.3 have taken the value of 8.3 °C which was the worst condition recorded in Section 4.1.

A sample calculation for the selected 3 in (80 mm) nominal diameter pipe used in the finalized EAHE prototype design was presented below. The rest of the calculation for different diameter can be found in Appendix B. The standard inner and outer diameter for PVC pipe of different nominal diameter can be found in Figure 3.15 given above.

From Figure 3.15,

$D_o = 88.7$ mm $= 0.0887$ m

$D_i = 86.9$ mm $= 0.0869$ m

Conductive thermal resistance of the pipe, $R_{conductive}$

$$R_{conductive} = \frac{\ln(D_o / D_i)}{2 \times \pi \times L \times k_p}$$

$$= \frac{\ln(0.0887 / 0.0869)}{2 \times \pi \times L \times 0.19}$$

$$= 0.01717 / L$$

Mass flow rate of air, $\dot{m}_a$

$$\dot{m}_a = \frac{\rho \times \pi \times D_i^2 \times V_{avg}}{4}$$

$$= \frac{1.205 \times \pi \times (0.0869)^2 \times 13.8}{4}$$

$$= 0.09864 \text{ kg/s}$$

Reynolds number of the pipe flow, Re

$$\text{Re} = \frac{4\dot{m}_a}{\pi \times D_i \times \mu}$$

$$= \frac{4(0.09864)}{\pi(0.0869)(0.000015573)}$$

$$= 92,793$$

Friction factor, f

$$f = (0.79\ln \mathrm{Re} - 1.64)^{-2}$$

$$= (0.79\ln(92,793) - 1.64)^{-2}$$

$$= 0.01828$$

Prantl number, Pr

$$\mathrm{Pr} = \frac{c_{pa} \times \mu}{k_a}$$

$$= \frac{1005 \times 0.000015573}{0.0257}$$

$$= 0.61$$

Nusselt number, Nu

$$Nu = \frac{\left(\dfrac{f}{8}\right)(\mathrm{Re} - 1000)\mathrm{Pr}}{1 + 12.7\left(\dfrac{f}{8}\right)^{0.5}(\mathrm{Pr}^{2/3} - 1)}$$

$$= \frac{\left(\dfrac{0.01828}{8}\right)(92,793 - 1000)0.61}{1 + 12.7\left(\dfrac{0.01828}{8}\right)^{0.5}(0.61^{2/3} - 1)}$$

$$= 155.59$$

Convective heat transfer coefficient, h_a

$$h_a = Nu \times \frac{k_a}{D_i}$$

$$= 155.59 \times \frac{0.0257}{0.0869}$$

$$= 46.0159 \ \mathrm{W/m^2 \cdot K}$$

Convective thermal resistance of the air, $R_{convective}$

$$R_{convective} = \frac{1}{\pi \times D_i \times h_a \times L}$$

$$= \frac{1}{\pi \times 0.0869 \times 46.0159 \times L}$$

$$= 0.08234 / L$$

The required length of the pipe, L

$$L = \frac{q_{load} \times R_{total}}{\Delta T_{room-ground}}$$

$$= \frac{952 \times 0.09676}{8.3}$$

$$= 11.1 \, m$$

Figure 4.24 to 4.27 show the calculation PVC pipes with 1 in, 2 in, 4 in and 5 in nominal diameter by utilizing the developed Microsoft Excel Spreadsheet.

For 1 in (25 mm) PVC pipe

Inner diameter of pipe, Di	0.0312	m
Outer diameter of pipe, Do	0.0334	m
Air velocity	13.8	m/s
Mass flow rate	0.01272	kg/s
Reynold number, Re	33316	
Friction factor, f	0.02305	
Prantl number, Pr	0.61	
Nusselt number, Nu	72.12	
Convective coefficient, ha	59.4106	
Rcond/L	0.05707	K/W
Rconv/L	0.17170	K/W
Rtotal/L	0.22877	K/W
Length, L	26.2397	m

Figure 4.24: Calculation for 25 mm PVC pipe by Microsoft Excel Spreadsheet

For 2 in (50 mm) PVC pipe

Inner diameter of pipe, Di	0.0577	m
Outer diameter of pipe, Do	0.0602	m
Air velocity	13.8	m/s
Mass flow rate	0.04349	kg/s
Reynold number, Re	61613	
Friction factor, f	0.01999	
Prantl number, Pr	0.61	
Nusselt number, Nu	113.99	
Convective coefficient, ha	50.7733	
Rcond/L	0.03552	K/W
Rconv/L	0.10864	K/W
Rtotal/L	0.14416	K/W
Length, L	16.5353	m

Figure 4.25: Calculation for 50 mm PVC pipe by Microsoft Excel Spreadsheet

For 4 in (100 mm) PVC pipe

Inner diameter of pipe, Di	0.1118	m
Outer diameter of pipe, Do	0.1141	m
Air velocity	13.8	m/s
Mass flow rate	0.16327	kg/s
Reynold number, Re	119381	
Friction factor, f	0.01734	
Prantl number, Pr	0.61	
Nusselt number, Nu	188.85	
Convective coefficient, ha	43.4115	
Rcond/L	0.01706	K/W
Rconv/L	0.06558	K/W
Rtotal/L	0.08263	K/W
Length, L	9.4778	m

Figure 4.26: Calculation for 100 mm PVC pipe by Microsoft Excel Spreadsheet

For 5 in (125 mm) PVC pipe

Inner diameter of pipe, Di	0.1374	m
Outer diameter of pipe, Do	0.14	m
Air velocity	13.8	m/s
Mass flow rate	0.24660	kg/s
Reynold number, Re	146717	
Friction factor, f	0.01661	
Prantl number, Pr	0.61	
Nusselt number, Nu	221.55	
Convective coefficient, ha	41.4404	
Rcond/L	0.01570	K/W
Rconv/L	0.05590	K/W
Rtotal/L	0.07160	K/W
Length, L	8.2121	m

Figure 4.27: Calculation for 125 mm PVC pipe by Microsoft Excel Spreadsheet

Table 4.8 summarized the result of calculation of the required length for PVC pipe with different diameter if were to be used in the EAHE prototype. Figure 4.28 shows the chart of required length of pipe and total cost for PVC pipe of different nominal diameter.

Table 4.8: Result of Calculation of Required Length and Total Cost for PVC with Different Nominal Diameter

Nominal pipe diameter, D (m)	Required length, L (m)	Cost per Meter (RM)	Total Cost (RM)
1 in (25 mm)	26.24	7.5	196.80
2 in (50 mm)	16.54	20.5	338.97
3 in (80 mm)	11.10	21.0	233.07
4 in (100 mm)	9.48	32.1	304.24
5 in (125 mm)	8.21	46.8	384.33
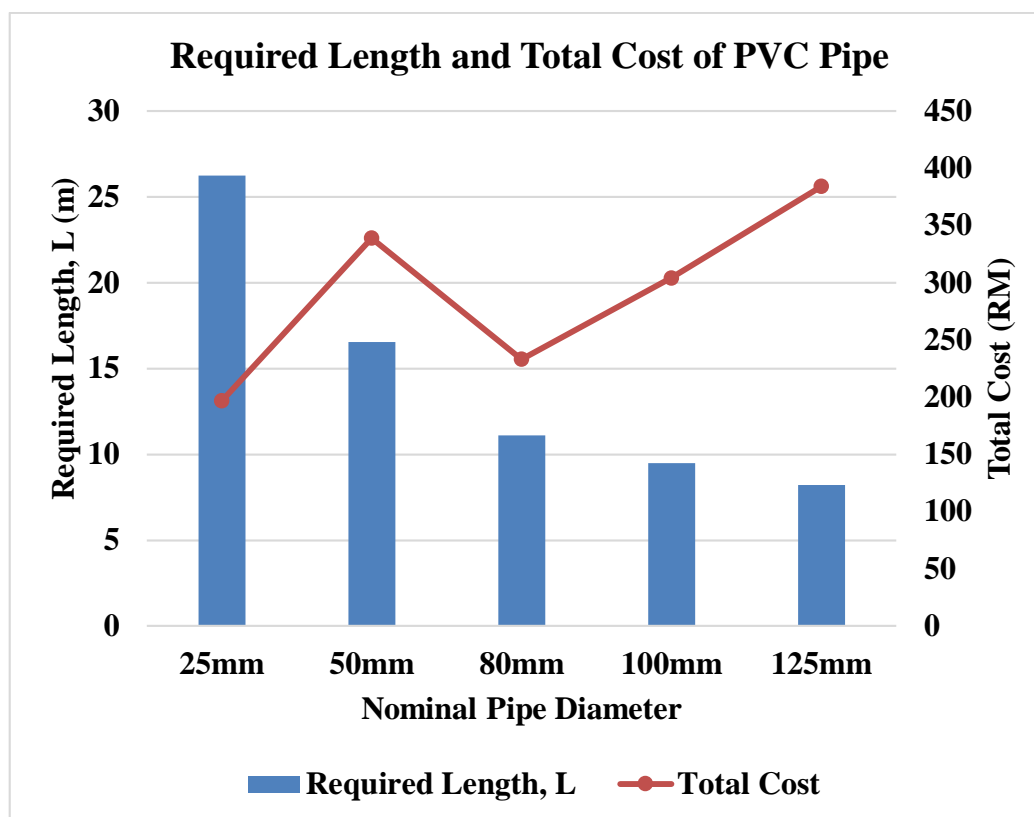
Figure 4.28: Required Length and Total Cost for PVC pipe of Different Nominal Diameter

For the finalized EAHE prototype design, PVC pipe with nominal diameter of 3 inch (80 mm) was selected because it hit the sweet spot of short required length and low total cost. PVC pipe with nominal diameter of 4 in (100 mm) and 5 in (125 mm) were not chosen because the total cost was too high. On the other hand, PVC pipe of diameter 1 in (25 mm) and 2 in (50 mm) were not chosen as well because it would be very impractical to dig a hole of 1.5 m depth that can fit in the required pipe length of 26.24 m and 16.54 m. Although the calculated pipe length required by the EAHE prototype to remove the imposed cooling load was 11.1 m. However, for the simplicity of design the length of the pipe has been designed to be 11.6 m (including the vertical portion being buried underground) as shown in Figure 4.29. In a nutshell, the pipe diameter and length of the designed EAHE prototype were 3 in (80 mm) and 11.6 m respectively based on the cooling load of the experimental residential room.
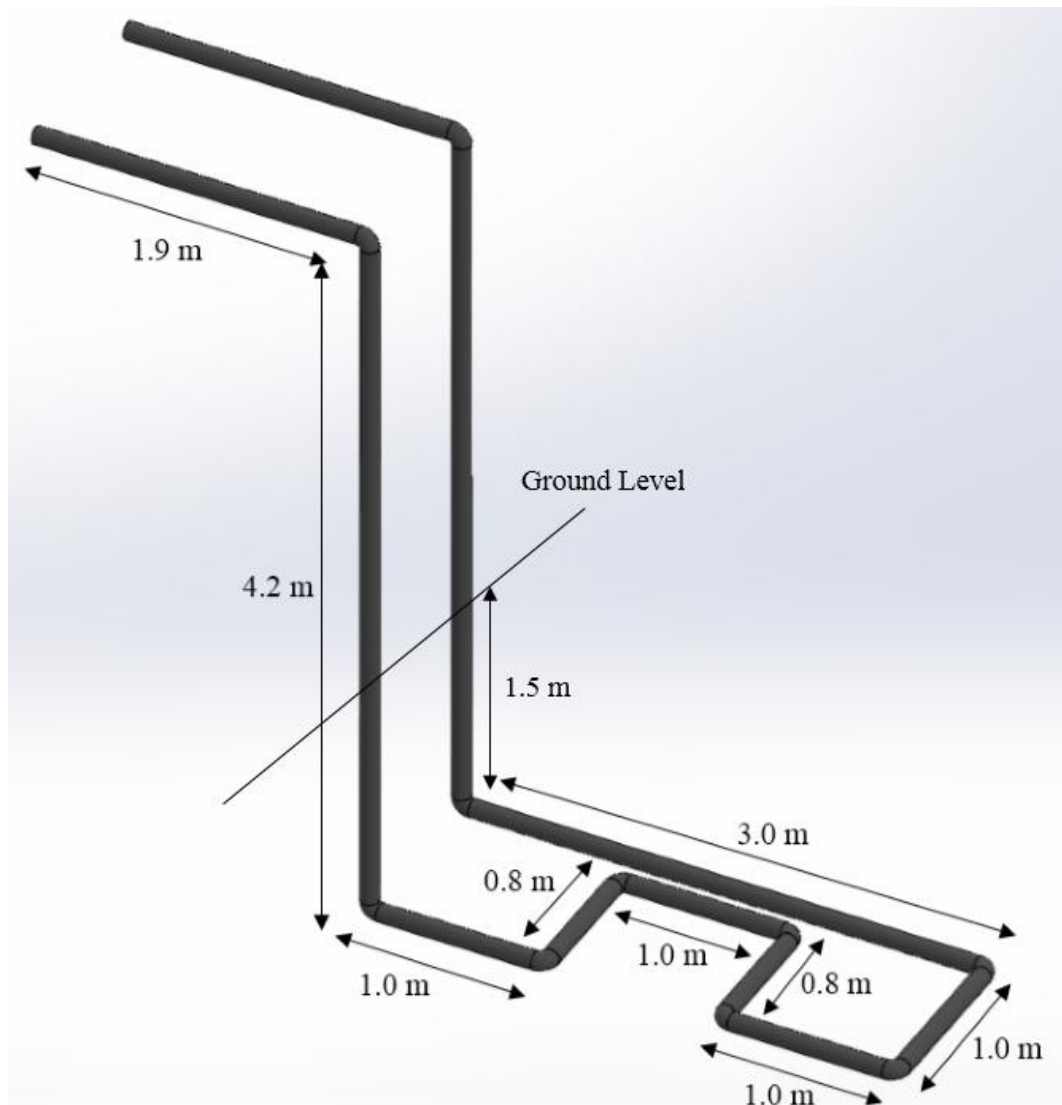
Figure 4.29: Pipe Layout of the EAHE Prototype with Dimensions Labelled

4.3.3   Full View of Designed EAHE Prototype System

The full view of the finalized EAHE prototype system was given in actual photo and solid modelling pictures in this section. Figure 4.30 shows the EAHE prototype's pipe layout along with the location where the temperature mentioned in Section 3.5 was collected being labelled on it. Figures 4.31 to 4.33 shows the EAHE system in solid modelling at different views. Figures 4.34 and 4.35 shows the actual EAHE pipe layout and prototype system on site.
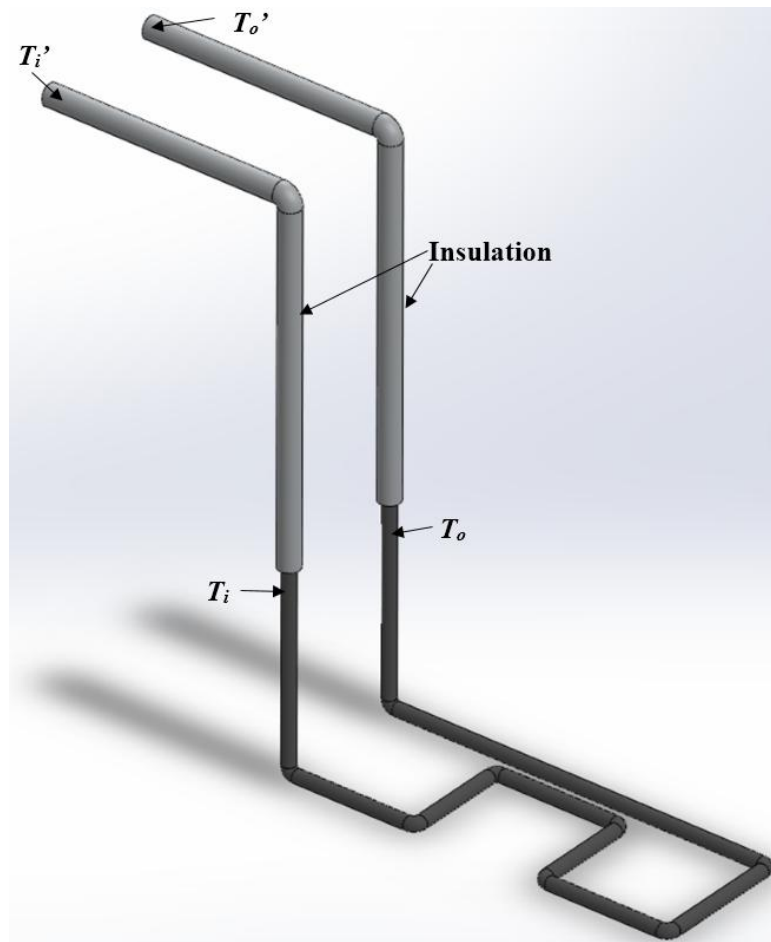
Figure 4.30: EAHE Pipe Layout with Insulation in Solid Modeling
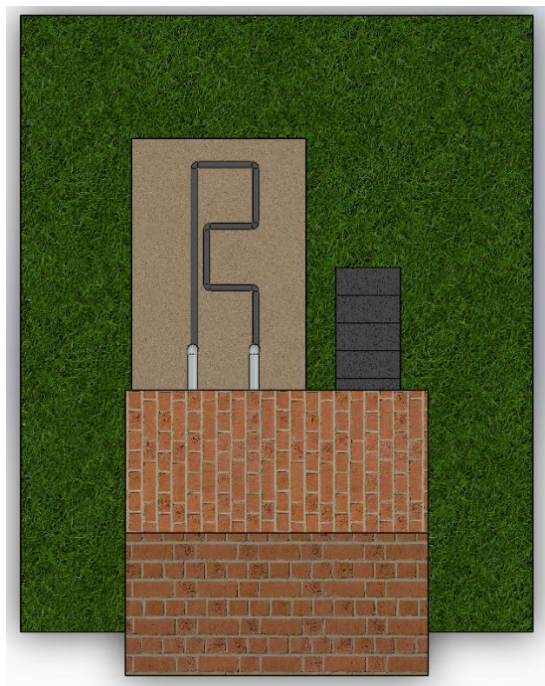
Figure 4.31: Top View of EAHE Prototype System in Solid Modeling
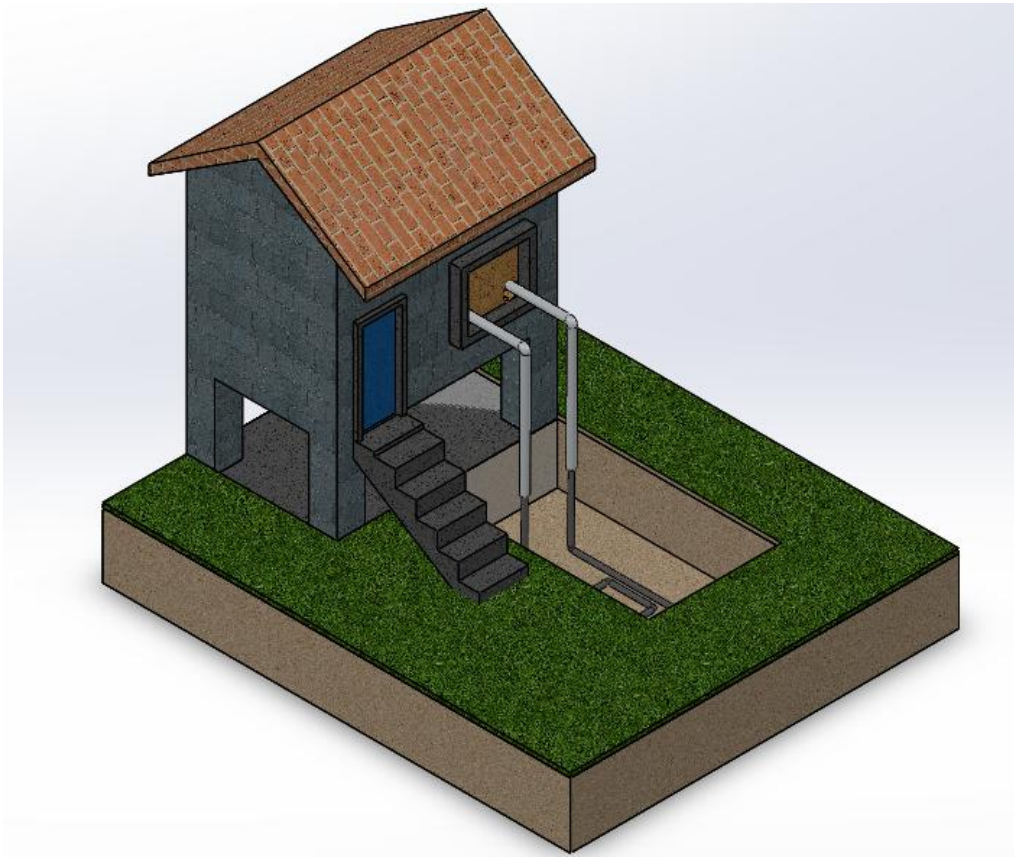
Figure 4.32: Isometric View of EAHE Prototype System in Solid Modeling
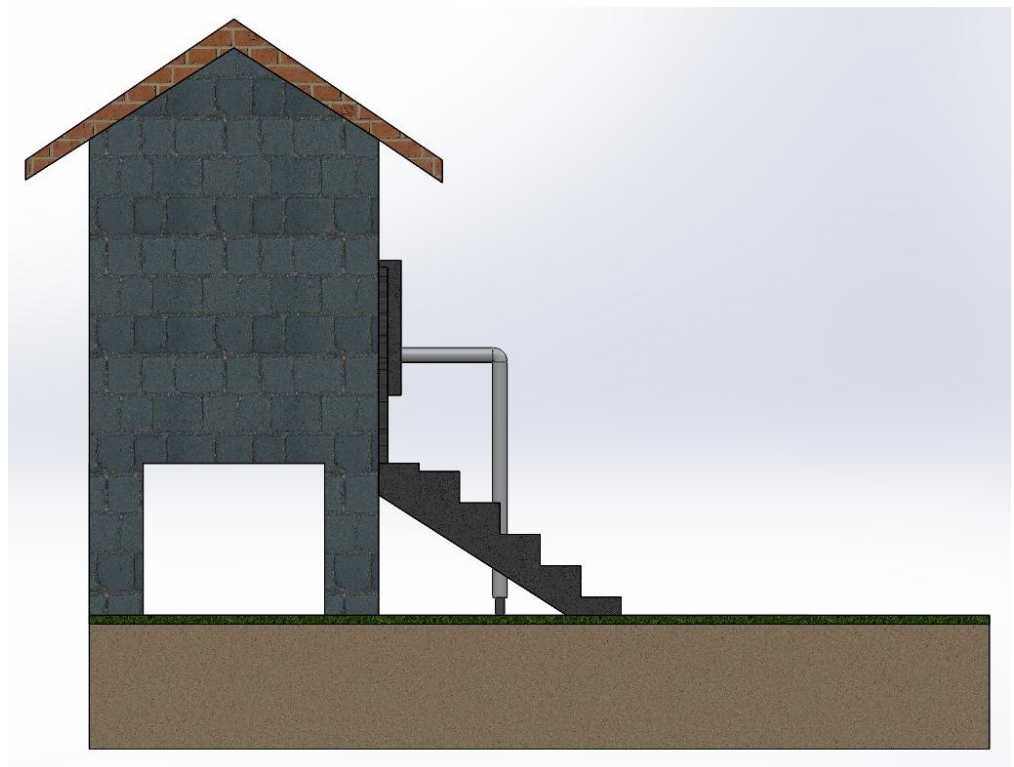
Figure 4.33: Side View of EAHE Prototype System in Solid Modeling

Figure 4.34: Actual EAHE Pipe Layout on Site
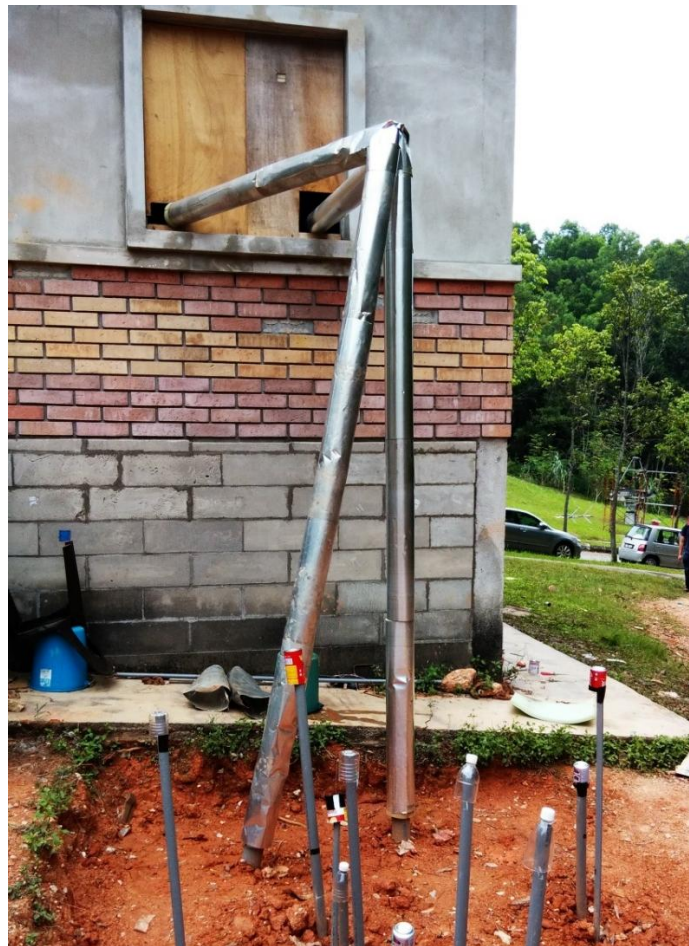
Figure 4.35: Actual EAHE Prototype on Site

4.4 Data Collection of the EAHE Prototype System

The actual measured EAHE inlet and outlet air velocity was measured and compared with the simulated value. Then, an average air velocity in the pipe can be obtained by using these values of air velocity. The average air velocity were then used in the calculation of air mass flow rate of the system since the inner diameter of the EAHE pipe had been finalized at this stage. All these simulated and experimental measured readings were summarized in Table 4.9. The calculation of the simulated and experimental mass flow rate of air was given below.

For simulated result,

$V_o = 17.1$ m/s

$V_i = 10.5$ m/s

$V_{avg} = \dfrac{V_o + V_i}{2}$

$\qquad = \dfrac{17.1 + 10.5}{2}$

$\qquad = 13.8$ m/s

$\overset{\bullet}{m}_a = \dfrac{\rho \times \pi \times D_i^2 \times V_{avg}}{4}$

$\qquad = \dfrac{1.205 \times \pi \times 0.0869^2 \times 13.8}{4}$

$\qquad = 0.09863$ kg/s

For experimental result,

$V_o = 16.5$ m/s

$V_i = 9.9$ m/s

$V_{avg} = \dfrac{V_o + V_i}{2}$

$\qquad = \dfrac{16.5 + 9.9}{2}$

$\qquad = 13.2$ m/s

$$\overset{\bullet}{m}_a = \frac{\rho \times \pi \times D_i^2 \times V_{avg}}{4}$$

$$= \frac{1.205 \times \pi \times 0.0869^2 \times 13.2}{4}$$

$$= 0.09434 \ \text{kg/s}$$

Table 4.9: Simulated and Experimental Values of Flow Properties of EAHE Prototype

Description	EAHE Outlet velocity, V_o (m/s)	EAHE Inlet Velocity, V_i (m/s)	Average Velocity, V_{avg} (m/s)	Mass Flow Rate, $\dot{m}_a$ (kg/s)
Simulated	17.1	10.5	13.80	0.09863
Experimental	16.5	9.9	13.20	0.09434

The following temperatures were collected on the EAHE prototype system each day from 8am to 6pm for three days.

1. Room temperature, T_r
2. EAHE inlet temperature, T_i
3. EAHE outlet temperature, T_o
4. Room Inlet temperature before insulation, $T_i{}'$
5. Room Outlet temperature after insulation, $T_o{}'$
6. Environment temperature, $T_{environ}$

These temperatures had been summed up and averaged to get the mean temperatures at the specific time. The aforementioned mean temperatures collected were tabulated in Table 4.10. Figure 4.36 shows the graph of the aforementioned mean temperatures plotted against time from 8am to 6pm. The particular temperature readings collected for each of the three days can be found in Appendix C. In the following Section 4.5, temperatures will be compared in the form of table and chart where it is relevant to relate them together. By doing so would allow a more in-depth analysis and discussion as compared to analysing and discussing all the temperatures collected in once.

Table 4.10: Various Mean Temperatures of the EAHE Prototype System

Description / Time	Ti (ºC)	To (ºC)	Ti' (ºC)	To' (ºC)	Tr (ºC)	Tenviron (ºC)
8:00 AM	28.1	27.4	28	27.5	28	27
9:00 AM	29.2	27.4	29.1	27.8	29.1	29.8
10:00 AM	29.7	27.4	29.5	27.9	29.6	32.1
11:00 AM	31.4	28	30.2	28.5	30.1	34
12:00 PM	32.7	29	31.1	29.5	31.1	35.6
1:00 PM	34.4	29.9	32.3	30.6	32.2	37
2:00 PM	35.4	30.5	32.9	31.1	32.7	36.8
3:00 PM	36.9	31.3	33.6	31.9	33.4	36.5
4:00 PM	37.4	31.9	34	32.2	33.8	35.7
5:00 PM	35.5	29.8	33.6	30.3	33.5	33.8
6:00 PM	34.3	29.2	33.1	29.7	33	31.9
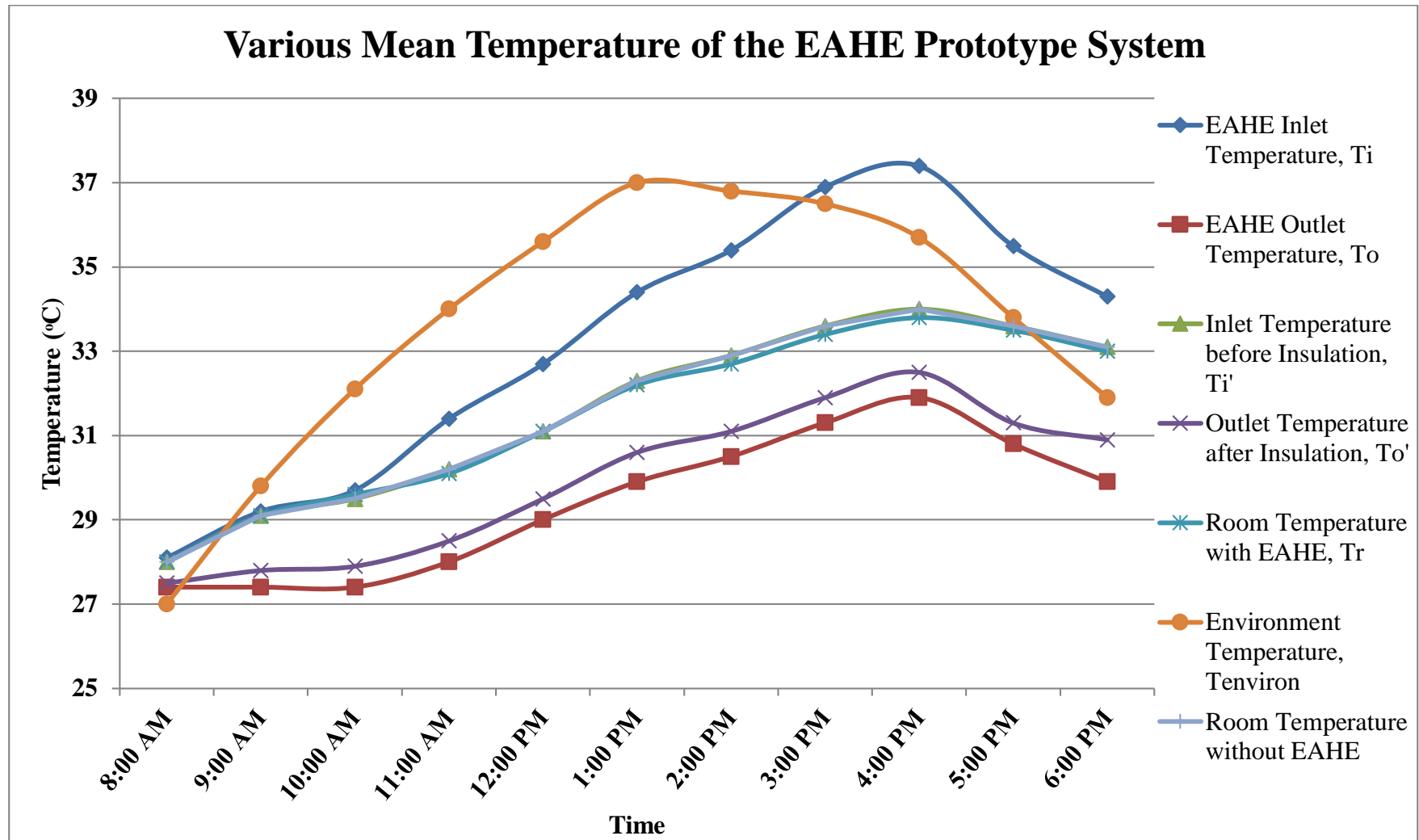
Figure 4.36: Various Mean Temperatures of the EAHE Prototype System

4.5   Temperatures Data Analysis of the EAHE Prototype System

4.5.1   Mean Room and Environment Temperatures with EAHE

Table 4.11 shows the tabulated mean room and environment temperature with the implementation of EAHE prototype system that was collected. On the other hand, Figure 4.37 shows the chart of mean room and environment temperature with EAHE prototype system against time that was plotted according to the tabulated data.

Table 4.11: Mean Room and Environment Temperatures with EAHE Prototype

Description / Time	Room Temperature with EAHE System, T_r (°C)	Environment Temperature, $T_{environ}$ (°C)	Temperature Difference, $T_{environ}$ - T_r (°C)
8:00 AM	28.0	27.0	-1
9:00 AM	29.1	29.8	0.7
10:00 AM	29.6	32.1	2.5
11:00 AM	30.1	34.0	3.9
12:00 PM	31.1	35.6	4.5
1:00 PM	32.2	37.0	4.8
2:00 PM	32.7	36.8	4.1
3:00 PM	33.4	36.5	3.1
4:00 PM	33.8	35.7	1.9
5:00 PM	33.5	33.8	0.3
6:00 PM	33.0	31.9	-1.1

As shown in the Table 4.11, Figure 4.36 and 4.37 that the room temperature is almost always lower than the environment temperature. At early in the morning of 8am and late evening in the 6pm, the room temperature was slight higher than the environment temperature by about 1 °C and 1.1 °C . The largest temperature difference between environment and room temperature was 4.8°C which occurred at 1pm in the afternoon. The EAHE prototype system was able to keep the room at about 30 °C from 8am in the early morning until 11am in the late morning. Then, the

room temperature kept increased from 31.1 ℃ at 12pm and reached the highest room temperature of 33.8 ℃ at 4pm. The increased in the room temperature was due to heat accumulation that caused by insufficient heat rejected by the EAHE prototype system as compared to the heat gained by the room.
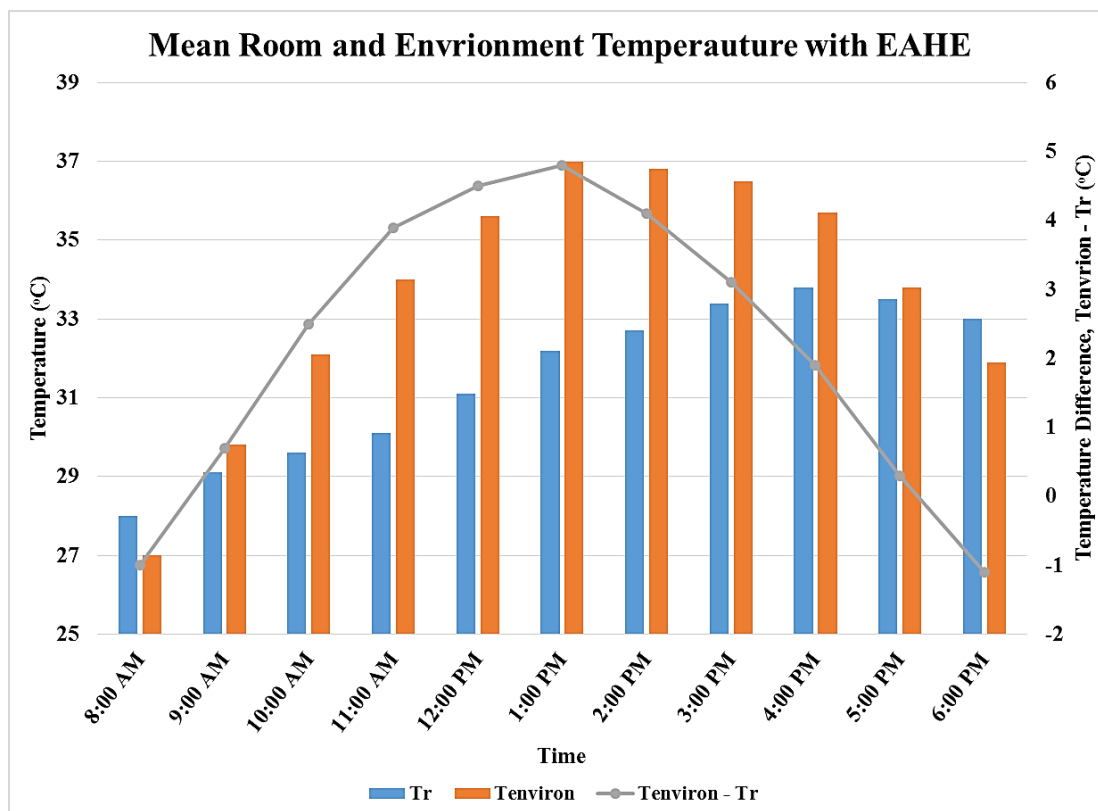
Figure 4.37: Mean Room and Environment Temperatures with EAHE Prototype

4.5.2   Mean Room and EAHE Outlet Temperatures

Table 4.12 shows the tabulated mean room and EAHE outlet temperature with the implementation of EAHE prototype system that was collected. On the other hand, Figure 4.38 shows the chart of mean room and EAHE outlet temperature with the implementation of EAHE prototype system against time that was plotted according to the tabulated data.

Table 4.12: Mean Room and EAHE Outlet Temperatures with EAHE Prototype

Description Time	Room Temperature with EAHE System, T_r (°C)	EAHE Outlet Temperature, T_o (°C)	Temperature Difference, $T_r - T_o$ (°C)
8:00 AM	28.0	27.4	0.6
9:00 AM	29.1	27.4	1.7
10:00 AM	29.6	27.4	2.2
11:00 AM	30.1	28	2.1
12:00 PM	31.1	29	2.1
1:00 PM	32.2	29.9	2.3
2:00 PM	32.7	30.5	2.2
3:00 PM	33.4	31.3	2.1
4:00 PM	33.8	31.9	1.9
5:00 PM	33.5	30.8	2.7
6:00 PM	33.0	29.9	3.1
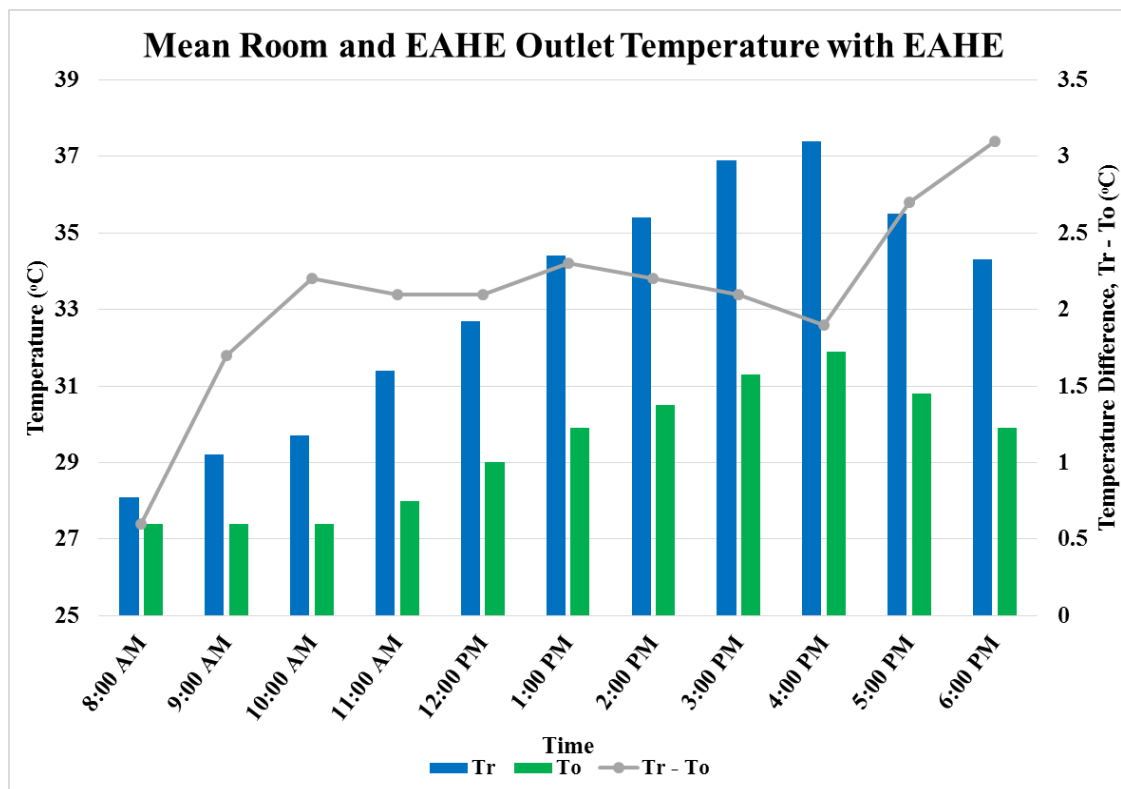
Figure 4.38: Mean Room and EAHE Outlet Temperatures with EAHE Prototype

As shown in the Table 4.12, Figure 4.36 and 4.38, the EAHE outlet temperature was lower than the room temperature at all the time. However, both the room and EAHE outlet temperature shown an increasing trend from 8am to 4pm. From 5pm onward, the outlet temperature decreases drastically and this trends was carried on until 6pm in the late evening. The largest temperature difference between room and EAHE outlet temperature occurred during 6pm in which a temperature difference of 3.1 ℃ was achieved. EAHE outlet temperature was able to remains below 30 ℃ until 1pm in the afternoon. After 1pm, the EAHE outlet temperature rises above 30 ℃ and reaches its peak value of 31.9 ℃ at 4pm in the afternoon. Then, the EAHE outlet temperature decreased until 6pm was reached.

The increased in EAHE outlet temperature could be due to the heat accumulation in the ground or in other words reservoir degradation. This can happen if the ground does not transfer the heat fast enough away and subsequently the ground temperature increases and would reduce the total amount of heat being rejected into the ground. A solution that could solve this problem is to increase the air velocity and pipe length of the EAHE system together. By having a longer pipe length, the rate of heat transfer could be reduced but still maintaining the same total heat rejection (or cooling capacity) if the air velocity was increased at the same time. As a result, the ground would not be saturated with heat and the ground temperature could be more stable all the time.

4.5.3   Mean Room and EAHE Inlet Temperatures

Table 4.13 shows the tabulated mean room and EAHE inlet temperature with EAHE prototype system that was collected. On the other hand, Figure 4.39 shows the chart of mean room and EAHE inlet temperature with the implementation of EAHE prototype system against time that was plotted according to the tabulated data.

Table 4.13: Mean Room and EAHE Inlet Temperatures with EAHE Prototype

Description / Time	Room Temperature with EAHE System, T_r (ºC)	EAHE Inlet Temperature, T_i (ºC)	Temperature Difference, $T_i - T_r$ (ºC)
8:00 AM	28	28.1	0.1
9:00 AM	29.1	29.2	0.1
10:00 AM	29.6	29.7	0.1
11:00 AM	30.1	31.4	1.3
12:00 PM	31.1	32.7	1.6
1:00 PM	32.2	34.4	2.2
2:00 PM	32.7	35.4	2.7
3:00 PM	33.4	36.9	3.5
4:00 PM	33.8	37.4	3.6
5:00 PM	33.5	35.5	2.0
6:00 PM	33	34.3	1.3
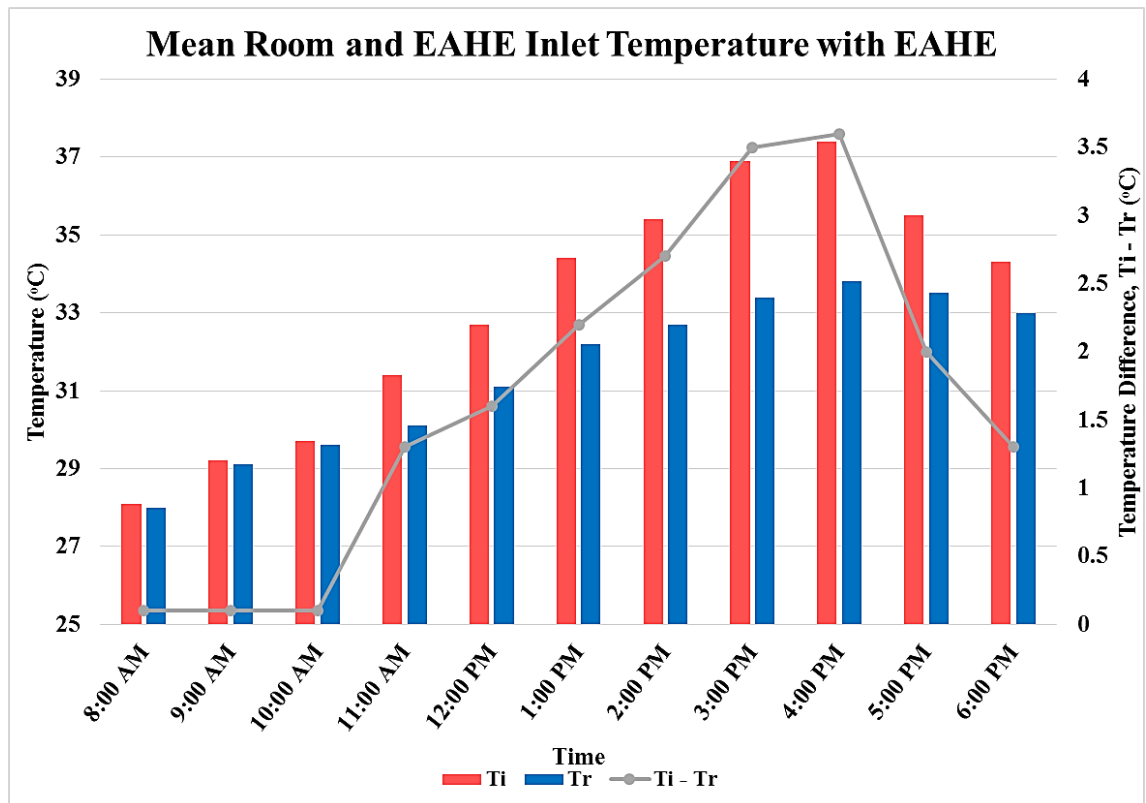
Figure 4.39: Mean Room and EAHE Inlet Temperatures with EAHE Prototype

As shown in the Table 4.13, Figure 4.36 and 4.39, the EAHE inlet temperature was higher than the room temperature almost all the time. However, both the EAHE inlet and room temperatures shown an increasing trend from 8am to 4pm. From 5pm onward, the EAHE inlet temperature decreased and this trend was carried on until 6pm in the late evening. The largest temperature difference between EAHE inlet and room temperature was 3.6 ℃ which occurred at 4pm. The highest EAHE inlet temperature recorded was 37.4 ℃ which occurred at 4pm. The lowest EAHE inlet temperature recorded was 28.1 ℃ which occurred at 8am.

The location where the measurement of EAHE inlet temperature was right after the insulation but before the pipe enter the ground as can be seen in Figure 4.30 above. The temperature difference between EAHE inlet temperature and room temperature could be caused by the heat gained by the insulation at the inlet segment as air flow through it. The heat gained by the insulation at the inlet segment was presented in Section 4.6.1.

4.5.4 Mean EAHE Inlet and Outlet Temperature

Table 4.14 shows the tabulated mean EAHE inlet and outlet temperature measured at the locations shown in Figure 4.30 which were just before and after the pipe enter into the ground. On the other hand, Figure 4.40 shows the chart of mean EAHE inlet and EAHE outlet temperatures against time that was plotted according to the tabulated data.

As shown in the Table 4.14, Figure 4.36 and 4.40 above, the EAHE inlet temperature was always above EAHE outlet temperature for all the time. Although both the EAHE inlet and outlet temperatures increases from 8am until 4pm, EAHE outlet temperature shown lesser increment as compared to EAHE inlet temperature. The peak EAHE inlet temperature recorded was 37.4 ℃ that occurred at 4pm. The peak EAHE outlet temperature recorded was 31.9 ℃ which also occurred at 4pm.

Table 4.14: Mean EAHE Inlet and Outlet Temperatures with EAHE Prototype

Description / Time	EAHE Inlet Temperature, T_i (ºC)	EAHE Outlet Temperature, T_o (ºC)	Temperature Difference, $T_i - T_o$ (ºC)
8:00 AM	28.1	27.4	0.7
9:00 AM	29.2	27.4	1.8
10:00 AM	29.7	27.4	2.3
11:00 AM	31.4	28	3.4
12:00 PM	32.7	29	3.7
1:00 PM	34.4	29.9	4.5
2:00 PM	35.4	30.5	4.9
3:00 PM	36.9	31.3	5.6
4:00 PM	37.4	31.9	5.5
5:00 PM	35.5	30.8	4.7
6:00 PM	34.3	29.9	4.4

Figure 4.40: Mean EAHE Inlet and Outlet Temperatures with EAHE Prototype

As can be observed from Figure 4.40, the temperature difference of the EAHE inlet and outlet temperature increased steadily from 8am until 5pm. The peak temperature difference recorded was 5.7 ℃ which occurred at 5pm. Besides, it can be observed that the temperature difference stay in the range of 4.9 to 5.7 ℃ throughout the afternoon from 1pm until 6pm. The temperature difference mentioned in here is an indication of the amount of heat rejected by the EAHE into the ground. Thus, the heat rejected by the EAHE prototype system increased and stayed in a maximum range in the afternoon.
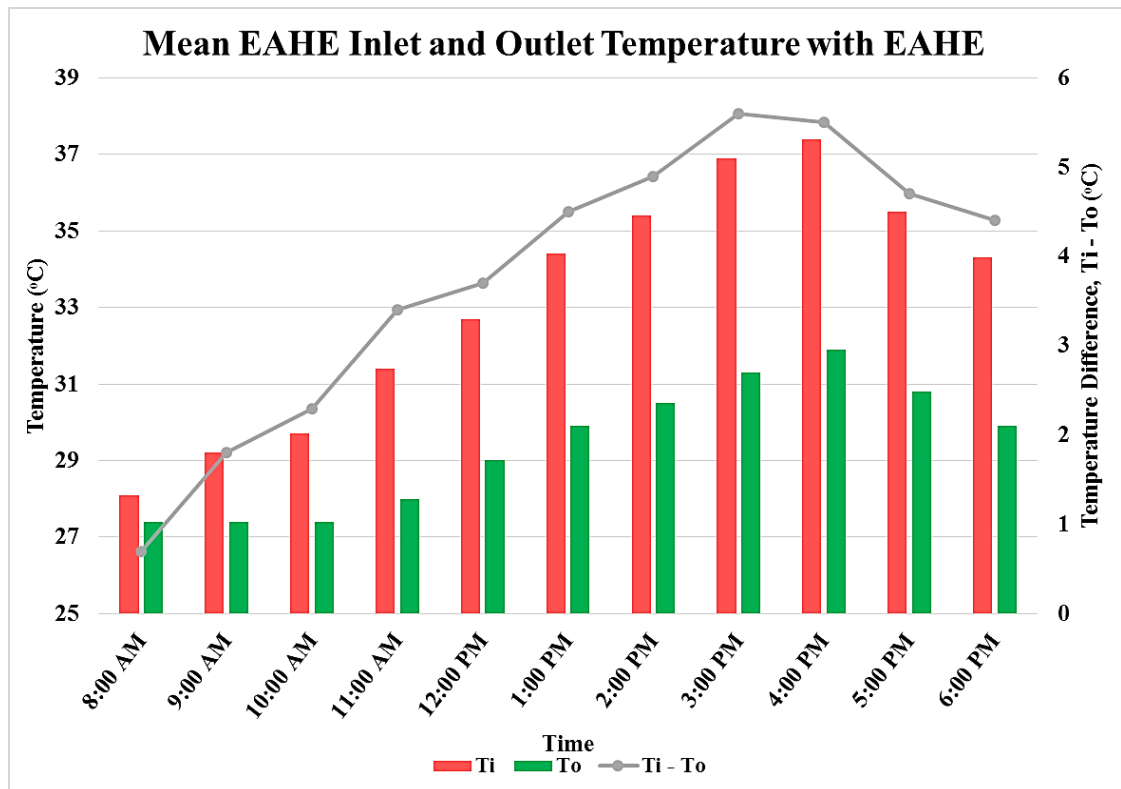
4.5.5   Mean Room Inlet and Outlet Temperature

Table 4.15 shows the tabulated mean room inlet and outlet temperature measured at the locations as shown in Figure 4.30 which were just before and after the insulation. On the other hand, Figure 4.41 shows the chart of mean EAHE inlet and EAHE outlet temperatures against time that was plotted according to the tabulated data.

Table 4.15: Mean Room Inlet and Outlet Temperatures with EAHE Prototype

Description \ Time	Room Inlet Temperature, T_i' (^{o}C)	Room Outlet Temperature, T_o' (^{o}C)	Temperature Difference, $T_i' - T_o'$ (^{o}C)
8:00 AM	28	27.5	0.5
9:00 AM	29.1	27.8	1.3
10:00 AM	29.5	27.9	1.6
11:00 AM	30.2	28.5	1.7
12:00 PM	31.1	29.5	1.6
1:00 PM	32.3	30.6	1.7
2:00 PM	32.9	31.1	1.8
3:00 PM	33.6	31.9	1.7
4:00 PM	34.0	32.5	1.5
5:00 PM	33.6	31.3	2.3
6:00 PM	33.1	30.9	2.2
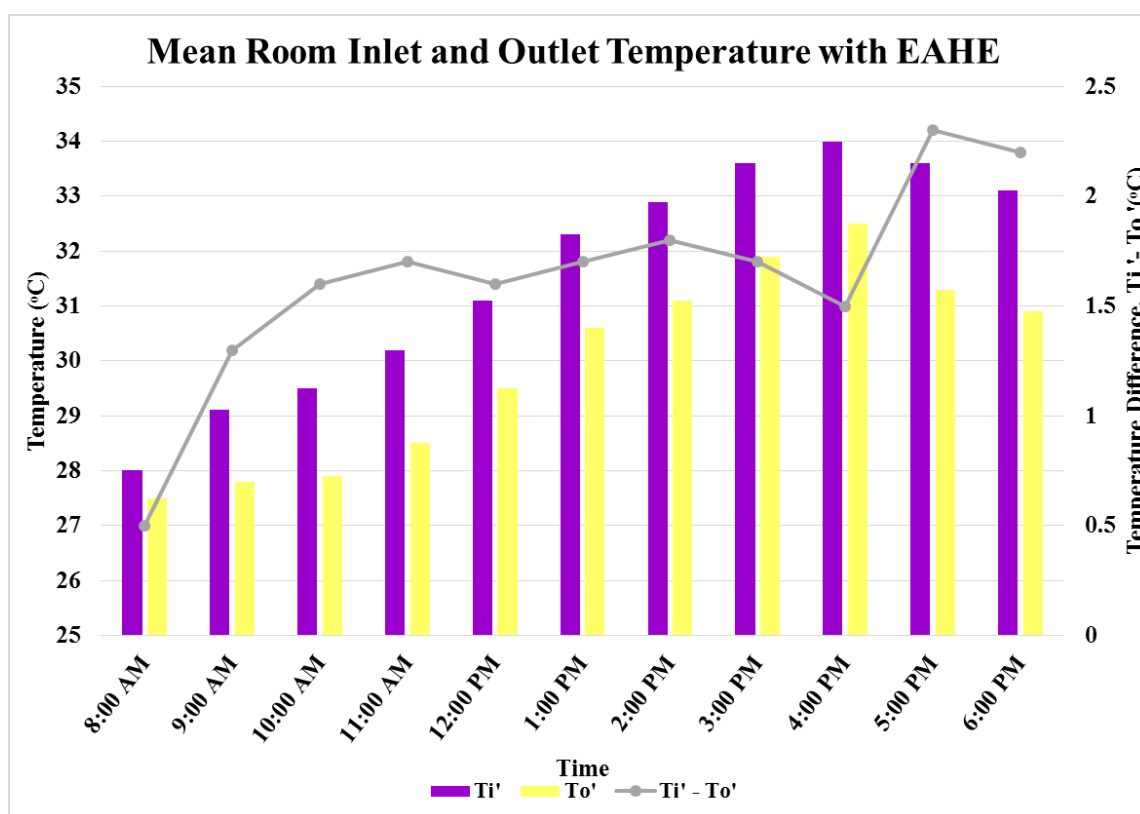
Figure 4.41: Mean Room Inlet and Outlet Temperature with EAHE Prototype

As shown in the Table 4.15, Figure 4.36 and 4.41 above, the room inlet temperature was above the room outlet temperature for all the time. The room inlet temperature constantly increased from 8am and reached its peak value of 34.0 ℃ at 4pm. On the other hand, the room outlet temperature stayed at a range of 27.5 to 27.9 ℃ from 8am to 10am. The room outlet temperature started to increase steadily from 11am until 4pm. Then, the room outlet temperature started to fall down from 5pm to 6pm. The highest room outlet temperature recorded was 32.5 ℃. Generally, the room inlet and outlet temperatures have the same increase trend from 11am to 4pm. Besides, the room inlet and outlet temperatures also have the same decrease trend from 5pm to 6pm. Therefore, it can be concluded that the room inlet and outlet temperatures are highly dependent on each other.

As can be observed from Figure 4.41, the temperature difference of the EAHE inlet and outlet temperature increases steadily from 8am to 10am. After that, the temperature difference stay in a relative constant range of 1.6 to 1.8 ℃ from

11am to 5pm. The peak temperature difference recorded was 2.3 ℃ which occurred at 5pm. The temperature difference mentioned in here is an indication of the amount of heat extracted from the room that is rejected to the ground. Thus, the heat extracted from the room by the EAHE prototype system stays in a constant range in from 11am to 5pm. The detail calculation and analysis of heat extraction from the room can be found in Section 4.6.4.

4.5.6   Mean Room Temperature without and with EAHE

Table 4.16 shows the tabulated mean room temperature with and without EAHE measured before and after the EAHE was being installed. On the other hand, Figure 4.42 shows the chart of mean room temperatures with and without EAHE against time that was plotted according to the tabulated data.

Table 4.16: Room Temperatures without and with EAHE Prototype

Description ⟍ Time	Room Temperature without EAHE, T_r' (℃)	Room Temperature with EAHE, T_r (℃)	Temperature Difference, $T_r'-T_r$ (℃)
8:00 AM	28.5	28	0.5
9:00 AM	29.8	29.1	0.7
10:00 AM	31.1	29.6	1.5
11:00 AM	32.3	30.1	2.2
12:00 PM	33.8	31.1	2.7
1:00 PM	35.2	32.2	3.0
2:00 PM	36.5	32.7	3.8
3:00 PM	37.3	33.4	3.9
4:00 PM	36.8	33.8	3.0
5:00 PM	35.9	33.5	2.4
6:00 PM	35	33	2.0
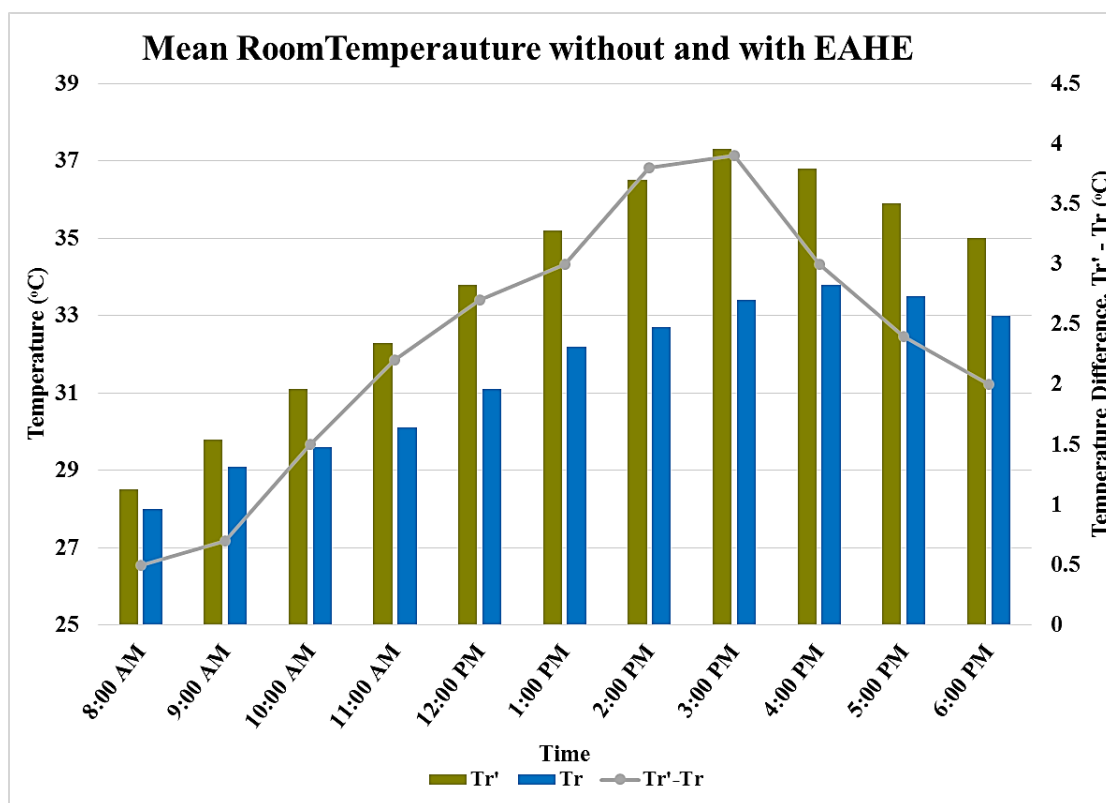
Figure 4.42: Room Temperature without and with EAHE Prototype

As can be observed from Table 4.16, Figure 4.36 and 4.21, the room temperature with EAHE prototype system was always lower than the room temperature without the system. Thus, the EAHE prototype system did reduced the room temperature at all the time. Both the room temperatures with and without EAHE increased from 8am but reached their peak value at different time. The room temperature with EAHE prototype system reached its peak temperature of 33.8 ℃ at 4pm. On the other hand, the room temperature without EAHE prototype system reached its peak value of 37.3 ℃ at 3pm.

The highest temperature difference between the room temperature with and without the EAHE prototype system was 3.9 ℃ which occurred at 3pm. During the afternoon from 12pm to 4pm the temperature difference stays in the range of 2.7 to 3.9 ℃. The temperature difference increased from 8am to 3pm and reached its peak value before it started to decrease again from 4pm to 6pm. Thus, it can be concluded that the EAHE prototype did reduced the room temperature significantly especially

during afternoon. It was also shown that at most the EAHE prototype system was able to bring down the room temperature by 3.9 °C.

4.6 Heat Analysis of the EAHE Prototype System

4.6.1 Heat Gained by the Insulation – Inlet Segment

Heat gained by the insulation can be calculated based on the Equation 3.20 given in Section 3.5.3. Firstly, heat gained by the insulation at the inlet segment has been presented here. It can be calculated based on temperature difference of the room inlet temperature before insulation, T_i' and EAHE inlet temperature after insulation, T_i. A sample calculation of heat gained at 3pm had been provided here. Heat gained from 8am to 6pm were summarized in Table 4.17.

At 3pm,

$$T_i = 36.9 \,°C$$

$$T_i^{'} = 33.6 \,°C$$

From Section 4.4,

$$\dot{m}_a = 0.09434 \,kg/s$$

while

$$c_{pa} = 1005 \,kJ/kg \cdot K$$

Therefore, heat gained by the insulation at the inlet segment is

$$q_{gained,in} = \dot{m}_a \, c_{pa} \left(T_i - T_i^{'} \right)$$
$$= 0.09434(1005)(36.9 - 33.6)$$
$$= 312.88 \,W$$

Table 4.17: Heat Gained by the Insulation – Inlet Segment

Description Time	Temperature Difference, $T_i - T_i{}'$ (°C)	Heat Gained - Inlet, $q_{gained,in}$ (W)
8:00 AM	0.1	9.48
9:00 AM	0.1	9.48
10:00 AM	0.2	18.96
11:00 AM	1.2	113.77
12:00 PM	1.6	151.70
1:00 PM	2.1	199.10
2:00 PM	2.5	237.03
3:00 PM	3.3	312.88
4:00 PM	3.4	322.36
5:00 PM	1.9	180.14
6:00 PM	1.2	113.77
Average	1.6	151.70

As can be observed from Table 4.17 above, the heat gained by the insulation at the inlet segment increases from 9am to 4pm and then it started to decrease until 6pm. The maximum heat gained by insulation at the inlet segment was 322.36 W which occurred at 4pm. This increasing and decreasing trends of the heat gained were because the sunlight start to shine on the inlet segment' insulation starting from 9am and the solar energy increased throughout the afternoon. The heat gained started to decrease when the sunlight finally moved away from the inlet segment' insulation which only occur after 5pm in the late evening. Last but not least, the average heat gained by insulation at inlet segment was calculated to be 151.70W.

4.6.2   Heat Gained by the Insulation – Outlet Segment

Heat gained by the insulation at the outlet segment has been presented here. It can be calculated by the temperature difference between the EAHE outlet temperature

before insulation, T_o and room outlet temperature after insulation, $T_o^{'}$. A sample calculation of heat gained by the insulation at 3pm has been provided here. Heat gained by insulation at the outlet segment from 8am to 6pm were summarized in Table 4.18.

At 3pm,

$$T_o = 31.3 \,°C$$

$$T_o^{'} = 31.9 \,°C$$

From Section 4.4,

$$\dot{m}_a = 0.09434 \,kg/s$$

while

$$c_{pa} = 1005 \;kJ/kg \cdot K$$

Therefore, heat gained by the insulation at the outlet segment is

$$q_{gained,out} = \dot{m}_a \, c_{pa} \left(T_o^{'} - T_o \right)$$
$$= 0.09434(1005)(31.9 - 31.3)$$
$$= 56.89 \,W$$

Table 4.18: Heat Gained by the Insulation – Outlet Segment

Description Time	Temperature Difference, $T_o^{'} - T_o$ (°C)	Heat Gained - Outlet, $q_{gained,out}$ (W)
8:00 AM	0.1	9.48
9:00 AM	0.4	37.92
10:00 AM	0.5	47.41
11:00 AM	0.5	47.41
12:00 PM	0.5	47.41
1:00 PM	0.7	66.37
2:00 PM	0.6	56.89
3:00 PM	0.6	56.89
4:00 PM	0.6	56.89
5:00 PM	0.5	47.41
6:00 PM	1.0	94.81

Average	0.6	51.72 W

As can be observed from Table 4.18 above, heat gained by the insulation at the outlet segment increased abruptly from 9am to 1pm and then it starts to decrease gradually and slowly until 6pm. The maximum heat gained by insulation at the outlet segment was 66.37 W which occurred at 1pm. This increasing trends of the heat gained was because the sunlight start to shine on the outlet segment' insulation starting from 9am and the solar energy reached its peak value at 1pm. The heat gained starts to decrease from 4pm to 5pm when the sunlight finally moved away from the outlet segment's insulation. However, there was an outlier in this set of data which was the heat gained at 6pm. Last but not least, the average heat gained by insulation at the outlet segment was calculated to be 51.72 W.

4.6.3   Heat Rejected by the EAHE

Heat rejected by the EAHE prototype system can also be calculated based on the Equation 3.20 given in Section 3.5.3. It can be calculated by the temperature difference between the EAHE inlet temperature after insulation, T_i and EAHE outlet temperature before insulation, T_o. A sample calculation of heat rejected by the EAHE prototype at 3pm has been provided here. Heat rejected by the EAHE prototype from 8am to 6pm were summarized in Table 4.19.

At 3pm,

$$T_i = 36.9 \,°\text{C}$$

$$T_o = 31.3 \,°\text{C}$$

From Section 4.4,

$$\overset{\bullet}{m}_a = 0.09434 \,\text{kg/s}$$

while

$$c_{pa} = 1005 \,\text{kJ/kg} \cdot \text{K}$$

Therefore, heat rejected by the EAHE prototype is

$$q_{rejected,EAHE} = \dot{m}_a \, c_{pa} \left(T_i - T_o \right)$$

$$= 0.09434(1005)(36.9 - 31.3)$$

$$= 530.95 \, W$$

Table 4.19: Heat Rejected by the EAHE Prototype

Description\Time	Temperature Difference, $T_i - T_o$ (°C)	Heat Rejected by EAHE, $q_{rejected,EAHE}$ (W)
8:00 AM	0.7	66.37
9:00 AM	1.8	170.66
10:00 AM	2.3	218.07
11:00 AM	3.4	322.36
12:00 PM	3.7	350.80
1:00 PM	4.5	426.65
2:00 PM	4.9	464.58
3:00 PM	5.6	530.95
4:00 PM	5.5	521.46
5:00 PM	4.7	445.61
6:00 PM	4.4	417.17
Average	3.8	357.70

As can be observed from Table 4.19 above, the heat rejected by the EAHE prototype into the ground increased abruptly from 9am to 3pm and then it starts to decrease until 6pm. The maximum heat rejected by the EAHE prototype was 530.95 W which occurred at 3pm On the other hand, the minimum heat rejected by the EAHE prototype was 66.37 W which occurred at 8am. From 12pm to 6pm, the heat rejected by the EAHE prototype stayed in the range of 322.36 to 530.95 W. The average temperature difference and heat rejected by the EAHE prototype were calculated to be 3.8°C and 357.70 W respectively.

4.6.4 Heat Rejected from the Room

Heat rejected by the room which appear to be part of the heat rejected by the EAHE can also be calculated based on the equation given in Section 3.5.3 above. This can be calculated by the temperature difference between the room inlet temperature before insulation, $T_i{}'$ and room outlet temperature after insulation, $T_o{}'$. A sample calculation of heat rejected by the room at 3pm will be provided below. Heat rejected by the room from 8am to 6pm were summarized in Table 4.20.

At 3pm,

$$T_i{}' = 33.6\,°C$$

$$T_o{}' = 31.9\,°C$$

From Section 4.4,

$$\dot{m}_a = 0.09434\,kg/s$$

while

$$c_{pa} = 1005\ kJ/kg \cdot K$$

Therefore, heat rejected by the EAHE prototype is

$$q_{rejected,EAHE} = \dot{m}_a\,c_{pa}\left(T_i{}' - T_o{}'\right)$$

$$= 0.09434(1005)(33.6 - 31.9)$$

$$= 161.18\,W$$

Table 4.20: Heat Rejected from the Room

Description / Time	Temperature Difference, $T_i{}' - T_o{}'$ (ºC)	Heat Rejected from Room , $q_{rejected,room}$ (W)
8:00 AM	0.5	47.41
9:00 AM	1.3	123.26
10:00 AM	1.6	151.70
11:00 AM	1.7	161.18
12:00 PM	1.6	151.70
1:00 PM	1.7	161.18

2:00 PM	1.8	170.66
3:00 PM	1.7	161.18
4:00 PM	1.5	142.22
5:00 PM	2.3	218.07
6:00 PM	2.2	208.59
Average	1.63	154.28

As can be observed from Table 4.20 above, the heat rejected from the room also increased suddenly from 9am to 2pm and then it started to decrease from 3pm to 4pm. However, the heat rejected from the room start to increase back from 5pm to 6pm. The maximum heat rejected from the room was 218.07 W which occurred at 5pm. From 10am to 3pm, the heat rejected from the room stayed within the range of 151.70 to 170.66 W. The average temperature difference and heat rejected from the room were calculated to be 2.2 ^{o}C and 208.59 W respectively.

4.7   Cooling Performance of the EAHE Prototype System

4.7.1   Summarized of Heat Analysis

Figure 4.43 shows the chart that summarized heat gained and rejected at various segments against time determined in Section 4.6. As can be observed from Figure 4.43, the portion of heat gained by the insulation at the inlet segment over the total heat rejected by the EAHE prototype shown an increasing trend from 10am to 4pm. After that, it also shown a decreasing trend from 5pm to 6pm. On the other hand, the heat gained by the insulation at outlet segment remain relatively constant as compared to its inlet segment counterpart. As can be observed from Figure 4.43, the portion of heat rejected from the room over the total heat rejected by the EAHE prototype remained relatively constant throughout the day from 10am to 4pm. There was an increase in the portion of heat rejected by the room from 8am to 9am and 5pm to 6pm only.
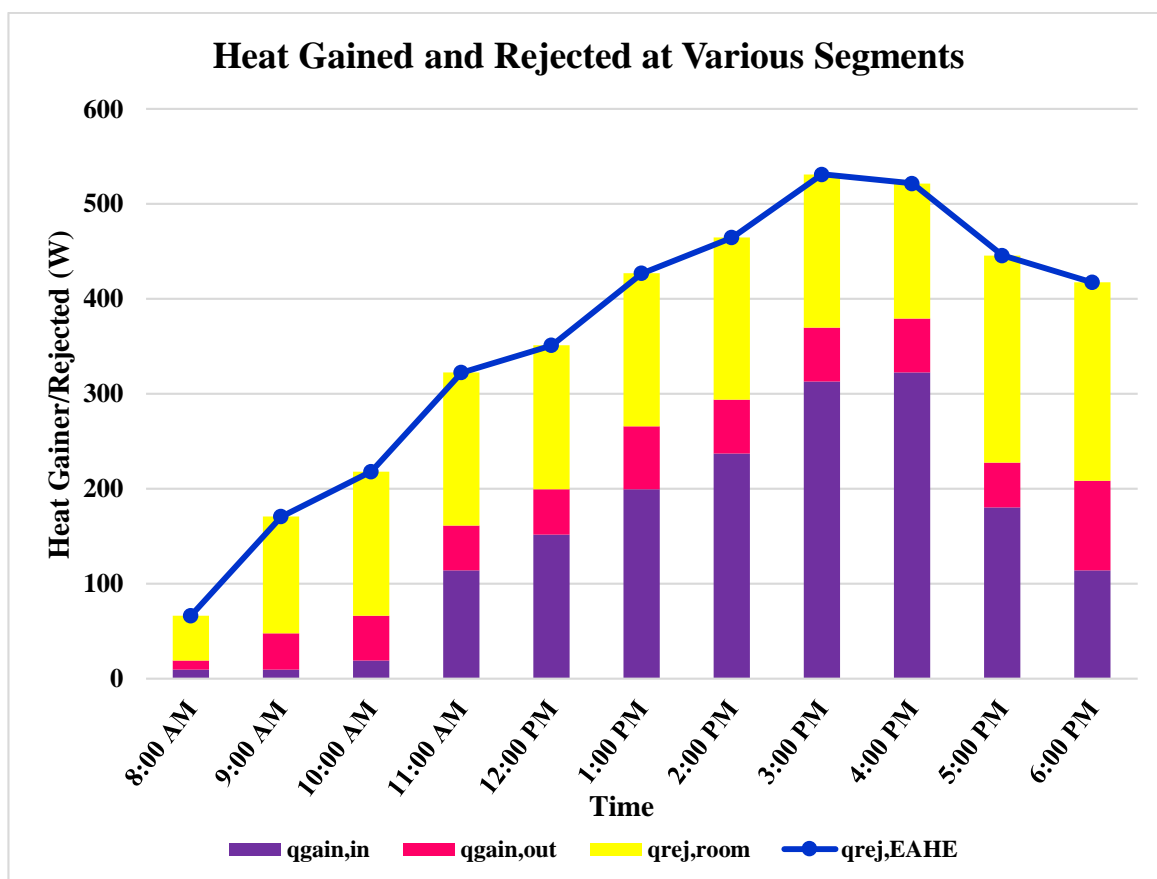
Figure 4.43: Heat Gained and Rejected at Various Segments

The portion of heat gained by the insulation at outlet segment remained almost constant because most of the segment was always shaded by the inlet segment when sunlight shone on it. However, the heat gained by the insulation at the inlet segment was being shone by sunlight that constantly increased its solar radiation intensity throughout the day from late morning until evening. After 5pm in the late evening, heat gained by the insulation at inlet segment start to decrease while the heat rejected from the room increased although the heat rejected by EAHE did not increased. Therefore, it could be concluded that heat rejected from the room was highly dependent on the heat gained at the insulation.

4.7.2   Percentage Reduction of Cooling Load Analysis

Percentage reduction of cooling load was defined as the fraction of heat rejected over the total cooling load either with or without the consideration of imperfect insulation. The ideal percentage reduction of cooling load is the fraction of heat rejected by the EAHE over the total cooling load without the consideration of imperfect insulation. On the other hand, actual percentage reduction of cooling is the fraction of heat rejected from the room over the total cooling load with the consideration of imperfect insulation. These can be calculated by Equation 3.21 and 3.22 that was given in Section 3.5.4. The maximum ideal and actual percentage reduction of cooling load has been provided here while the others were summarized in Table 4.21.

$$\text{Max \% Reduction of Cooling Load (ideal)} = \frac{Max(q_{rejected,EAHE})}{q_{load}} \times 100\%$$

$$= \frac{530.95}{952} \times 100\%$$

$$= 55.77\%$$

$$\text{Max \% Reduction of Cooling Load (actual)} = \frac{Max(q_{rejected,room})}{q_{load}} \times 100\%$$

$$= \frac{218.07}{952} \times 100\%$$

$$= 22.91\%$$

Table 4.21: Ideal and Actual Percentage Reduction of Cooling Load

Description / Time	Ideal Percentage Reduction of Cooling Load (%)	Actual Percentage Reduction of Cooling Load (%)
8:00 AM	6.97	4.98
9:00 AM	17.93	12.95
10:00 AM	22.91	15.93
11:00 AM	33.86	16.93
12:00 PM	36.85	15.93
1:00 PM	44.82	16.93

2:00 PM	48.80	17.93
3:00 PM	55.77	16.93
4:00 PM	54.78	14.94
5:00 PM	46.81	22.91
6:00 PM	43.82	21.91
Average	37.57	16.21
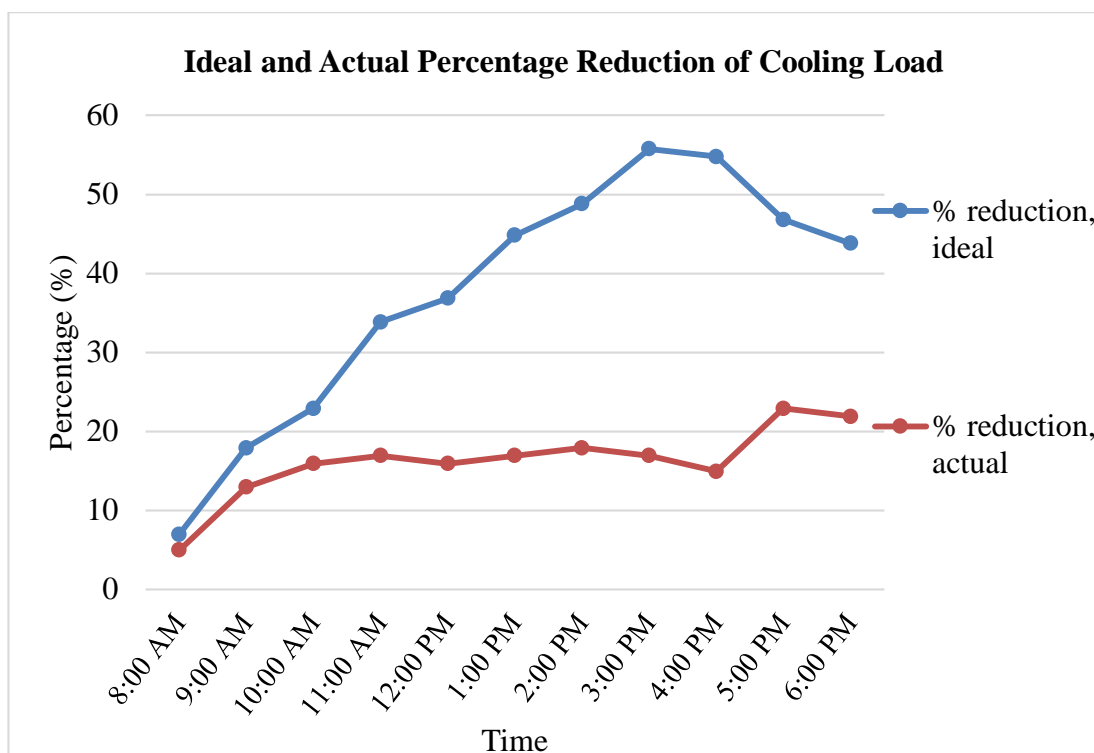
Figure 4.44: Ideal and Actual Percentage Reduction of Cooling Load

As can be observed from Figure 4.44, the ideal percentage reduction of cooling load increased almost linearly from 8am to 3pm. Then, it started to decrease from 4pm to 6pm. The maximum and average ideal percentage reduction of cooling load recorded was 55.77 % and 37.57 % respectively. Besides, the actual percentage reduction of cooling almost remained constant from 10am to 3pm follow by a drop at 4pm and increased abruptly from 4pm to 5pm. The maximum and average actual percentage reduction of cooling load recorded was 22.91 % and 16.21 % respectively. These findings indicated that the cooling capacity provided by the EAHE was not fully utilized by the room as the actual reduction in cooling load remained constant

when the ideal reduction in cooling load actually increased. Therefore, the actual percentage of reduction of cooling load could have been increased provided that a better insulation had been done.

4.7.3   EAHE Efficiency Analysis

EAHE efficiency was defined as the fraction of heat rejected from the room to the total heat rejected by the EAHE into the ground and can be calculated by Equation 3.21 given in Section 3.5.4. Table 4.22 tabulated the heat rejected by the room and EAHE and the associated EAHE efficiency at various time. Figure 4.45 shows the chart of heat rejected and EAHE efficiency.

Table 4.22: Heat Rejected and EAHE Efficiency

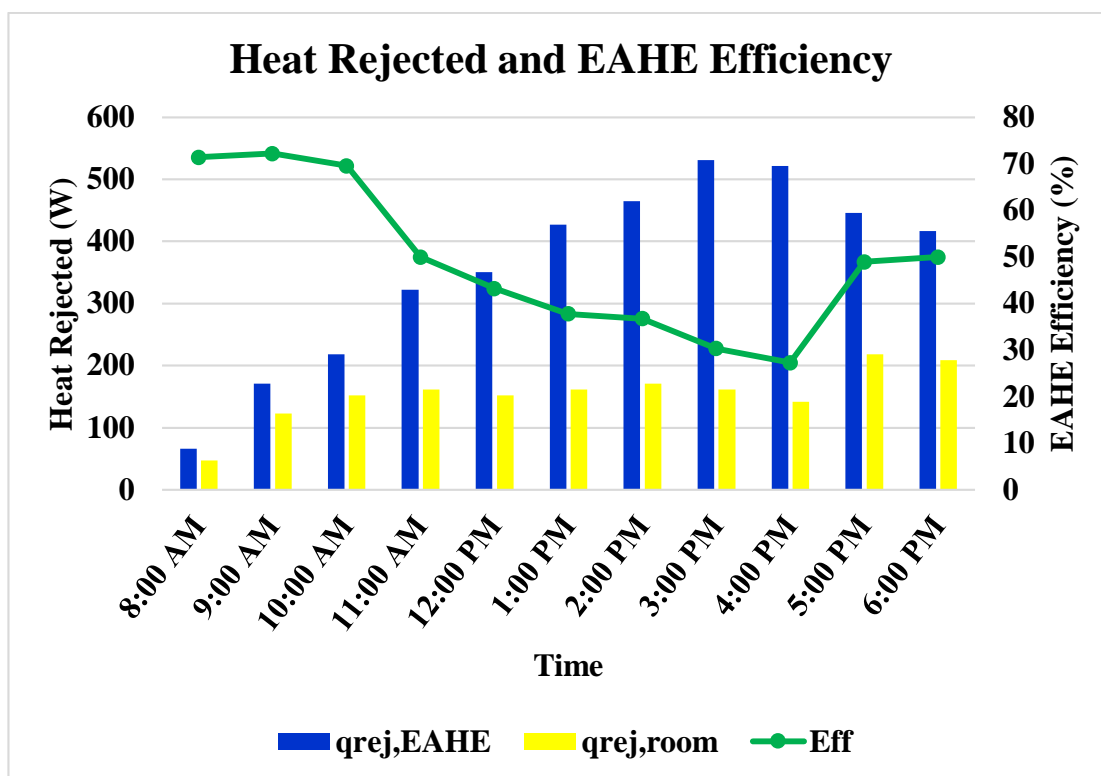| Description Time	Heat Rejected by EAHE, $q_{rejected,EAHE}$ (W)	Heat Rejected from Room , $q_{rejected,room}$ (W)	EAHE Efficiency $\dfrac{q_{rejected,room}}{q_{rejected,EAHE}} \times 100\%$ (%)
8:00 AM	66.37	47.41	71.43
9:00 AM	170.66	123.26	72.22
10:00 AM	218.07	151.70	69.57
11:00 AM	322.36	161.18	50.00
12:00 PM	350.80	151.70	43.24
1:00 PM	426.65	161.18	37.78
2:00 PM	464.58	170.66	36.73
3:00 PM	530.95	161.18	30.36
4:00 PM	521.46	142.22	27.27
5:00 PM	445.61	218.07	48.94
6:00 PM	417.17	208.59	50.00
Average	357.70	154.28	48.87

Figure 4.45: Heat Rejected and EAHE Efficiency

EAHE efficiency shown a decreasing trend from 10am to 4pm as shown in Table 4.22 and Figure 4.45. After that, the EAHE efficiency started to recover back from 5pm to 6pm. The maximum EAHE efficiency achieved by the prototype was 72.22 % at 9am in the morning while the lowest EAHE efficiency recorded was 27.27 % at 4pm. This trend was due to the increased of heat gained by the insulation which caused lesser portion of the heat rejected from room as the heat rejected by the EAHE had to remain at its maximum constant value. Besides, the average EAHE efficiency achieved by the EAHE prototype was 48.87 %. Last but not least, the result obtained also shown that the EAHE efficiency stayed in the range of 30 - 50 % for most of the time.

4.7.4   Coefficient of Performance (COP) Analysis

Two different COPs of the EAHE prototype were analysed which are the COP_{ideal} and COP_{actual}. COP_{ideal} is the ideal coefficient of performance of the EAHE prototype without the consideration of imperfect insulation. It was defined as the ratio of heat rejected by the EAHE system over the power dissipated which was fan power. On the other hand, COP_{actual} is the actual coefficient of performance of the EAHE prototype with the consideration of imperfect insulation. It was defined as the ratio of heat rejected from the room over the power dissipated. The formula for the calculation of COP_{ideal} and COP_{actual} were shown in Section 3.5.4 and had been provided again here.

$$COP_{ideal} = \frac{q_{rejected,EAHE}}{P_{fan}} = \dot{m}_a \, c_{pa} \left(T_i - T_o \right)$$

$$COP_{actual} = \frac{q_{rejected,room}}{P_{fan}} = \dot{m}_a \, c_{pa} \left(T_i^{'} - T_o^{'} \right)$$

Table 4.23 summarized the ideal and actual coefficient of performance of the EAHE prototype at various time. Figure 4.46 shown the graph of ideal and actual coefficient of performance of the EAHE prototype plotted against time according to the tabulated data in Table 4.23.

Table 4.23: Ideal and Actual COP of EAHE Prototype

Description Time	Ideal COP, COP_{ideal}	Actual COP, COP_{actual}
8:00 AM	1.33	0.95
9:00 AM	3.41	2.47
10:00 AM	4.36	3.03
11:00 AM	6.45	3.22
12:00 PM	7.02	3.03
1:00 PM	8.53	3.22
2:00 PM	9.29	3.41

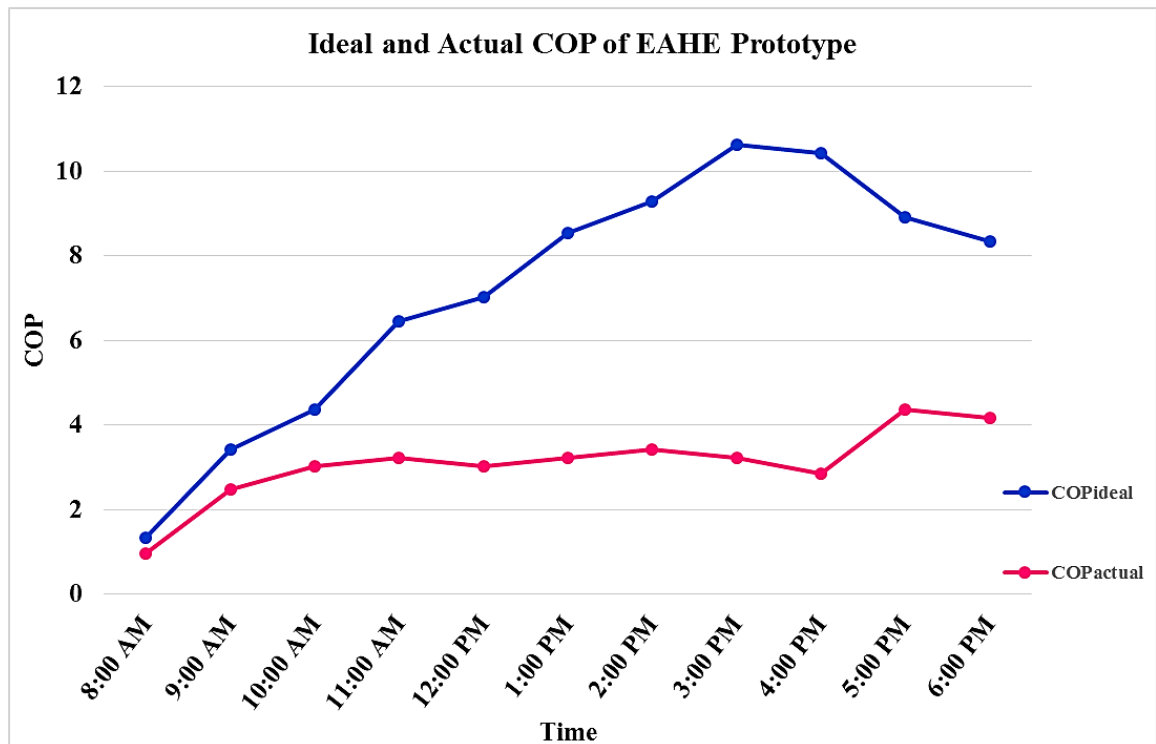|		
3:00 PM	10.62	3.22
4:00 PM	10.43	2.84
5:00 PM	8.91	4.36
6:00 PM	8.34	4.17
Average	7.15	3.09

Figure 4.46: Ideal and Actual COP of EAHE Prototype

Based on Table 4.23 and Figure 4.46, the maximum ideal and actual COPs achieved by the EAHE prototype were 10.62 and 4.36. These maximum ideal and actual COPs were achieved at 3pm and 5pm respectively. Both the ideal and actual COP of the EAHE prototype attained the lowest value at 8am in the morning. The lowest ideal and actual COPs attained were 1.33 and 0.95 respectively. Although ideal COP of the EAHE prototype increased throughout the day from morning to late afternoon, actual COP stayed in the range of 3.0 – 4.4 for most of the time. The ideal and actual average COPs achieved by the EAHE prototype were 7.15 and 3.09 respectively.

As can be observed from Figure 4.46, the difference between the ideal and actual COPs increased as time progressed from 10am to 4pm. This could be due to the decreased of heat rejected from the room that caused by increased of heat gained by insulation as explained previously in Section 4.6.4. On the other hand, the difference between the ideal and actual COPs reduced as time progress from 5pm to 6pm. This could be due to increase of heat rejected from the room as a result of the decreased of heat gained by insulation as the solar radiation intensity reduced in the evening.

Another reason that might have caused the increased of difference between ideal and actual COPs was the heat accumulation in the ground after prolong period of EAHE operation. The ground temperature near the EAHE pipe might have increased throughout the day rather than staying at a constant value as assumed due to heat rejected by the EAHE prototype. The maximum heat rejected by EAHE would be reduced if the ground temperature have increased. Thus, a detail investigation are required to determine whether there were heat accumulated and the effect corresponding effects on EAHE prototype.

In a nutshell, the actual COP of the EAHE could theoretically be increased if the heat gained by the insulation and heat accumulation in the ground could be reduced. These and the aforementioned findings again further reinforced the insight that cooling performance of the EAHE prototype system could be increased if the heat gained by the insulation could be reduced to a reasonable extent. Although the actual average COP (3.09) achieved was not low, there was plentiful of room for improvement to get it closer to the ideal average COP recorded (7.15).

CHAPTER 5

CONCLUSION AND RECOMMENDATIONS

5.1 Conclusion

One of the most important design aspect of the Earth-to-Air Heat Exchanger (EAHE) system was the determination of the suitable depth for the installation of the pipe. By experimental measurement, the most ideal or suitable depth for the installation of the EAHE prototype was determined to be 1.5m. The difference of ground temperature at the depth of 1.5 m and 2.0 m was very small during all the period of the time. The measured difference in mean maximum and minimum temperature at the depth of 1.5 m and 2.0 m was just $0.1\,°C$. Thus, it would be impractical to go for another 0.5 m deeper for the slight improvement in mean daily temperature range because it cannot be justified by the additional costing and time that might be incurred.

To design the EAHE prototype system, the cooling load imposed by the experimental residential room at UTAR LKCFES has been determined before others design parameters of the EAHE prototype could be established. For the aforementioned purpose, the Residential Load Factor (RLF) method has been used to conduct a cooling load analysis. The indoor and outdoor design temperature has been defined to be $29.4\,°C$ and $35\,°C$. The total cooling load determined using RLF method was 952 W. The EAHE prototype was designed to reject heat imposed by the cooling load determined under the worst condition recorded with temperature difference of room and ground, $\Delta T_{room\text{-}ground}$ of $8.3\,°C$. The finalized EAHE prototype design has selected PVC pipe of 3 in (80 mm) nominal diameter because it was well balanced in terms of space saving and total cost. The required pipe length of the EAHE prototype

using 3 in (80 mm) nominal diameter PVC pipe was calculated to be 11.1 m. However, the pipe length has been designed to be 11.6 m for simplicity of design.

A centrifugal exhaust fan has been designed and fabricated in this project that was being used in the EAHE prototype system to provide the static pressure, air velocity and mass flow rate required by the system. The centrifugal exhaust fan was designed through a trial-and-error approach using Flow Simulation of SolidWorks. Some of the important aforementioned specifications of the finalized centrifugal fan design was simulated using Flow Simulation and experimentally tested after it is fabricated. The simulated and experimental suction velocity was determined to be 17.1 m/s and 16.5 m/s with a percentage difference of 3.64%. The simulated and experimental mass flow rate was determined to be 0.16186 kg/s and 0.15618 kg/s with a percentage difference of 3.64% as well.

From the result obtained from experiment, the ideal and actual maximum percentage reduction of cooling load achieved were 55.77 % and 22.91 %. The average ideal and actual percentage reduction of cooling load achieved were 37.57 % and 16.21 % respectively. The maximum heat rejected by the EAHE and from the room were 530.95 W and 218.07 W. The average heat rejected by EAHA and from the room achieved were 357.70 W and 154.28 W respectively. On the other hand, the maximum and minimum EAHE efficiency achieved by the designed EAHE prototype were 72.22 % and 27.27% respectively. However, the result obtained shown that the EAHE efficiency stays in the range of 30 - 50 % only for most of the time and had achieved an average EAHE efficiency of 48.87 %.

The maximum ideal and actual COPs achieved by the EAHE prototype were 10.62 and 4.36. The lowest ideal and actual COPs attained by the EAHE prototype were 1.33 and 0.95. Although ideal COP of the EAHE prototype increased throughout the day from morning to late afternoon, actual COP stays in the range of 3.0 – 4.4 for most of the time. Besides, the average ideal and actual COPs achieved by the EAHE prototype were 7.15 and 3.09 respectively. In conclusion, the EAHE did achieve reasonably good cooling performance in terms of COP. However, it did not perform very well in terms of percentage of reduction of cooling load and EAHE efficiency due to too much heat gained by the insulation. Therefore, it is feasible to

implement EAHE cooling system in Malaysia if thermal insulation of the system could be carefully designed and monitored.

5.2   Recommendation

The thermal insulation on the pipe exposed to solar radiation could be improved in order to improve the cooling performance of the EAHE prototype. This is because result of the experiment has shown that the increases of heat gained by the insulation reduced the heat rejected from the room and hence reduced the actual coefficient of performance. To solve this problem, the EAHE pipes that is exposing to solar radiation could be covered with rock wool blanket or neoprene insulation foam.

Besides this, a larger centrifugal exhaust fan with a larger rated power could be used in place of the 50 W fan but with the condition that it must be placed outside the building to avoid unnecessary heat dissipation. By using a larger centrifugal exhaust fan, the air velocity and pipe length could be increased in the EAHE design. This will increase the amount of heat rejected in to the ground by the EAHE system and at the same will avoid heat accumulation in the ground. This is because higher air velocity means lower heat transfer as the air would have lesser time to transfer heat across the pipe but the loss in that amount of heat transfer can be made up by having a longer pipe. The benefit of having higher air velocity is that heat will not accumulate easily in the ground near where the EAHE pipes were buried.

REFERENCES

ASHRAE, 2009. 2009 *ASHRAE Handbook – Fundamentals. Chapter 14.*

Al-Ajmi, A., Loveday, D.L., Hanby, V.I., 2006. The cooling potential of earth-air heat exchangers for domestic buildings in a desert climate. *Building and Environment*, 41(3), pp. 235-244.

ATKC e-Commerce Warehouse, 2015. *PVC Pipes & Fittings*. [online]. Available at: <http://www.ewarehouse.atkc.com.my/plumbing/pvc-pipe-fittings&filter=161> [Assessed 1 January 2015].

EIA U.S. Energy Information Administration, 2013. *International Energy Outlook 2013.* [online] Available at: <http://www.eia.gov/forecasts/ieo/world.cfm> [Accessed 5 August 2014]

Energy Commission, 2011. *Malaysia Energy Information Hub: Electricity - Final Electricity Consumption.* [online] Available at < http://meih.st.gov.my/statistics> [Accessed 6 August 2014]

Germany Energy Agency, 2002. *Geothermal energy.* [online] Available at: < http://www.renewables-made-in-germany.com/en/renewables-made-in-germany-start/geothermal.html> [Accessed 7 August 2014]

Ghosal, M.K., Tiwari, G.N., 2006. Modeling and parametric studies for thermal performance of earth to air heat exchanger integrated with a greenhouse. *Energy Conversion and Management*, 47(13-14), pp. 1779-1798.

Incopera, F. P., 2002. *Introduction to Heat Transfer.* 4th ed. Singapore: John Wiley & Sons.

Malaysia Metrological Department, 2015. *Buletin Cuaca Bulana*n. [online]. Available at: <http://www.met.gov.my/index.php?option=com_content&task=view&id=842&Itemid=1586> [Assessed 29 February 2015].

Mongkon, S., Thepa, S., Namprakai, P., Pratinthong, N., 2014. Cooling performance assessment of horizontal earth tube system and effect on planting in tropical greenhouse. *Energy Conversion and Management,* 78, pp. 225-236.

Nik, A.R., Kasran, B. and Hassan, A., 1986. Soil Temperature Regimes under Mixed Dipterocarp Forests of Peninsular Malaysia. *Pertanika*, 9(3), 277-284.

Ozgener, L., 2011. Ozgener, O., 2011. A review on the experimental and analytical analysis of the earth to air heat exchanger (EAHE) systems in Turkey. *Renewable and Sustainable Energy Reviews,* 15(9), pp. 4483-4490.

Peretti, C., Zarella, A., Carli, M.D., Zecchin, R., 2013. The design and environmental evaluation of earth-to-air heat exchangers (EAHE). A literature review. Renewable and Sustainable Energy Reviews, 28, pp. 107-116.

Pfafferott, J., 2003. Evaluation of earth-to-air heat exchangers with a standardised method to calculate energy efficiency. *Energy and Building*, 35(10), pp. 971-983.

Reimann, G., 2007. Ground Cooling of Ventilation Air for energy Efficient House in Malaysia: A Case Study of the CoolTek House. In: *Conference on Sustainable Building South East Asia.* Malaysia, 5-7 November 2007. Johor, Malaysia: Institute Sultan Iskandar of Urban Habitat and Highrise. Available at <http://www.irbnet.de/daten/iconda/CIB11369.pdf> Accessed date [19 August 2014].

Sanusi, A.N.Z., Li, S. and Zamri, A.A.A., 2014. Seeking Underground for Potential Heat Sink in Malaysia for Earth Air Heat Exchanger (EAHE) Application. *Australian Journal of Basic and Applied Sciences*, 8 (8), pp. 54-57.

Tan, K. S., 2013. Investigation into Effectiveness of Heat Transfer for Water-Circulated Geothermal Cooling System with Polyethylene Ground Heat Exchange Loop.

The European Technology Platform on Renewable Heating and Cooling, 2012. *Strategic Research Priorities for Geothermal Technology.* [online] Available at: <http://www.rhc-platform.org/fileadmin/Publications/Geothermal_SRA.pdf> [Accessed 6 August 2014]

Woodson, T., Coulibaly, Y. and Traore, E.S., 2012. Earth-air Heat Exchangers for Passive Air Conditioning: Case Study Burkina Faso. *Journals of Construction in Developing Countries*, 17(1), pp. 21-32.

Wu, H., Wang, S., Zhu, D., 2007. Modelling and evaluation of cooling capacity of earth-air-pipe systems. *Energy Conversion and Management*, 48(5), pp. 1462-1471.

APPENDICES

APPENDIX A: Tables and Graph of Ground, Room and Environment Temperature

Table A-1: Ground, Room and Environment Temperature on 1 March 2015 (Day 1)

Description / Time	0.5 m (°C)	1.0 m (°C)	1.5 m (°C)	2.0 m (°C)	Room temperature, $T_r{'}$ (°C)	Environment temperature, T_{env} (°C)
08:00 AM	28.1	27.9	27.6	27.6	27.2	28.7
09:00 AM	28	27.8	27.5	27.5	28	30
10:00 AM	28.6	28.1	27.4	27.4	32.2	31.3
11:00 AM	29.5	28.4	27.4	27.3	34.3	32.6
12:00 PM	30.2	28.9	28	27.7	36	34.2
01:00 PM	30.9	29.1	28.6	28.2	37.3	35.5
02:00 PM	31.4	29.7	28.9	28.7	37	36.8
03:00 PM	31.9	30.9	29.4	29.1	36.6	37.7
04:00 PM	31	31.2	29.7	29.6	35.9	37.2
05:00 PM	30	30.4	30	29.9	34	36.4
06:00 PM	28.9	29.1	29.1	29	30.8	35.1

Figure A-1: Ground, Room and Environment Temperature on 1 March 2015 (Day 1)
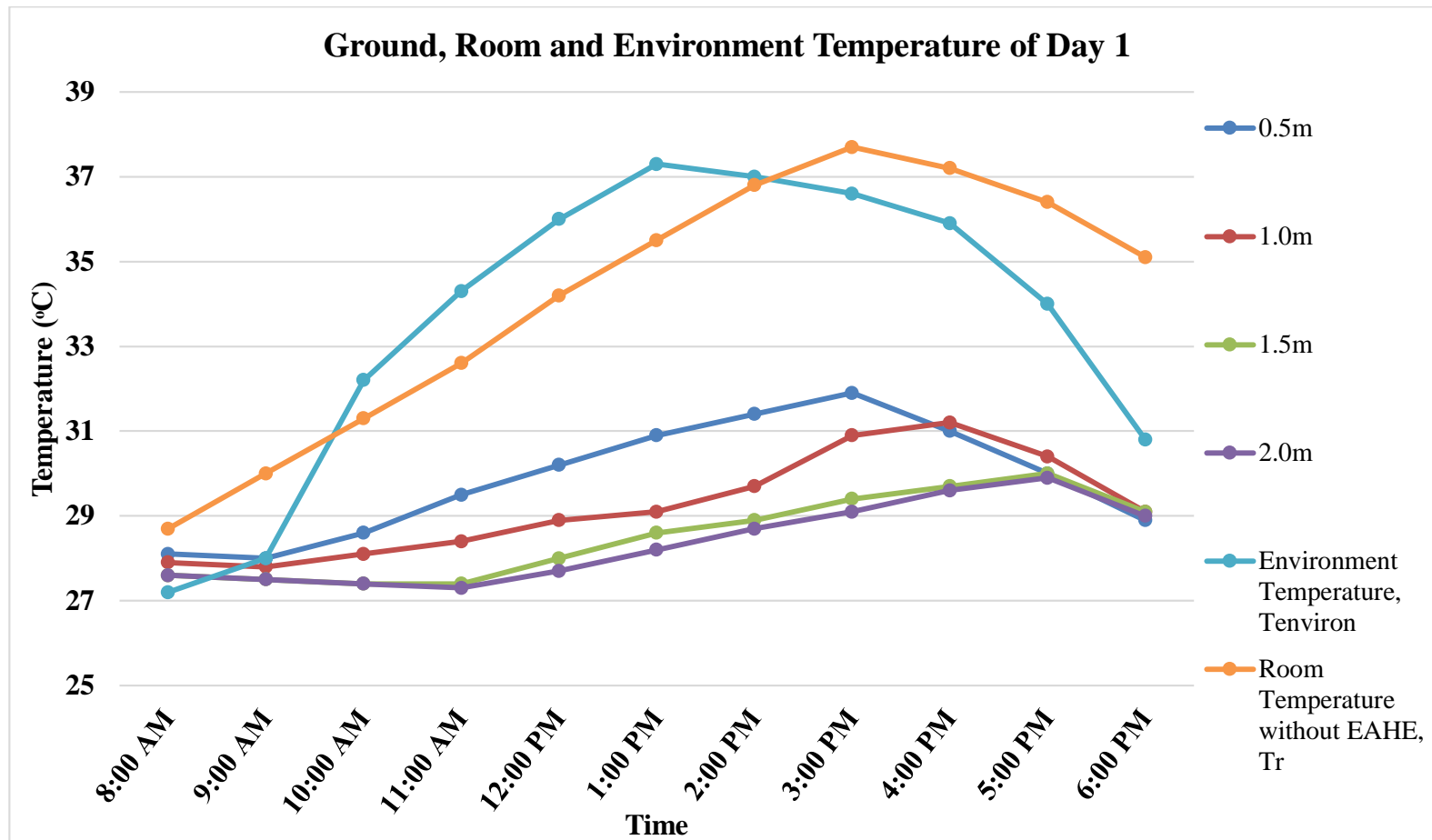
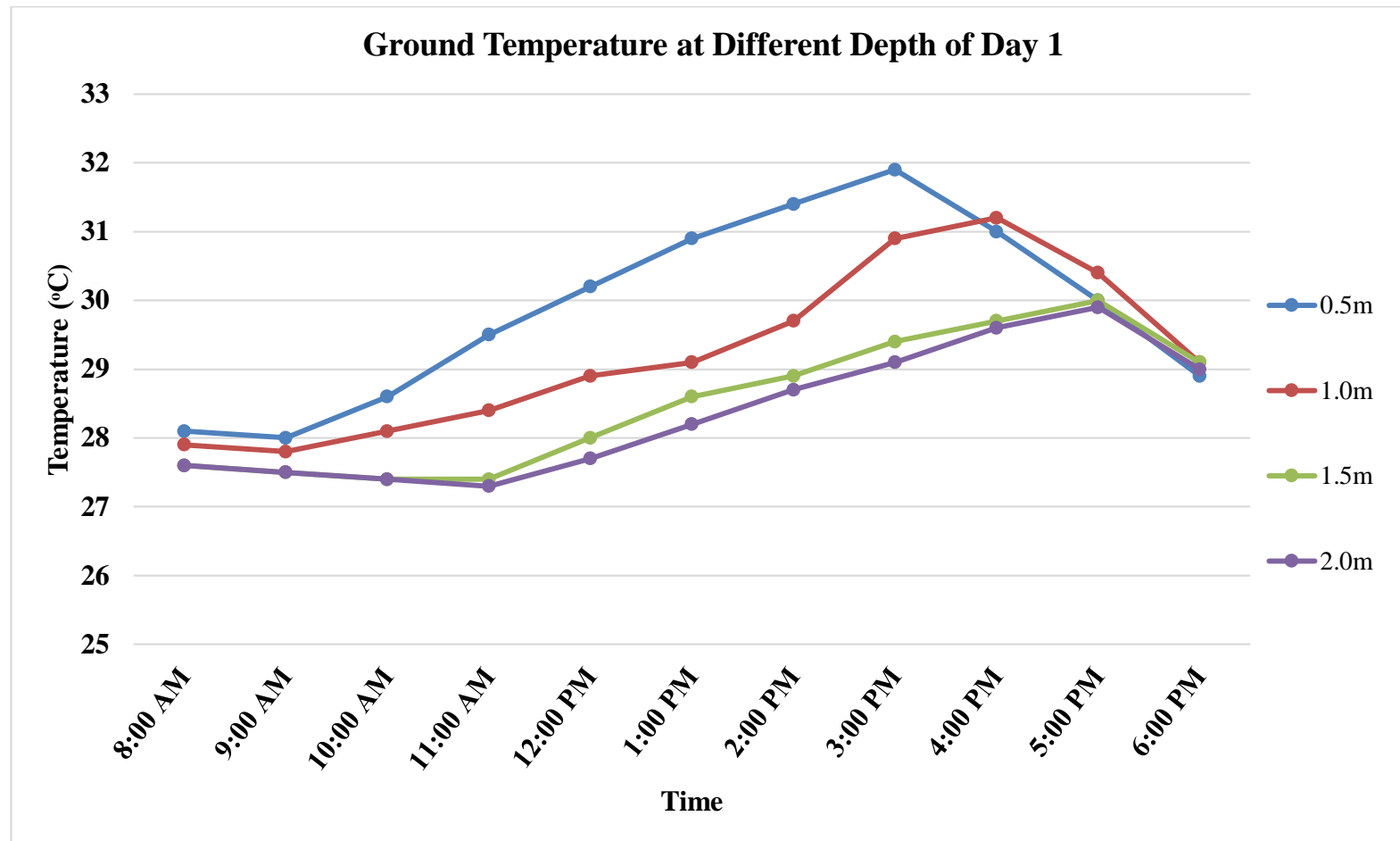**Figure A-2: Ground Temperature at Different Depth on 1 March 2015 (Day 1)**

Table A-2: Ground, Room and Environment Temperature on 2 March 2015 (Day 2)

Description / Time	0.5 m (°C)	1.0 m (°C)	1.5 m (°C)	2.0 m (°C)	Room temperature, T_r' (°C)	Environment temperature, T_{env} (°C)
08:00 AM	27.9	27.7	27.4	27.4	27	28.5
09:00 AM	27.8	27.6	27.3	27.3	27.8	29.8
10:00 AM	28.4	27.9	27.2	27.2	32	31.1
11:00 AM	29.2	28.1	27.1	27	34	32.3
12:00 PM	29.7	28.4	27.5	27.2	35.5	33.7
01:00 PM	30.6	28.8	28.3	27.9	37	35.2
02:00 PM	31	29.3	28.5	28.3	36.6	36.4
03:00 PM	31.4	30.4	28.9	28.6	36.1	37.2
04:00 PM	30.5	30.7	29.2	29.1	35.4	36.7
05:00 PM	29.2	29.6	29.2	29.1	33.2	35.6
06:00 PM	28.8	29	29	28.9	30.7	35

Figure A-3: Ground, Room and Environment Temperature on 2 March 2015 (Day 2)
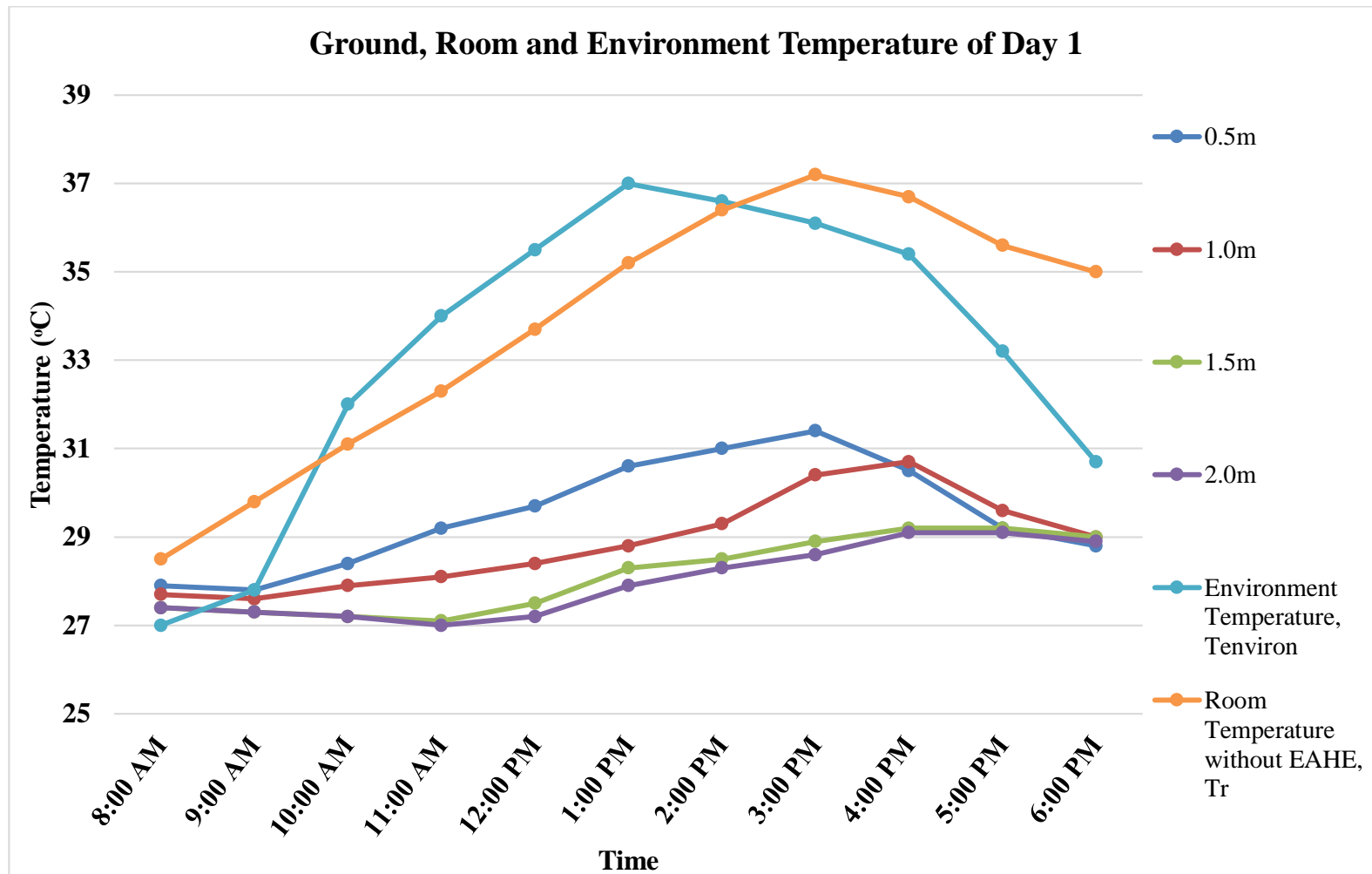
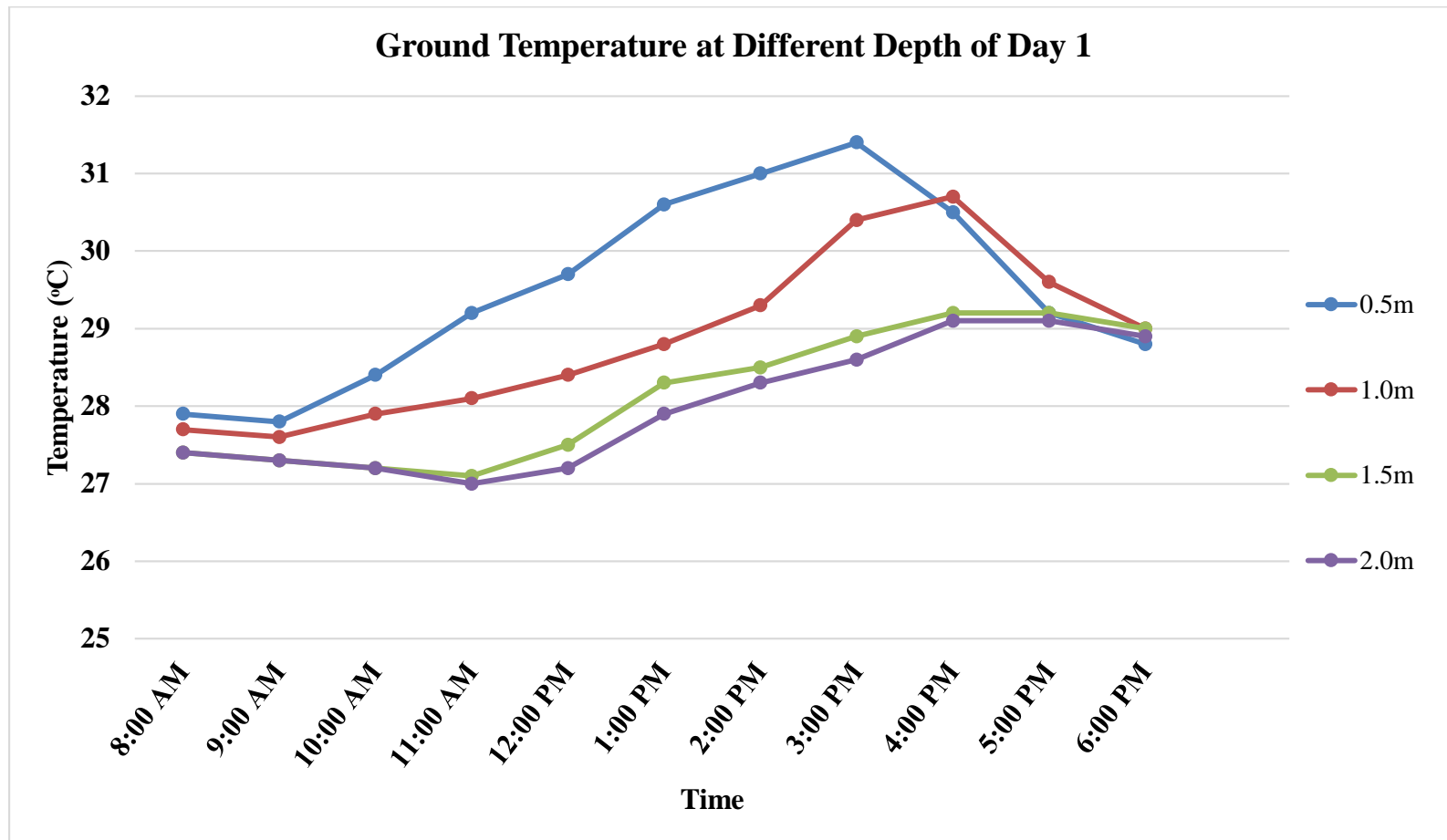**Figure A-4: Ground Temperature at Different Depth on 2 March 2015 (Day 2)**

Table A-3: Ground, Room and Environment Temperature on 3 March 2015 (Day 3)

Description / Time	0.5 m (°C)	1.0 m (°C)	1.5 m (°C)	2.0 m (°C)	Room temperature, $T_r{'}$ (°C)	Environment temperature, T_{env} (°C)
08:00 AM	27.7	27.5	27.2	27.2	26.8	28.3
09:00 AM	27.6	27.4	27.1	27.1	27.6	29.6
10:00 AM	28.2	27.7	27	27	31.8	30.9
11:00 AM	28.9	27.8	26.8	26.7	33.7	32
12:00 PM	29.5	28.2	27.3	27	35.3	33.5
01:00 PM	30.3	28.5	28	27.6	36.7	34.9
02:00 PM	30.9	29.2	28.4	28.2	36.5	36.3
03:00 PM	31.2	30.2	28.7	28.4	35.9	37
04:00 PM	30.3	30.5	29	28.9	35.2	36.5
05:00 PM	29.3	29.7	29.3	29.2	33.3	35.7
06:00 PM	28.7	28.9	28.9	28.8	30.6	34.9

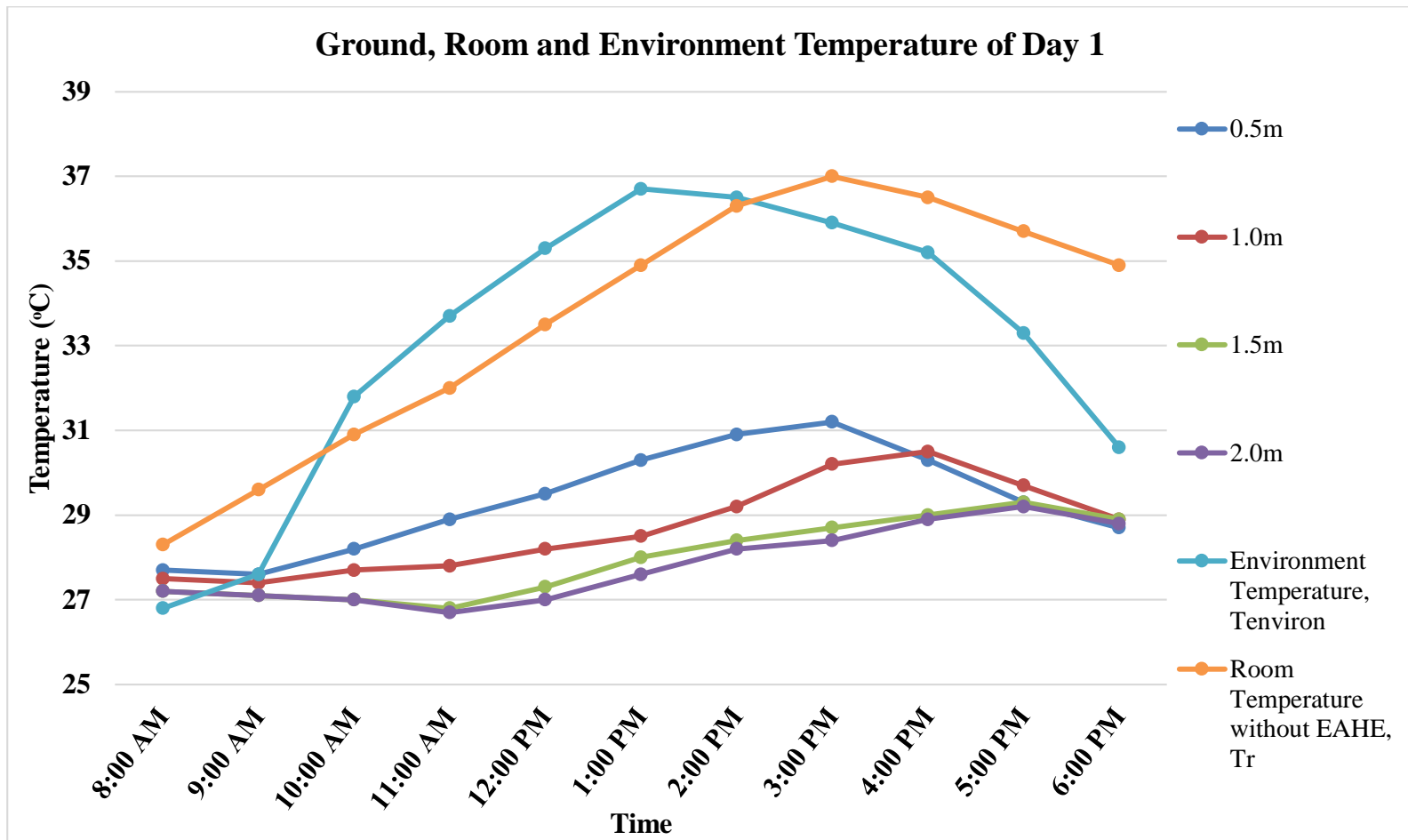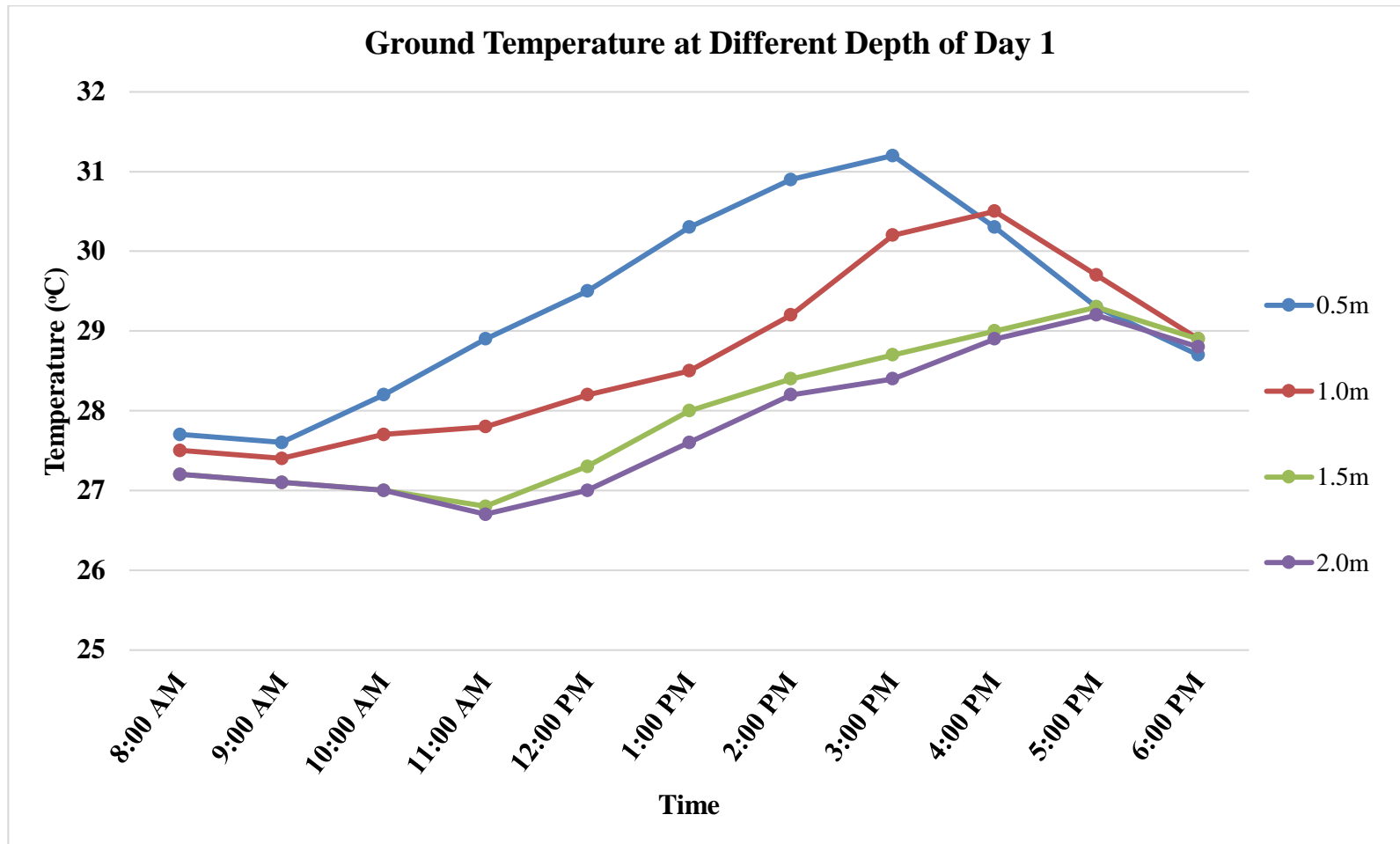**Figure A-5: Ground, Room and Environment Temperature on 3 March 2015 (Day 3)**

Figure A-6: Ground Temperature at Different Depth on 3 March 2015 (Day 3)

APPENDIX B: Calculation of Required Length for Different Diameter

1. For nominal diameter of 25 mm

From Figure 3.15,

D_o = 31.2 mm = 0.0312 m

D_i = 33.4 mm = 0.0334 mm

Conductive thermal resistance of the pipe, $R_{conductive}$

$$R_{conductive} = \frac{\ln(D_o / D_i)}{2 \times \pi \times L \times k_p}$$

$$= \frac{\ln(0.0334 / 0.0312)}{2 \times \pi \times L \times 0.19}$$

$$= 0.05707 / L$$

Mass flow rate of air, $\dot{m}_a$

$$\dot{m}_a = \frac{\rho \times \pi \times D_i^2 \times V_{avg}}{4}$$

$$= \frac{1.205 \times \pi \times (0.0312)^2 \times 13.8}{4}$$

$$= 0.01272 \text{ kg/s}$$

Reynolds number of the pipe flow, Re

$$Re = \frac{4\dot{m}_a}{\pi \times D_i \times \mu}$$

$$= \frac{4(0.01272)}{\pi(0.0312)(0.000015573)}$$

$$= 33,316$$

Friction factor, f

$$f = (0.79 \ln \mathrm{Re} - 1.64)^{-2}$$

$$= (0.79 \ln(33,312) - 1.64)^{-2}$$

$$= 0.02305$$

Prantl number, Pr

$$\mathrm{Pr} = \frac{c_{pa} \times \mu}{k_a}$$

$$= \frac{1005 \times 0.000015573}{0.0257}$$

$$= 0.61$$

Nusselt number, Nu

$$Nu = \frac{\left(\dfrac{f}{8}\right)(\mathrm{Re} - 1000)\mathrm{Pr}}{1 + 12.7\left(\dfrac{f}{8}\right)^{0.5}(\mathrm{Pr}^{2/3} - 1)}$$

$$= \frac{\left(\dfrac{0.02305}{8}\right)(33,316 - 1000)0.61}{1 + 12.7\left(\dfrac{0.02305}{8}\right)^{0.5}(0.61^{2/3} - 1)}$$

$$= 72.12$$

Convective heat transfer coefficient, h_a

$$h_a = Nu \times \frac{k_a}{D_i}$$

$$= 72.12 \times \frac{0.0257}{0.0334}$$

$$= 59.4106 \ \text{W/m}^2 \cdot \text{K}$$

Convective thermal resistance of the air, $R_{convective}$

$$R_{convective} = \frac{1}{\pi \times D_i \times h_a \times L}$$

$$= \frac{1}{\pi \times 0.0312 \times 59.4106 \times L}$$

$$= 0.17170/L$$

The required length of the pipe, L

$$L = \frac{q_{load} \times R_{total}}{\Delta T_{room-ground}}$$

$$= \frac{952 \times 0.22877}{8.3}$$

$$= 26.24 \ \text{m}$$

2. For nominal diameter of 50 mm

From Figure 3.15,

D_o = 57.7 mm = 0.0577 m

D_i = 60.2 mm = 0.0602 m

Conductive thermal resistance of the pipe, $R_{conductive}$

$$R_{conductive} = \frac{\ln(D_o / D_i)}{2 \times \pi \times L \times k_p}$$

$$= \frac{\ln(0.0602/0.0577)}{2 \times \pi \times L \times 0.19}$$

$$= 0.03552/L$$

Mass flow rate of air, $\dot{m}_a$

$$\dot{m}_a = \frac{\rho \times \pi \times D_i^2 \times V_{avg}}{4}$$

$$= \frac{1.205 \times \pi \times (0.0577)^2 \times 13.8}{4}$$

$$= 0.04349 \ \text{kg/s}$$

Reynolds number of the pipe flow, Re

$$Re = \frac{4\dot{m}_a}{\pi \times D_i \times \mu}$$

$$= \frac{4(0.04349)}{\pi(0.0577)(0.000015573)}$$

$$= 61{,}613$$

Friction factor, f

$$f = (0.79 \ln Re - 1.64)^{-2}$$

$$= (0.79 \ln(61{,}613) - 1.64)^{-2}$$

$$= 0.01999$$

Prantl number, Pr

$$Pr = \frac{c_{pa} \times \mu}{k_a}$$

$$= \frac{1005 \times 0.000015573}{0.0257}$$

$$= 0.61$$

Nusselt number, Nu

$$Nu = \frac{\left(\dfrac{f}{8}\right)(\text{Re}-1000)\text{Pr}}{1+12.7\left(\dfrac{f}{8}\right)^{0.5}(\text{Pr}^{2/3}-1)}$$

$$= \frac{\left(\dfrac{0.01999}{8}\right)(61{,}613-1000)0.61}{1+12.7\left(\dfrac{0.01999}{8}\right)^{0.5}(0.61^{2/3}-1)}$$

$$= 113.99$$

Convective heat transfer coefficient, h_a

$$h_a = Nu \times \frac{k_a}{D_i}$$

$$= 113.99 \times \frac{0.0257}{0.0577}$$

$$= 50.7733 \ \text{W/m}^2 \cdot \text{K}$$

Convective thermal resistance of the air, $R_{convective}$

$$R_{convective} = \frac{1}{\pi \times D_i \times h_a \times L}$$

$$= \frac{1}{\pi \times 0.0577 \times 50.7733 \times L}$$

$$= 0.10864/L$$

The required length of the pipe, L

$$L = \frac{q_{load} \times R_{total}}{\Delta T_{room-ground}}$$

$$= \frac{952 \times 0.10864}{8.3}$$

$= 16.54 \ \text{m}$

3. For nominal diameter of 100 mm

From Figure 3.15,

$D_o = 111.8 \ \text{mm} = 0.1118 \ \text{m}$

$D_i = 114.1 \ \text{mm} = 0.1141 \ \text{m}$

Conductive thermal resistance of the pipe, $R_{conductive}$

$$R_{conductive} = \frac{\ln(D_o / D_i)}{2 \times \pi \times L \times k_p}$$

$$= \frac{\ln(0.1141 / 0.1118)}{2 \times \pi \times L \times 0.19}$$

$$= 0.01706 / L$$

Mass flow rate of air, $\dot{m}_a$

$$\dot{m}_a = \frac{\rho \times \pi \times D_i^2 \times V_{avg}}{4}$$

$$= \frac{1.205 \times \pi \times (0.1118)^2 \times 13.8}{4}$$

$$= 0.16327 \ \text{kg/s}$$

Reynolds number of the pipe flow, Re

$$Re = \frac{4 \dot{m}_a}{\pi \times D_i \times \mu}$$

$$= \frac{4(0.16327)}{\pi(0.1118)(0.000015573)}$$

$$= 119{,}381$$

Friction factor, f

$$f = (0.79 \ln \text{Re} - 1.64)^{-2}$$
$$= (0.79 \ln(119{,}381) - 1.64)^{-2}$$
$$= 0.01734$$

Prantl number, Pr

$$\text{Pr} = \frac{c_{pa} \times \mu}{k_a}$$
$$= \frac{1005 \times 0.000015573}{0.0257}$$
$$= 0.61$$

Nusselt number, Nu

$$Nu = \frac{\left(\dfrac{f}{8}\right)(\text{Re} - 1000)\text{Pr}}{1 + 12.7\left(\dfrac{f}{8}\right)^{0.5}(\text{Pr}^{2/3} - 1)}$$

$$= \frac{\left(\dfrac{0.01734}{8}\right)(119{,}381 - 1000)0.61}{1 + 12.7\left(\dfrac{0.01734}{8}\right)^{0.5}(0.61^{2/3} - 1)}$$

$$= 188.85$$

Convective heat transfer coefficient, h_a

$$h_a = Nu \times \frac{k_a}{D_i}$$
$$= 188.85 \times \frac{0.0257}{0.1118}$$
$$= 43.4115 \ \text{W/m}^2 \cdot \text{K}$$

Convective thermal resistance of the air, $R_{convective}$

$$R_{convective} = \frac{1}{\pi \times D_i \times h_a \times L}$$

$$= \frac{1}{\pi \times 0.1118 \times 43.4115 \times L}$$

$$= 0.06558/L$$

The required length of the pipe, L

$$L = \frac{q_{load} \times R_{total}}{\Delta T_{room-ground}}$$

$$= \frac{952 \times 0.08263}{8.3}$$

$$= 9.48 \text{ m}$$

4. For nominal diameter of 125 mm

From Figure 3.15,

$D_o = 134.7 \text{ mm} = 0.1374 \text{ m}$

$D_i = 140.0 \text{ mm} = 0.1400 \text{ m}$

Conductive thermal resistance of the pipe, $R_{conductive}$

$$R_{conductive} = \frac{\ln(D_o / D_i)}{2 \times \pi \times L \times k_p}$$

$$= \frac{\ln(0.1374 / 0.1400)}{2 \times \pi \times L \times 0.19}$$

$$= 0.01570/L$$

Mass flow rate of air, $\dot{m}_a$

$$\dot{m}_a = \frac{\rho \times \pi \times D_i^2 \times V_{avg}}{4}$$

$$= \frac{1.205 \times \pi \times (0.1374)^2 \times 13.8}{4}$$

$$= 0.24660 \ \text{kg/s}$$

Reynolds number of the pipe flow, Re

$$Re = \frac{4\dot{m}_a}{\pi \times D_i \times \mu}$$

$$= \frac{4(0.24660)}{\pi(0.1374)(0.000015573)}$$

$$= 146{,}717$$

Friction factor, f

$$f = (0.79 \ln Re - 1.64)^{-2}$$

$$= (0.79 \ln(146{,}717) - 1.64)^{-2}$$

$$= 0.01661$$

Prantl number, Pr

$$Pr = \frac{c_{pa} \times \mu}{k_a}$$

$$= \frac{1005 \times 0.000015573}{0.0257}$$

$$= 0.61$$

Nusselt number, Nu

$$Nu = \frac{\left(\dfrac{f}{8}\right)(Re-1000)Pr}{1+12.7\left(\dfrac{f}{8}\right)^{0.5}(Pr^{2/3}-1)}$$

$$= \frac{\left(\dfrac{0.01661}{8}\right)(146,717-1000)0.61}{1+12.7\left(\dfrac{0.01661}{8}\right)^{0.5}(0.61^{2/3}-1)}$$

$$= 221.55$$

Convective heat transfer coefficient, h_a

$$h_a = Nu \times \frac{k_a}{D_i}$$

$$= 221.55 \times \frac{0.0257}{0.1374}$$

$$= 41.4404 \ W/m^2 \cdot K$$

Convective thermal resistance of the air, $R_{convective}$

$$R_{convective} = \frac{1}{\pi \times D_i \times h_a \times L}$$

$$= \frac{1}{\pi \times 0.1374 \times 41.4404 \times L}$$

$$= 0.05590/L$$

The required length of the pipe, L

$$L = \frac{q_{load} \times R_{total}}{\Delta T_{room-ground}}$$

$$= \frac{952 \times 0.07160}{8.3}$$

$$= 8.21 \ m$$

APPENDIX C: Tables and Graph Various Temperature of the EAHE Prototype System

Table A-4: Various Temperature of the EAHE Prototype System on 26 March 2015 (Day 1)

Description Time	T_i (ºC)	T_o (ºC)	T_i' (ºC)	T_o' (ºC)	T_r (ºC)	$T_{environ}$ (ºC)
8:00 AM	28.1	27.4	28	27.5	28	27
9:00 AM	29.1	27.4	29.1	27.8	29.1	29.8
10:00 AM	29.8	27.5	29.6	28	29.7	32.2
11:00 AM	31.3	27.9	30.1	28.4	30	33.9
12:00 PM	32.2	28.5	30.6	29	30.6	35.1
1:00 PM	34	29.5	31.9	30.2	31.8	36.6
2:00 PM	35.1	30.2	32.6	30.8	32.4	36.5
3:00 PM	36.7	31.1	33.4	31.7	33.2	36.3
4:00 PM	37.1	31.6	33.7	32.6	33.5	35.4
5:00 PM	35.5	30.7	33.6	31.2	33.5	33.8
6:00 PM	34.4	29.7	33.2	30.8	33.1	32

Figure A-7: Various Temperature of the EAHE Prototype System on 26 March 2015 (Day 1)
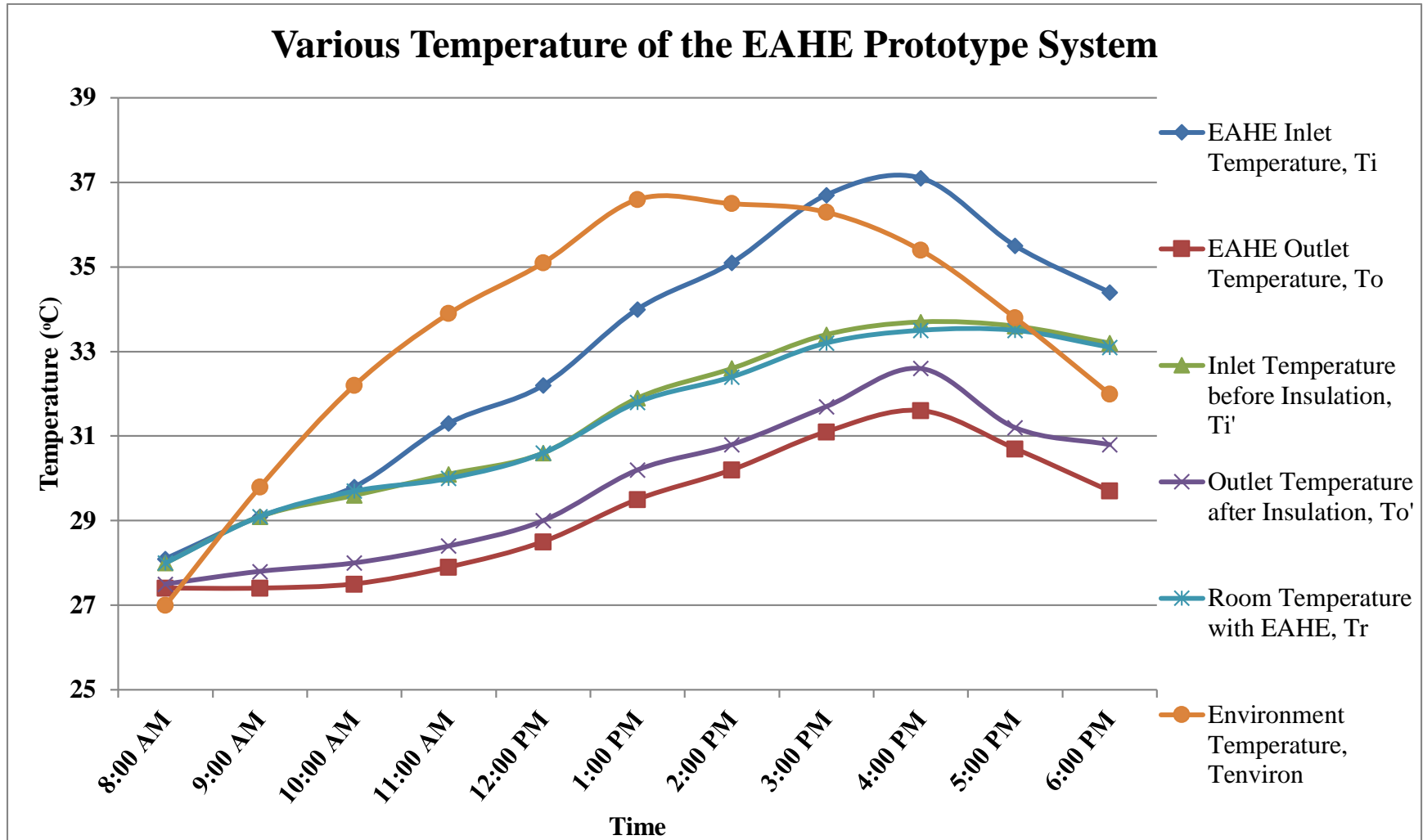
Table A-5: Various Temperature of the EAHE Prototype System on 27 March 2015 (Day 2)

Description / Time	T_i (ºC)	T_o (ºC)	T_i' (ºC)	T_o' (ºC)	T_r (ºC)	$T_{environ}$ (ºC)
8:00 AM	27.9	27.2	27.8	27.3	27.8	26.8
9:00 AM	29.4	27.2	28.9	27.6	28.9	29.6
10:00 AM	29.8	27.6	29.7	28.1	29.8	32.3
11:00 AM	31.6	28.2	30.4	28.7	30.3	34.2
12:00 PM	32.9	29.2	31.3	29.7	31.3	35.8
1:00 PM	34.7	30.2	32.6	30.9	32.5	37.3
2:00 PM	35.6	30.7	33.1	31.3	32.9	37
3:00 PM	37.1	31.5	33.8	32.1	33.6	36.7
4:00 PM	37.5	32	34.1	32.6	33.9	35.8
5:00 PM	35.7	30.9	33.8	31.4	33.7	34
6:00 PM	34.9	30.1	33.7	31	33.6	32.5

Figure A-8: Various Temperature of the EAHE Prototype System on 27 March 2015 (Day 2)
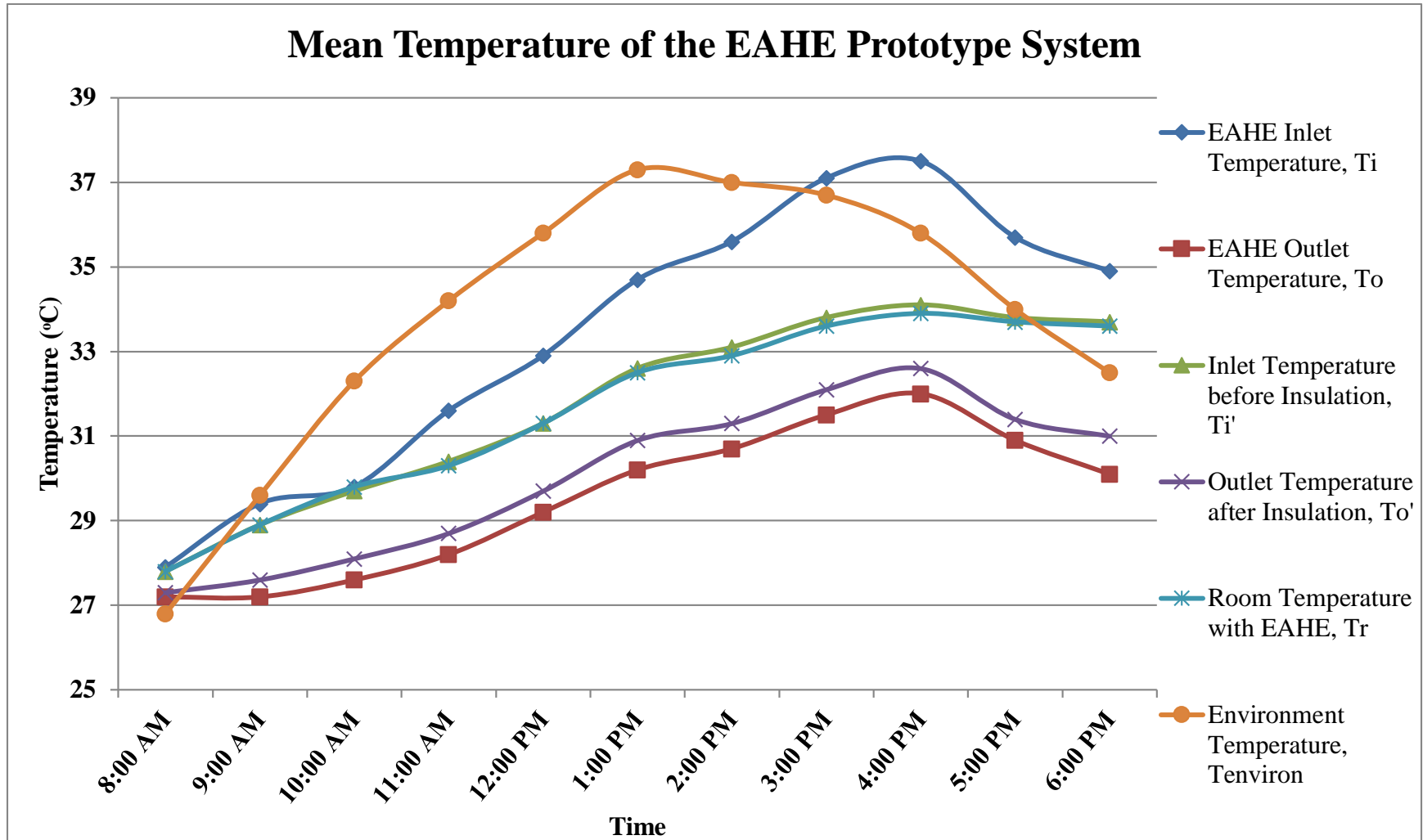
Table A-6: Various Temperature of the EAHE Prototype System on 28 March 2015 (Day 3)

Description / Time	T_i (°C)	T_o (°C)	T_i' (°C)	T_o' (°C)	T_r (°C)	$T_{environ}$ (°C)
8:00 AM	28.3	27.6	28.2	27.7	28.2	27.2
9:00 AM	29.1	27.6	29.3	28	29.3	30
10:00 AM	29.5	27.1	29.2	27.6	29.3	31.8
11:00 AM	31.3	27.9	30.1	28.4	30	33.9
12:00 PM	33	29.3	31.4	29.8	31.4	35.9
1:00 PM	34.5	30	32.4	30.7	32.3	37.1
2:00 PM	35.5	30.6	33	31.2	32.8	36.9
3:00 PM	36.9	31.3	33.6	31.9	33.4	36.5
4:00 PM	37.6	32.1	34.2	32.3	34	35.9
5:00 PM	35.3	30.8	33.4	31.3	33.3	33.6
6:00 PM	33.6	29.9	32.4	30.9	32.3	31.2

Figure A-9: Various Temperature of the EAHE Prototype System on 28 March 2015 (Day 3)